Ivan Vidović, Dipl.-Ing. BSc

Railway Infrastructure Condition Monitoring
and
Asset Management –
The Case of Fibre Optic Sensing

DOCTORAL THESIS

to achieve the university degree of

Doktor der technischen Wissenschaften

submitted to

Graz University of Technology

Supervisor

Stefan Marschnig
Graz University of Technology

Second Supervisor

Sebastian Stichel
KTH Royal Institute of Technology

Graz, July 2020

AFFIDAVIT

I declare that I have authored this thesis independently, that I have not used other than the declared sources/resources, and that I have explicitly indicated all material which has been quoted either literally or by content from the sources used. The text document uploaded to TUGRAZonline is identical to the present doctoral thesis.

8.7.2020	
Date	Signature

Preface

The beginning of this work is doubtless the appropriate place to thank all those people who made this work possible and accompanied me on the way to compiling it.

First of all, I would like to thank Peter Veit for the support provided in recent years. He made it possible to work at the institute, to build up a worthwhile network and to develop on a personal level.

Very special thanks to Stefan Marschnig, supervisor, co-author and collaboration partner on many projects and papers. Stefan, sitting next to you provides both the opportunity to gain valuable knowledge and experience but also means countless hours of discussions on subject-related issues in and outside the walls of the university as well. Thank you for challenging me and making sure that I never lost my focus. Your involvement has been integral in bringing this work to fruition.

Furthermore, I would like to thank Sebastian Stichel for being available as the second reviewer and examiner of this work.

Many thanks to all my project partners I had the pleasure to work with in recent years. Above all, I will never forget the track inspections and discussions with Simon Züger who helped me to overcome the one or other obstacle and brought light into the darkness.

I would like to express my sincerest gratitude to Matthias Landgraf. The discussions with you have taught me new perspectives and paths to finding answers and motivation in some difficult times. Thanks for the constructive work together and the invaluable and amicable conversations.

Johannes Neuhold, Martin Smoliner and Michael Fellinger shared the burden of finishing a dissertation with me. It has been a joy to share this path with you. Well, we've almost made it.

My colleagues at the institute, with whom I had the pleasure of working with in the past 4+ years, enlivened my days at the institute with a lot of fun, social distractions and vivid discussions. Many thanks, Martina Zeiner, Petra Wilfling, Markus Enzi, Georg Neuper, Armin Berghold, Stefan Walter, Markus Loidolt and Stefan Offenbacher. Claudia Kaufmann, the institute's manager behind the scenes and when necessary fighter on the frontline, has

Abstract

The condition monitoring and assessment of railway infrastructure are vital tasks of infrastructure managers. Economically and technically optimal maintenance measures and strategies are planned and executed based on the condition assessments.

Almost all infrastructure managers use track recording vehicles for track measurements and monitoring. In addition, sensors can be attached to assets of interest and provide continuous information over time. Furthermore, it is also feasible to use optical fibres laid in cable troughs along railway tracks as a data source. The present work examines the potential of fibre optic cables, which are already installed in cable troughs alongside railway tracks, for railway infrastructure condition monitoring and assessment. Distributed Acoustic Sensing (DAS) transforms the fibre optic cable into a linear sensor detecting all structure-borne sound waves and vibrations. In principle, the signal detected is the response of the track to the load of a train passing.

The results presented in the scope of this thesis demonstrate the applicability of DAS for infrastructure condition monitoring. Not only the current condition but also the emergence or deterioration of e.g. white spots over time can be assessed and quantified. Furthermore, both the quality of maintenance work and its effect can be evaluated. The methodology developed enables a measurement data-based condition monitoring of crossing noses, switch panels and insulated rail joints. Based on this, it permits conclusions on the current condition of individual assets and sections as well as the effectiveness of a component exchange. It has also been shown that, in addition to a distinction between freight and passenger trains and the associated train operation monitoring, maintenance work, such as tamping, can be unambiguously classified as such and essential parameters evaluated.

This work provides a basis for future developments and shows that a holistic and permanent condition monitoring, as well as condition assessment of the railway infrastructure, can be achieved utilising the already available infrastructure of optical fibres.

Kurzfassung

Die Erfassung des Fahrwegzustands der Eisenbahn ist eine der wichtigsten Aufgaben von Infrastrukturbetreibern. Basierend auf den Zustandsbewertungen werden wirtschaftlich und technisch optimale Instandhaltungsmaßnahmen und -strategien geplant und ausgeführt.

Zur Erfassung des Fahrwegzustands werden bei nahezu allen Infrastrukturbetreibern in erster Linie Gleismesswagen eingesetzt. Zusätzlich können Sensoren an Anlagen von Interesse angebracht werden und liefern zeitlich kontinuierliche Informationen. Neben derartigen Punktsensoren, besteht auch die Möglichkeit, entlang der Schieneninfrastruktur in Kabeltrögen verlegte Glasfaserkabel als Datenquelle heranzuziehen. Die gegenständliche Arbeit untersucht die Möglichkeit bereits verlegte Lichtwellenleiter zur Zustandserfassung des Fahrwegs zu verwenden. Distributed Acoustic Sensing (DAS) verwandelt den Lichtwellenleiter in einen linearen Sensor, der alle Körperschallwellen und Vibrationen erfasst. Das Signal spiegelt im Prinzip die Reaktion des Fahrwegs zufolge der Belastung einer Zugüberfahrt wider.

Die Ergebnisse der Arbeit zeigen, dass anhand der entwickelten Methodik DAS zur Zustandsüberwachung des Fahrwegs eingesetzt werden kann. Es kann nicht nur der aktuelle Zustand, sondern auch die Entwicklung bzw. Verschlechterung von weißen Spritzern über die Zeit gemessen und quantifiziert werden kann. Darüber hinaus, können sowohl die Qualität von Instandhaltungsarbeiten als auch deren Effekt bewertet werden. Des Weiteren wird eine Methodik entwickelt, die eine messdatenbasierte Zustandsüberwachung von Herzstücken ermöglicht. Daraus lassen sich Rückschlüsse sowohl auf den aktuellen Zustand von einzelnen Weichen ziehen als auch die Wirksamkeit eines Komponententausches aufzeigen. Außerdem hat sich gezeigt, dass neben einer Unterscheidung zwischen Güter- und Personenzügen und der damit einhergehenden Zuglaufüberwachung auch Instandhaltungsarbeiten, wie beispielsweise Stopfen, eindeutig als solche klassifiziert und wesentliche Parameter davon analysiert werden können.

Diese Arbeit bietet eine Grundlage für zukünftige Entwicklungen und zeigt wie sich eine holistische und permanente Zustandsüberwachung als auch Zustandsbewertung des Eisenbahnfahrwegs gestalten lässt.

CONTENTS

Index of abbreviations

AM	*asset management*
Anabel	*analyse und auswertung belastungsdaten*
A/D converter	*analogue-to-digital converter*
BPF	*bandpass filter*
BLS	*bern-lötschberg-simplon railway company*
(C)OTDR	*(coherent) optical time-domain reflectometry*
CAGR	*compound annual growth rate*
CM	*condition monitoring*
CU	*control unit*
DAS	*distributed acoustic sensing*
DOFS	*distributed optical/optic fibre sensing/sensors*
ERRI	*european rail research institute*
EM	*electromagnetic*
FOS	*fibre optic sensing*
FUT	*fibre under test*
GB	*gigabyte*
GT	*gross-tonnes*
HDF5	*hierarchical data format*
IC	*intercity*
IM	*infrastructure manager*
ITU	*international telecommunication union*
IU	*interrogator unit*

kHz	*kiloHertz*
LCC	*life cycle costs*
LVEL	*limit value exhaustion level*
m	*metre*
µm	*micrometre*
nm	*nanometre*
OLA	*opta sense linear asset*
OS	*operating system*
PC	*personnel computer*
PU	*processing unit*
RQ	*research question*
RU	*railway undertaking*
SBB	*swiss federal railways*
SD	*standard deviation*
STFT	*short-time fourier transform*
S&C	*switches & crossings*
TRV/TRC	*track recording vehicle/track recording car*

Note that geographical names shall be written in their native form, i.e. *Guemligen* will be written in the German form *Gümligen*, regardless of whether English-language forms exist.

Index of figures

Index of tables

1   INTRODUCTION

1.1   Overview

Railways as a means of mass transport as we know it today transfer and carry people and cargo from one destination to another. Especially in challenging times like these (increased mobility demand – climate change – green deal – emission-free travelling – sustainable infrastructure) the importance of this mode of transport is impossible to ignore. From the early beginnings in the first half of the 19th century, it revolutionised the mobility sector and soon became a success story. What the exceptional comfort was for passenger traffic, the almost unlimited transport load was for freight transport. As a consequence of the increased travelling speed, previously unimaginable distances could be overcome. Some unique aspects, however, have remained, while others have been improved or become obsolete. The principal technology is still the same as it was 150 years ago, but the technical standards have unequivocally changed, not at least because of altered requirements and demands.

Higher train speeds, an increasing number of trains and thus loads have a massive impact on the railway system, the wear and tear of the components and consequently the infrastructure. These are among the many challenges infrastructure managers (IM) face nowadays. After all, the construction and operation of infrastructure assets are associated with tremendously high costs covered by mainly public money. In 2019, the Austrian Federal Railways Infrastructure AG (ÖBB Infra AG) received an amount of EUR 2,328.1 million in grants of which some EUR 883.2 million are grants for expansion and reinvestment of the infrastructure and further EUR 861.4 million are subsidies for operation. The smallest share – some EUR 583.5 million is associated with inspection, maintenance, disposal and repair of existing infrastructure (ÖBB-INFRASTRUKTUR AG, 2019). In Switzerland, the public sector granted subsidies for the Swiss Federal Railways (SBB) at a total amount of CHF 4,374 million (~EUR 4,158 million) in 2019, upon which almost half of the granted money is foreseen as contributions directly related to rail infrastructure and one-third of the infrastructure money is spent on infrastructure maintenance (SBB Swiss Federal Railway, 2019). Furthermore, the EU has allocated more than EUR 33 billion in grants to investments in the rail sector in the current EU financial framework (2014–2020) (European Commission, 2019).

In light of recent events, it is expected that this amount will increase significantly over the next few years.

Hence, operations with mainly public resources must be carefully planned and allocated. It is only the prudent use of both funds and the assets themselves that guarantees that resources are used appropriately, in the proper location and in a demand-based manner. This is the key to justifying the high investment costs and ensuring the assets can last as long as possible, ultimately leading to a sustainable railway system. However, a system can only ever be considered sustainable when it encompasses a wide range of aspects as economic, social and environmental implications, which for railways is undoubtedly true. The economic aspect, moreover, is even more important for railways than for many other areas and requires the implementation of an asset strategy that considers both maintenance and renewal of existing infrastructure in order to reach the expected service life or even to prolong it resulting in the lowest life cycle costs (LCC) of an asset (UIC, 2016).

Any asset management (AM) strategy requires decision-making with regard to maintenance tasks, which tasks to carry out and to what extent considering the budget and technical asset condition. Several maintenance strategies exist and are discussed briefly.

Fail & fix concepts lead to very few interferences and track closures necessary for inspection and condition evaluations, because an asset is only repaired in case of breakdown. In such a case, costs for track closure and repairs are high. Another corrective/reactive approach is the find & fix concept. Here, visual inspection (time-based) or measurements are prerequisites as they must detect a failure immediately before the asset or – at worst – the system breaks down. The costs added by inspection are counteracted by reduced system downtime for repair measures. A more advanced strategy – namely do & prevent – is a rather cyclic concept and to some extent a preventive concept. Maintenance tasks, e.g. grinding, are carried out after some millions of gross-tonnes and minimise risks of component or asset break downs. Naturally, such a strategy results in higher maintenance costs. The most common concept is to monitor & prevent, which is rather an improvement of the measuring-based find & fix concept. Monitor & prevent applies time-series analyses of measurands and maintenance tasks are carried out before a defect occurs. Improved maintenance schedules and lower costs are positive effects of such a strategy but require both sophisticated condition evaluation methods and knowledge about the system's behaviour. An even more mature concept and advancement

of the former is the predict & prevent concept, which predicts the quality and behaviour of an asset over the entire time. This includes as a prerequisite, of course, exact knowledge about the effect of maintenance on quality and behaviour and the particular damage mechanisms. Such a regime, as well as the install & forget concept (maintenance-free components), is desirable but not ready for implementation yet. Except for the fail & fix concept, any mentioned strategy requires a more or less precise asset condition monitoring and evaluation. This enables trend analyses of quality and behaviour and planning of purposeful maintenance tasks. The more often an asset's condition is evaluated reliably, the more accurate the necessary measures can be planned and executed. IMs have to take care of various assets (bridges, tunnels, tracks, turnouts, and more) with naturally different service lives, inspection cycles and maintenance demands, each of which is a topic for itself.

Nowadays, various data sources for determining the condition of assets exist. Some of them are related directly to infrastructure condition monitoring while others certainly influence railway operations and may affect the asset condition as a consequence of malfunctioning. A classification may look as follows: 1) vehicle measures infrastructure; 2) vehicle measures vehicle; 3) infrastructure measures infrastructure and 4) infrastructure measures vehicle. A brief overview of the current state of the art/knowledge/practice is given at this point and reviews both the strengths and shortcomings of such.

Track recording vehicles ((TRV), sometimes also referred to as track measurement cars (TMC) or track recording cars (TRC)) are commonly used by almost every infrastructure manager mainly for track geometry measurements of the entire network. Measurement data from TRVs are well-known, reliable and state of the art, but are by no means a modern concept. The first automatic recording vehicle capable of detecting track failures was invented around 1928 by Dr Sperry (Solomon, 2001). Along with the advantages, some shortcomings can be identified. These vehicles do not observe the network continuously, which means the local measurements over a specific distance only take place on a now and then basis. These measurement intervals are adequate of course, for sections deteriorating at a moderate pace, but may be too long for critical sections including isolated track defects (white spots), hollow layers (hanging sleepers), subgrade lowerings, (insulated) rail joints or even broken rails. Furthermore, measurements from TRVs are not capable of performing condition monitoring (CM) of turnouts and bridges, in particular. These assets are assessed mainly by visual inspection executed by dedicated experts

in cyclic intervals every few weeks. Current developments aim to go beyond a pure track geometry observation, as several additional measuring systems are equipped on vehicles for detection of e.g. rail and catenary profiles or tunnel clearance measurements (Auer, 2013). Furthermore, it is even possible to mount an additional antenna on the TRV to perform measurements with a Ground Penetrating Radar (GPR) (Fontul *et al.*, 2018) delivering information on superstructure and substructure condition (e.g. humidity and fouling). Measurements with GPR need additional track closures (if not mounted on conventional TRVs) and rain events during or in the proximity of the measurements may have some effects on data quality and reliability. Furthermore, data analyses are carried out mainly by the suppliers and are expensive. A method for increasing the measurement frequency to assess the condition of tracks provides sensors mounted on in-service vehicles/trains (onboard measurement (OBM)) including axle box accelerometers (Yazawa and Takeshita, 2002; Erhard, Wolter and Zacher, 2009) or bogie movement measurements (McAnaw, 2003; Weston, Ling, Goodman, *et al.*, 2007; Weston, Ling, Roberts, *et al.*, 2007). This data could be a valuable data source for critical assets and sections and has been examined for almost 20 years. Nevertheless, measurements on a broad scale are still not available and many measurement campaigns struggle to deliver reliable data and thus are not proven yet. These systems are assigned to the first group *vehicle measures infrastructure*. The latter systems aim not only to deliver data on track condition, but also to assess the health status of vehicle components. Such systems can be classified into the second group *vehicle measures vehicle*.

In recent years, the application of sensors on turnouts (Kassa, Sramota and Kaynia, 2017) and bridges (Loendersloot and Mostafa, 2018) has been thoroughly investigated not only within the scope of various EU projects. These approaches are very useful to gain knowledge about the condition and behaviour of these assets, but, only deliver information about certain turnouts or bridges at one location. Furthermore, gaining knowledge on the health status of these assets is becoming more and more decisive as experienced experts – know-how owners with long manual inspection experience – retire from service and their valuable knowledge is lost with them. Manual inspections are highly subjective procedures, they are not to be regarded as reproducible and are naturally time-consuming and costly. Some of the aspects of this call for equipping thousands of turnouts and bridges with sensors and measures on this scale scarcely

affordable for any IM. Sensors mounted on assets of interest are assigned to the third group *infrastructure measures infrastructure*.

Lastly, another noteworthy data source IMs rely on are wayside train monitoring systems (WTMS); *infrastructure measures vehicle*. The main field of application is, accordingly, monitoring and assessment of rolling stock's condition. WTMS have been gradually expanded and provide additional information about infrastructure-damaging conditions of vehicles such as dragging equipment or whether vehicles comply with the clearance profile (Barke and Chiu, 2005; Bisang, Frey and Koller, 2017). Trackside sensors for rolling stock observations have been used for a long time, are proven systems and monitor the condition of each train passing at the location where they are deployed. Nonetheless, these are local measurements at specific points installed at neuralgic points within the network. For instance, SBB has some 200 train monitoring systems with different levels of sophistication distributed over a net length of more than 3,200 km. The effective extent of the measurement system is determined by the quantity of equipment in use and inevitable gaps can lead to some undetected failures and incidents.

Condition monitoring, assessment and decision-making lead to a final, vital task for IMs: planning, executing and documentation of maintenance. Mostly, maintenance planning bases on thresholds, limit values or quality figures and depend, as mentioned before, on the strategy carried out. External contractors are primarily responsible for the execution of e.g. tamping or grinding. While these routines are fairly straightforward, the question of documentation of maintenance work arises. Where are the executed tasks documented and what is documented? Are there only notifications of discrepancies between planned and executed work and what time is reported? The time of execution or the time when it was documented? These issues are especially of great interest if maintenance is completely outsourced and the IM has no influence and information on such works, but it is not of insignificance for any IM.

1.2 Research demand and objective

The overview of various data and information sources given before outlines the need to close the lack of data for assets and boundary conditions, in particular. Additional data shall increase the information about the condition of assets, close the gap of knowledge and ultimately provide IMs with additional and valuable information for track asset management. Hereby, the focus is laid on gathering data and information without adding additional sensors to infrastructure because every IM strives to avoid affecting the daily railway's operations. For this purpose, fibre optic cables seem to be a suitable source as they are laid in thousands of kilometres alongside railway tracks.

Using optical fibres in a sense of distributed optical fibre sensing for monitoring of infrastructure systems was mainly driven by the oil and gas industry. With the exception of the oil and gas industry, there have long been only a few areas of application and especially in railways, hardly any field of application could be identified. This is primarily because of the aforementioned measurement methods in this area used for infrastructure condition monitoring. However, fibre optic sensors are well-known and widely used in railways nowadays. Du (Du *et al.*, 2020) gives an overview of sensors (grating/reflectometry and interferometry based sensors) applied in railways currently and in the past years.

For IMs, sensing methods capable of monitoring extensive sections of the infrastructure are of particular interest. In the case of distributed sensors Distributed Acoustic/Vibration Sensing fulfils this requirement. Since 2010, it has also been used for detection of natural hazard management, landslides, avalanches and mudslides. With this method, up to 40 km can be monitored with one sensing unit whereby optical fibres already laid in the cable trough can be used.

However, this work examines the capability of distributed fibre optic sensing for railway infrastructure condition monitoring and focuses on two main aspects: condition monitoring and evaluation of 1) track and turnouts and 2) assessment of planned/executed maintenance tasks. An extensive literature review on DOFS is presented in Chapter 2 where the basics of optical fibres are discussed.

1.3 Scope, limitations and delimitations

In this thesis, a thorough investigation of a distributed optical fibre sensor is carried out to essentially determine its full potential for railway infrastructure condition monitoring and asset management. The focus hereby is neither the development of a new sensing technology nor its evaluation to enhance the distributed sensing performance, but rather a thorough applicability examination of distributed fibre optic sensing for infrastructure condition monitoring.

The system must demonstrate its efficiency under realistic operating conditions. Therefore, the system's default settings have been used and consequently no amendments regarding spatial resolution, sampling rate modifications or adaptions were made.

The monitored track is an existing mostly double line partly owned by both SBB and BLS. Some track sections have very heavy loads with an average of nine trains per hour and direction (this is an average number of freight and passenger trains over the entire day). More passenger trains naturally run during the day, whereas at night, freight trains predominate. As a consequence, train headways under two minutes are achieved in morning rush hours leaving no room for operational disturbances. For those reasons, it was not possible to deploy a new optical fibre cable and the existing glass fibre infrastructure installed along tracks was used for this project. Furthermore, no improvements were made regarding the bedding, routing and distance of the optical fibre to the track.

Besides the boundary conditions regarding the optical fibre, there are also limitations with regards to track condition, component exchange and thus maintenance measures. Firstly, the track condition was not changed to evocate a specific type of failure, such as isolated track defects or hollow sleepers. Thus, although detecting track failures poses an apparent field of application for fibre optic sensing, they were not created especially for this purpose. Secondly, as the condition, type and age of the superstructure and components vary along the route it may turn out that the comparability is limited. In this respect again, no adaptions were made. Last but not least, as the assessment and documentation of maintenance measures is an essential part of this thesis, all planned and unplanned measures were recorded. In case some planned tasks could not be performed, they were not repeated and executed for the sole purpose of data collection.

1.4 Research environment

A substantial part of this dissertation has been developed within the context of a pilot project with Swiss Federal Railways (SBB) to examine the potential of DAS in railways. The Institute of Railway Engineering and Transport Economy (EBW) can look back on long and tremendously successful cooperation with SBB, exploring issues predominantly regarding railway asset management. While the project's overall aim was the entropy of fibre optic sensors, the title of the thesis "Railway infrastructure condition monitoring and asset management: The case of fibre optic sensing" implies that this applied research goes beyond a pure disciplinary perspective.

The latter is highly dedicated to structural health monitoring (SHM) which has evolved to become a new discipline in countless fields in recent years, including civil engineering. Facing the problem of outdated civil infrastructures including e.g. bridges and tunnels it becomes more and more crucial to determine when the structures need to be repaired or reinforced. SHM applications include large infrastructures (e.g. bridges and tunnels), oil and gas pipelines, vehicles (e.g. aircraft, ships and cars), and biomedical devices at which a detection of the changed condition is the main focus of SHM. This holds true for new structures too. Furthermore, well maintained civil infrastructures lead to prolonged service life and decreasing life cycle costs. Therefore, any new installation shall be able to reliably produce information regarding its condition and any change in this and pass on the information to operators and/or decision-makers. As optical fibre sensors come with numerous advantages (e.g. small size, lightweight, high sensitivity and resistance to electromagnetic interference and corrosion) it is no wonder that the use of fibre optic sensors in the field of SHM has been examined thoroughly in the past two decades. The results were quite promising and encouraging. However, fibre optics is a field for itself with a myriad of R&D projects examining fibre and laser properties for enhancing the sensing capabilities. The global fibre optics market is estimated to be worth USD 4.3 billion in 2019 increasing to USD 6.9 billion in 2024. The Compound Annual Growth Rate (CAGR) in this period is expected to stand at 10.0% (*Fiber Optics Market by Cable Type, Optical Fiber Type, Application & Geography*, 2020). At Graz University of Technology, where this thesis was written, a considerable part of ongoing research at the Institute of Engineering Geodesy and Measurement Systems (IGMS) is dedicated to fibre optic sensors.

What is true for the market of optical fibres is all the more the case for the railways. Railway operation goes beyond moving goods and transferring passengers from one point to another. Rather, it must be seen as an interplay of many different disciplines that finally enables the movement of trains. Sophisticated signalling solutions for traffic management, designing user-friendly ticketing systems and construction of comfortable vehicles are just a few examples necessary for successful railway operations. Striving for the enhancement of customer experience and the adaption of automation technologies to increase and speed up optimisation in railways are few industry representatives, namely smart railways worth USD 20.5 billion in 2019. This value is expected to increase to USD 39 billion by 2024 (*Smart Railways Market by Solution*, 2020) where solutions for asset management and maintenance are vital aspects.

The former – asset management and condition monitoring – however, calls for a broader scope and is certainly not a means for itself but rather needs integration of various knowledge dimensions, such as economical and technical expertise. The construction and operation of railway infrastructure are associated with high investment and maintenance costs. The aim is, therefore, to achieve the longest possible service life, taking into account sustainable and economically optimal investment and maintenance strategies. Consequently, railway infrastructure condition monitoring and assessment is critical for achieving this overall goal. Among the first, Professor Veit (Head of the Institute of Railway Engineering and Transport Economy since 2010) started to consider both economical and technological aspects for railway infrastructure renewal and maintenance strategies. The "Standard Element Approach" (StdE) – formerly also known as "Normkilometer" – allows describing infrastructure costs as a consequence of maintenance and renewal tasks for a certain set of boundary conditions (e.g. load, superstructure, radii). Within the framework leading the four-year project "Strategie Fahrweg (1998–2002)" of the Austrian Federal Railways (ÖBB), such Normkilometers were set up describing almost 90 % of the entire network. The success was sweeping and reflected in the postdoctoral thesis "Projekt Strategie Fahrweg" (Veit, 1999). In the following years, various IMs (Croatia (HŽ), Switzerland (SBB), Sweden (TVK)) set up this or similar approaches. Keeping economic aspects in mind, the behaviour and the quality of the infrastructure, as well as wear and tear of components, were further investigated in the framework of theses and projects in the subsequent years. A further, no least significant milestone and a highlight of the Institute's achievements was Marschnig's postdoctoral thesis

"iTAC – innovative Track Access Charges" (Marschnig, 2016), where significant considerations were adapted from SBB and are part of the track access charging scheme set up in 2017.

In an environment constantly dealing with the interaction economy-technology, the awarded master's thesis "The track behaviour after formation rehabilitation" (Vidovic, 2016) was conducted dealing with major issues regarding track quality and behaviour after high investment costs to improve the substructure condition and behaviour. Results of the thesis and major findings from Hansmann and Landgraf (Hansmann and Landgraf, 2013) resulted in a paper (Vidovic, Landgraf and Marschnig, 2017) presented at the "3rd International symposium Railway geotechnical engineering" in Paris. The starting point for the dissertation was a visit from Dr Jochen Holzfeind in April 2017 (at that time asset manager track at SBB) including a workshop on further research and collaboration activities between SBB and EBW. Besides this workshop, the keynote "Fiber Optic Sensing – a new data source for asset management" held in Berlin at the *2nd European conference on Wayside Train Monitoring Systems* in April 2018 was another cornerstone of the work. Further activities in that year include a presentation at the *4th Track Access Charges Summit* in Amsterdam on Mark-ups in track access charging and chairing a session at the same conference. First major findings of the dissertation work were presented in Malmö, Sweden in late 2018 at the *Intelligent Rail Summit 2018*. In that period also the first papers were written concerning hypothesis and core findings of the thesis. The most noteworthy activities in 2019, which was a year full of highlights, were firstly the reviewed and finally accepted paper (Vidovic and Landgraf, 2019) published by the *Cambridge Centre for Smart Infrastructure & Construction,* secondly the invited presentations at the *Smart Maintenance Conference* at the ETH in Zurich and the *22nd Internationale Tagung des Arbeitskreises Eisenbahntechnik* in Salzburg. Conclusively, the year was rounded off with a presentation at the *12th World Congress on Railway and Research* in Tokyo, Japan. Additionally, a reviewed paper was published in the congress' proceedings (Vidovic and Marschnig, 2019). Beside the mentioned publications and presentations, further activities as co-author were published involving track geometry data analyses (Neuhold, Vidovic and Marschnig, 2020), benchmarking of implemented track access charges in Europe (Marschnig, Vidovic and Brantegger, 2019) and estimating future tamping demands based on a sophisticated wear formula (Marschnig and Vidovic, 2019). In the time to come, more articles will be published, some of which have already been accepted, some of which are still under review. Among them are some directly related to

the dissertation, others solely in the extended research environment. Table 1.1 and Table 1.2 give an overview of the research carried out in the past four years. Note that those do not include supervised thesis, project reports and presentations given.

Ivan Vidovic, Stefan Marschnig	in revision 2020	Optical fibres for condition monitoring of railway infrastructure – encouraging data source or errant effort?	Applied Sciences
Ivan Vidovic, Anna Oprandi, Stefan Marschnig	2020	Innovative railway infrastructure condition monitoring through Fibre Optic Sensing	ZEVrail
Ivan Vidovic, Stefan Marschnig	2019	FOSphAT – Fiber optic sensing for permanent and holistic assessment of track	Proceedings of 12th World Congress on Railway Research
Ivan Vidovic, Matthias Landgraf	2019	Fibre Optic Sensing as Innovative Tool for Evaluating Railway Track Condition?	ice Publishing, Cambridge Centre for Smart Infrastructure & Construction
Ivan Vidovic, Matthias Landgraf	2019	Higher railway track availability achieved with innovative data analytics?	Proceedings of the International Heavy Haul Association STS Conference (IHHA 2019)

Table 1.1: Core research in the course of the thesis.

Ivan Vidovic, Stefan Marschnig	in submission (2020)	Working title: "Track deterioration models comprehensive literature review"	---
Ivan Vidovic, Markus Loidolt, Stefan Marschnig	in submission (2020)	Working title: "Harmonised TAC"	---
Markus Loidolt, Ivan Vidovic, Stefan Marschnig	accepted (08/2020)	Das Performance Regime (RL 34/2012/EU) als Tool zur Systemoptimierung	ZEVrail
Johannes Neuhold, Ivan Vidovic, Stefan Marschnig	2020	Preparing track geometry data for automated maintenance planning	Journal of Transportation Engineering, Part A: Systems
Stefan Marschnig, Ivan Vidovic	2019	Estimating future tamping demands using the Swiss Wear Factor	Proceedings of 12th World Congress on Railway Research
Stefan Marschnig, Ivan Vidovic, Michela Brantegger	2019	Trassenpreise auf Basis der Richtlinie 2012/24 EU – ein erster Benchmark?	Der Eisenbahningenieur
Ivan Vidovic, Matthias Landgraf, Stefan Marschnig	2017	Impact of substructure improvement on track quality	Proceedings of the 3rd International symposium Railway geotechnical engineering

Table 1.2: Further research.

1.5 Research questions

The main research question in this thesis is as follows:

(How) Can IMs utilise DAS to increase knowledge about track condition?

Based on the main research question, the background and the research demand the following five sub-questions (RQ1-5) were formulated during the research project.

RQ1: Can DAS describe different asset conditions?

RQ2: Is this technology able to detect potential track failures (e.g. isolated track defects)?

The research questions one and two are answered in sub-chapter 6.2. The signal characteristics of sections with track defects are compared with those without any defects and will reveal whether this system can distinguish between different asset conditions. Furthermore, sub-chapter 6.3 investigates DAS' suitability for turnout condition monitoring.

RQ3: Does the system allow for time series and trend analyses?

Following the conclusions from the previous research questions, the system's capability for condition monitoring and behaviour over time is evaluated. Thereby the development of a reported track failure over time is analysed in sub-chapter 6.2.1. Furthermore, Chapter 6.3 is devoted to both turnout condition monitoring and the influence of maintenance on the signal pattern and characteristic.

RQ4: Can DAS replace other types of monitoring/measuring technology and be a stand-alone application?

Research question four is partly theoretical in nature whereby it elaborates on "what can be done in the future/what already has been investigated" and is partly based on facts and results presented within this thesis. Answers to this question are given in Chapter 6.4, 8 and 9.

RQ5: Can DAS assess executed maintenance work?

Chapter 7 tackles research question five. On the one hand, it examines whether the system can detect executed maintenance measures and specify its type. Moreover, in-depth analyses are carried out to reveal distributed optical fibre sensing's potential for the assessment of maintenance tasks.

1.6 Outline of the thesis

The content of this thesis is arranged as follows:

Chapter 2 "Fibre optic sensing – Basics and working principle" presents a basic understanding of optical effects inside the fibre, which are of importance for the sensing principle. An overview and classification of fibre optic sensors are presented and light scattering processes inside the fibre, i.e., Brillouin, Raman and Rayleigh scatterings, are theoretically described. Then some fundamental concepts of distributed fibre sensing are introduced and the working principles of OTDR (optical time-domain reflectometry) sensors based on Rayleigh scattering processes are explained. Also, an extensive literature review of DOFS in railways is presented.

In Chapter 3 "Sensing properties and signal characteristics", the applied monitoring system is described and signal patterns and the statistical properties over the whole distance are analysed. The chapter concludes with some aspects of the imperative of comparing track layout and cable routing.

Chapter 4 outlines the data acquisition and pilot project. Firstly, the pilot line and the components, such as sleeper and rail type will be analysed. It will highlight the vast amount of information IM already have about a track and its structure, as well as the traffic and the operating train types on specific lines. Afterwards, the developed methodology for further analyses will be discussed. Especially, the mandatory link between channel and asset is described. The chapter concludes with the description of the data processing cycle.

In Chapter 5, the obtained data is analysed. In the first step, it is possible to display the events taking place on or next to the monitored track. By displaying the train traffic on the track, fibre optic sensing enables live train traffic monitoring and reveals the potential of this technology in regard to railway operations. As railway operations are not the main objective of the thesis, the influence of train composition and track condition is analysed afterwards.

Based on the results of the previous chapter, Chapter 6 is devoted to analyses regarding the infrastructure condition. In addition to the track, the condition of turnouts is also analysed and assessed.

Chapter 7 elaborates on asset management's additional aspects – maintenance measures. The most important maintenance tasks within a track's life cycle, tamping and grinding, are recorded, analysed and evaluated.

In Chapter 8, conclusions are drawn on the main achievements in this thesis and the research questions are answered.

Finally, Chapter 9 presents a few perspectives on the further potential of distributed fibre optic sensing. Furthermore, it gives insight on how this holistic and permanent monitoring technology can be used in the decision-making processes for a sustainable AM. Additionally, this chapter reviews what else is necessary to implement and use this data in the daily business of IM in the future.

2   FIBRE OPTIC SENSING – BASICS AND WORKING PRINCIPLE

2.1   Basics of optical fibres

Since the focus of this thesis is neither the development of measuring systems nor the assessment of such technologies, this basic introduction shall facilitate an initial understanding of distributed optical fibre sensors and its capabilities.

2.1.1   Structure

The core, cladding and coating form the basic construction of an optical fibre. Also, these are the three fundamental layers of any fibre. With a diameter between 4–62.5 micrometre (µm), the core is the thinnest part of the fibre and has a fixed connection to the cladding. Generally, the refractive index of the core is slightly higher than that of the cladding (~1 %). Therefore, when light travels through the core and hits the interface with the cladding at a specific angle its direction, caused by total internal reflection, is diverted. The standard diameter of the cladding is 125 µm and is fixed to the coating (Ø 155–900 µm) which surrounds the cladding. Many fibre optic cables also have a strength member and an outer jacket (Figure 2.1) (Hecht, 2015).
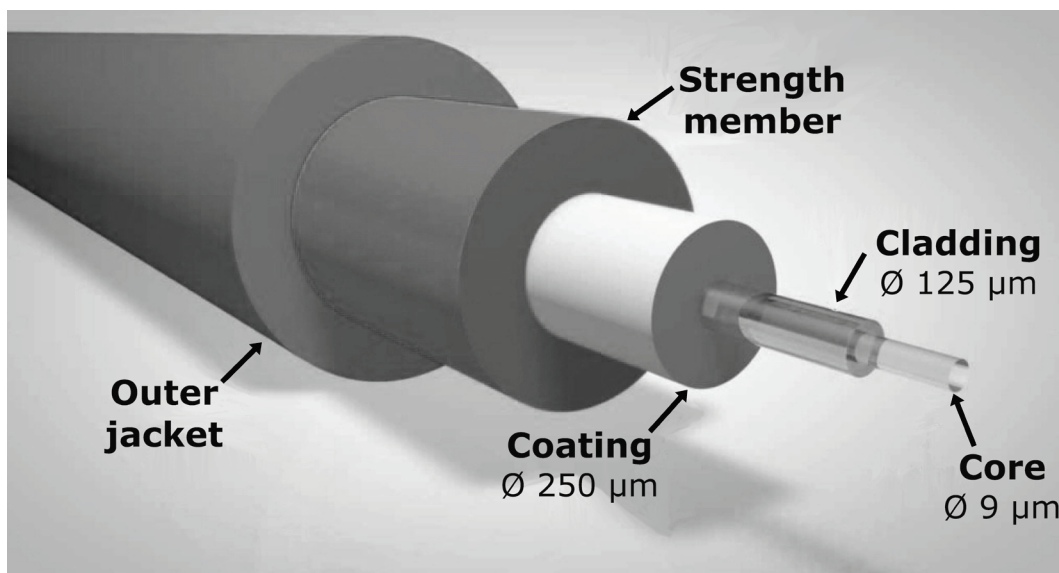
Figure 2.1: Schematic diagram of the optical fibre structure.

While the strength member provides the rigidity to protect the fibre from buckling, the outer jacket protects the inner parts from the surrounding environment and thus from moisture, extreme temperature and water ingress into the fibre. Although fibre optic cables find use in many areas, the core and cladding of the vast majority of fibres are made of silica (*SiO$_2$*), commonly known as pure glass. Furthermore, plastic or polymer-based cores and claddings are applied for the mass market; e.g. luminaires or local networks (Hui and O'Sullivan, 2009; DeCusatis, 2014).

2.1.2 Light guiding

The speed of light *c* is constant in a given medium. In a vacuum, it is considered as the universal speed limit and slows down when passing a transparent material. Hence, the speed of light depends on the medium it travels through and changes when it passes from one medium into another. Light refraction occurs when the angle between a light ray, which hits the surface of a medium, is not perpendicular to or parallel with the boundary. In such a case, the light ray changes its speed and direction, but the frequency of light remains the same.

"The refractive index[1] n is the ratio of the speed of light in a vacuum to the speed of light in the material (Hecht, 2015)*":*

$$n = \frac{c_{vac}}{c_{mat}}$$

EQ 2.1

where *c$_{vac}$* is the speed of light in vacuum and *c$_{mat}$* the speed of light in a material.

The refractive index indicates how difficult it is for the light to travel through a medium. Therefore, if *n* increases, the light speed in the material decreases and travels the slower the higher *n* is. When a light ray strikes the surface of a material with a different refractive index another phenomenon can be observed: the light is bent. This effect depends on the one hand

---

[1] Refractive index: vacuum ≈ 1; air ≈ 1.0002926.

on the different refractive indexes of the two materials and on the other hand on the angle at which the light ray hits the surface of the other medium. The relationship between angles of incident and refraction is described by the following equation (Thyagarajan and Ghatak, 2007):

$$n_1 \sin \gamma_1 = n_2 \sin \gamma_2$$

EQ 2.2

with

n_1 refractive index of material 1

n_2 refractive index of material 2

γ_1 angle of incidence

γ_2 angle of refraction.

EQ 2.2 is also known as *Snell's law* and derives after mathematical relations the critical angle γ_c:

$$\gamma_c = \arcsin\left(\frac{n_2}{n_1}\right)$$

EQ 2.3

The critical angle describes the limit value up to which total internal reflection takes place. The angles of incidence and refraction are measured from the normal, which is an imaginary line perpendicular to the surface. As an example, Figure 2.2 shows the relationship between the angle of incidence – refraction – and total internal reflection when light travels towards the boundary with a lower refractive index ($n_1 > n_2$). If a light ray strikes the surface of the lower dense medium with an angle less than the critical angle ($\gamma_2 < \gamma_c$) refraction will occur and the light ray is bent away from the normal. Otherwise, if the angle of incidence is bigger than the critical angle ($\gamma_1 > \gamma_c$) the light ray will bounce back from the boundary of the less dense material and the light will undergo total internal reflection. A third, less common case, is when the angle of incidence reaches the critical angle ($\gamma_2 = \gamma_c$). In such a case, the refracted ray lies along the boundary, having an angle of refraction of 90-degrees (Thyagarajan and Ghatak, 2007; Hecht, 2015).
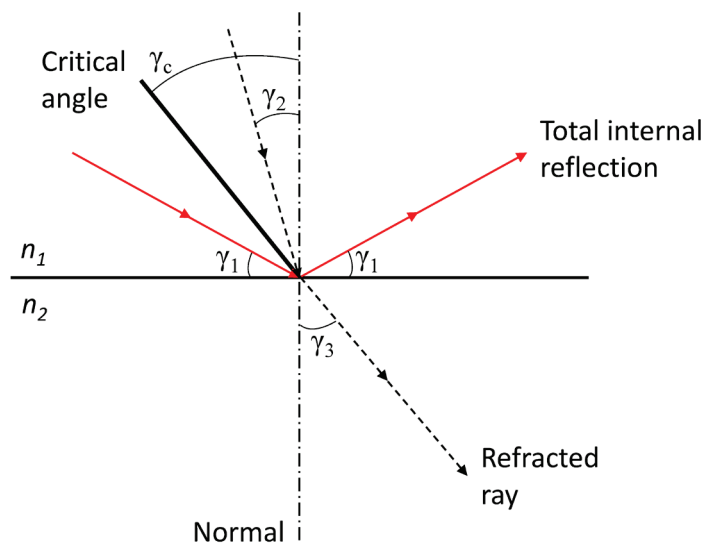
Figure 2.2: Refraction and total internal reflection

(adapted from (Thyagarajan and Ghatak, 2007)*).*

The total internal reflection is the basic concept behind light propagation in optical fibres and only takes place when both of the following conditions are met:

1) a light ray is in the medium with the higher refractive index and approaching the less dense medium

2) the angle of incidence for the light ray is greater than the so-called critical angle.

Based on the general principles, Figure 2.3 illustrates the light propagation in an optical fibre. The refractive index of the core is slightly higher than that of the cladding $(n_0 > n_1)$, causing the effect of total internal reflection.
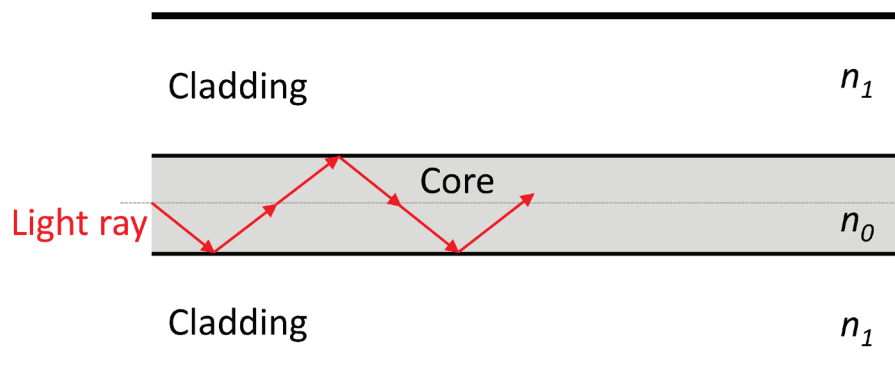
Figure 2.3: Light guiding in an optical fibre (adapted from (Hecht, 2015)*).*

2.1.3 Transmission

The transmission of signals through optical fibres is affected by three effects leading to signal degradation (Hecht, 2015):

1) attenuation
2) dispersion *and*
3) crosstalk.

The effects will be briefly discussed in the following section, whereby the focus will be on the effect of attenuation.

2.1.3.1 Attenuation

The attenuation of an optical fibre is characterised by the amount of loss between the incident light and the output. Losses from imperfect light coupling, absorption and fibre are considered as total attenuation. Attenuation is the main factor on which the distance a pulse can travel in a fibre depends before it becomes too weak to detect. The effects of absorption and scattering cumulate over a fibre's length. While losses due to absorption and scattering occur along the fibre, coupling losses only occur at a fibre's end. For shorter fibres attenuation and scattering are less important than end losses. For a system's performance, total attenuation is the decisive parameter. For communication fibres, the attenuation is measured in decibels per kilometre. Figure 2.4 illustrates the contributions from scattering and absorption to total loss in fibre. The peaks arising of metal impurities of the glass look smaller in other plots and also may be smaller in other communication fibres. For wavelengths greater than 1.6 µm the absorptions arise due to silicon-oxygen bonds in the glass. Furthermore, as visible, the absorption increases with longer wavelengths. In the case of Rayleigh scattering, the most attenuation is observed at shorter wavelengths. The lowest loss occurs for longer wavelengths at 1.55 µm where upon both infrared absorption and Rayleigh scattering show the losses. For example, in the wavelength range of 1550 nm an attenuation of approximately 0.2 dB/km results in an intensity loss of the signal of 5 % per kilometre. The absorption loss is represented by the space between the measured total attenuation and theoretical scattering curve. The closer the two lines, the larger the fraction of total attenuation that arises from scattering (Hecht, 2015).
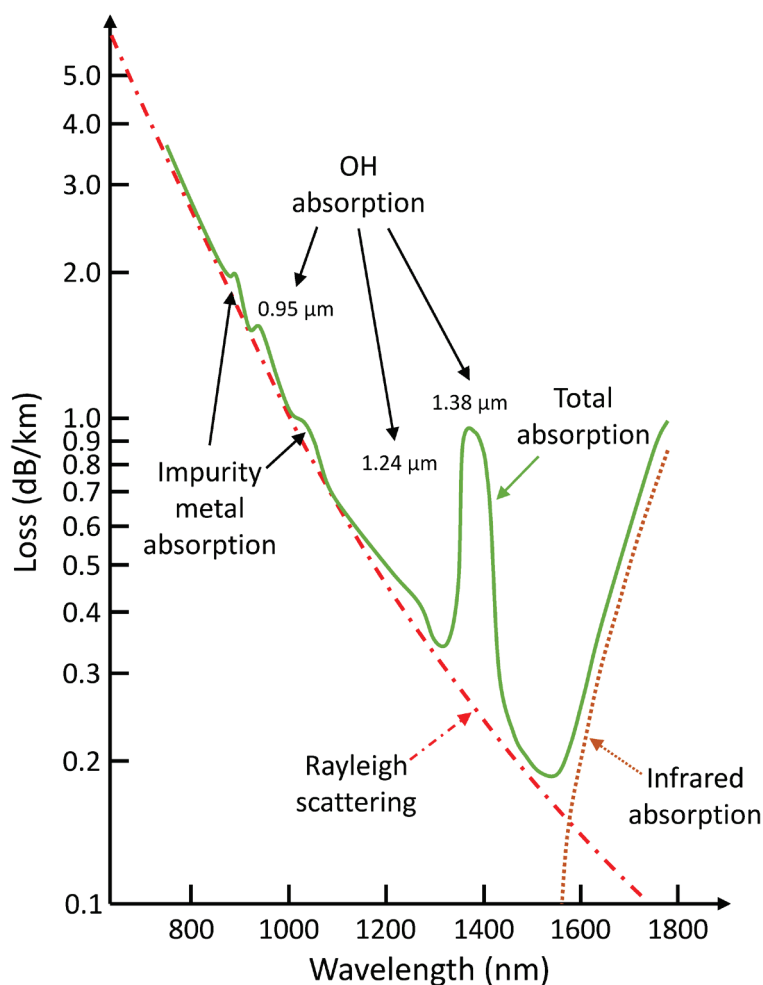
Figure 2.4: Total loss in a fibre (adapted from (Hecht, 2015)*).*

2.1.3.2   *Dispersion and bandwidth*

One of the main advantages of optical fibres is that they can transmit signals at high speed over long distances at a low loss with high bandwidth. Generally, the more information needs to be transmitted the faster the signal has to vary, and this can cause problems when transmitting high-bandwidth signals. The speed of signals in electrical wires is limited due to the nature of electrical currents. The impedance of wires increases with the speed at which the signal varies. This is mainly because the moving electrons induce currents in the copper around them. As a result, higher frequencies result in higher attenuation for coaxial cables and the loss increases exponentially as the signal frequency increases. On the contrary, optical fibres have almost the same attenuation at all frequencies.

Dispersion is another effect limiting the signal transmission in optical fibres. As light travels along a fibre, some photons spread out and travel in many distinct paths called "modes" leading to high dispersion. The speed of light varies (slightly) within the glass with wavelength and differences in the photon wavelength cause chromatic dispersion. The farther the light travels the more the photons spread out and the higher the dispersion is (Hecht, 2015).

2.1.3.3 Crosstalk

If signals cross barriers which are meant to separate them from each other crosstalk occurs. The common crosstalk, rather electronic crosstalk, happens between phone lines and radio broadcasts because the communication channels of both can leak into each other one. As fibres do not carry electrical current they are immune to such electrical crosstalk. However, as the technique "wavelength-division multiplexing" was developed, fibres are able to carry multiple optical channels at different wavelengths and such technology is vulnerable to crosstalk (Hecht, 2015).

2.2 Classification of fibre optic sensors

While for communication purposes it is preferred to minimise external perturbations of the optical fibre, for fibre optic sensing such effects are desired and even enhanced. The reduction of external disturbances provides reliable signal transmission and reception. On the other hand, geometrical and optical changes to an optical fibre caused by external disturbances can be measured. In general, there are two different types of sensors: intrinsic and extrinsic. For the first one, the optical fibre is the sensitive part. Consequently, sensing takes place within the fibre itself, whereby any environmental event can modulate the light ray within the fibre and can be converted and interpreted. In a truly intrinsic system, the light ray never leaves the fibre. For the latter, an optical fibre can be utilised as an information carrier connected to a black box to impress information on a light beam that propagates to a remote receiver. The black box can contain several mechanisms such as mirrors or liquid cells to modulate, transform or generate the light beam (Li, Li and Song, 2004; Udd and Spillman Jr., 2011). Furthermore, each of these sensors can be divided into sub-classes and even sub-sub classes.

Another method of classifying fibre optic sensors is to consider the type of modulation of the light beam such as intensity or phase modulation. Furthermore, it is also possible to arrange fibre optic sensors according to the spatial resolution[2] of the measuring points (Figure 2.5). For instance, single point sensors are applied when measurements are required solely at specific points. Moreover, for the measurement at more discrete points, quasi-distributed sensors are applied. For civil engineering monitoring applications, both single point sensors and quasi-distributed sensors have been widely used (Tennyson *et al.*, 2001; Di Sante, 2015).
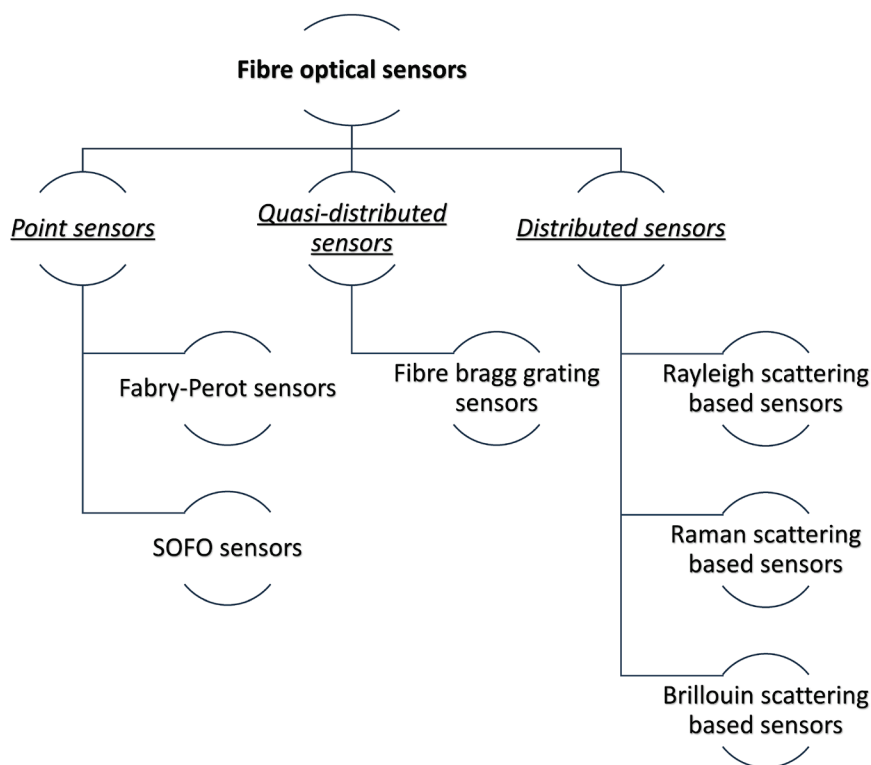
Figure 2.5: Overview of fibre optic sensor technologies

(adapted from (Udd and Spillman Jr., 2011)*).*

Distributed sensors are mainly based on optical scattering such as Rayleigh, Brillouin and Raman scattering (Rogers, 1999). They are useful for monitoring and measuring long linear assets including areas such as 1) leakage detection of pipelines; 2) embedded sensors in composite

---

[2] The spatial resolution is the smallest length of fibre over which any sensible change in the spatial variation of the measurand can be detected (Rogers, 1999).

materials; 3) temperature monitoring in reactor systems and 4) stress monitoring of bridges and buildings (Udd and Spillman Jr., 2011).

A light wave, which travels in a medium, interacts with the individual atoms and molecules. As each medium has its resonance, the electric field will only induce a time-dependent polarisation dipole, if the light wave's wavelength is far from a medium resonance. A secondary electromagnetic wave is generated by the induced dipole, which is light scattering. Compared to the wavelength of light the distances between the scattering particles are smaller and lead to coherent secondary light waves. Consequently, the resulting intensity is the addition of scattered fields. However, light scattering is a random statistical process and occurs in all directions. Small inhomogeneities and impurities within the fibre are the reason for density variations and attenuate the forward propagating signal, that is proportional[3] to $1/\lambda^4$, as well as the creation of the backward propagating wave. This effect is called Rayleigh scattering and is known as an elastic and linear scattering without any frequency shift. Hence, the frequency of the incident light is the same as that of the scattered light and the scattered power is proportional to the incident power.

The frequency spectrum of Rayleigh, Brillouin and Raman scattered light is illustrated in Figure 2.6. The scattering peaks on both sides of the central Rayleigh peak are called Brillouin scattering components. They originate from light interactions with propagating sound waves. The interaction between the incident light and molecular vibrations is called Raman scattering. In contrast to Rayleigh scattering, both Brillouin and Raman scatterings are associated with frequency shifts and thus characterised as inelastic scatterings. If scattering is shifted down to lower frequencies, it is called Stokes components. Otherwise, in the case of upshifted frequencies, it is called anti-Stokes (Boyd, 2008; Santos and Farahi, 2014).

In addition to the classification made previously, a further distinction is made between spontaneous and stimulated scattering. While for the former, the optical properties of the medium do not change during the process, for the latter they are altered by interaction with the incident light.

---

[3] λ = wavelength of the propagating wave.
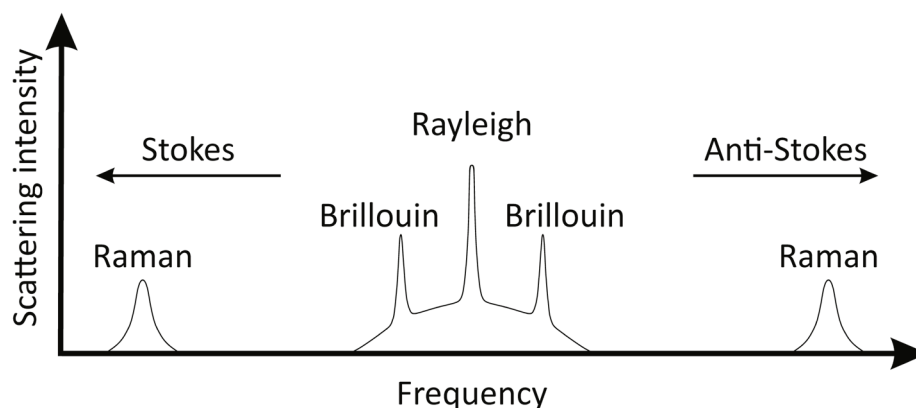
Figure 2.6: Typical spontaneous light scattering spectrum

(adapted from (Santos and Farahi, 2014)*).*

All mentioned scattering processes are useful in distributed fibre optic sensing and have been widely used and examined. For diverse applications, various sensors were to be developed and applied. For instance, Raman scattering highly depends on a fibre's temperature which has been investigated thoroughly in order to develop various techniques for different applications and areas (Abalde-Cela *et al.*, 2010; Delepine-Lesoille *et al.*, 2010; Oakley *et al.*, 2011). In contrast, Brillouin scattering depends on the fibre density and has been exploited in Brillouin based DOFS (Matta *et al.*, 2008; Motil, Bergman and Tur, 2016).

In the course of the pilot project, a coherent Rayleigh based DOFS has been applied. Thus, the basic principle of such a system is described in the next sub-chapter.

2.3 Distributed optical fibre sensing based on Rayleigh backscattering

2.3.1 Rayleigh scattering

In a perfectly homogenous medium without imperfections and impurities scattering would never occur. Hence, because there are no minuscule particles present that the incident light can interact with, only a forward propagating wave would be observed. Therefore, scattering is characterised by optical properties intrinsic to the scattering medium where upon Rayleigh scattering is typically related to the refractive index of fluctuations resulting from density and compositional inhomogeneities that are frozen into the structure of the fibre during the fibre fabrication when the temperature cools from glass softening temperature to room temperature (Agrawal, 2006).

In the case of Rayleigh scattering, which is characterised as elastic and linear scattering, the frequency of the scattered light is the same as that of the incident pulse. The main losses in an optical fibre are caused by the effect of Rayleigh scattering. While the direction of a photon may change during the scattering process, its energy is conserved. The reason for this type of scattering is caused by the scattering of light from particles of refractive index fluctuations much smaller than the optical wavelength. Therefore, there is a strong relationship between scattering wavelength and scattering intensity which is proportional to $1/\lambda^4$. According to that, the wavelength dependence results in a greater scattering amount for shorter wavelengths and consequently in larger losses for shorter wavelengths. Scattering intensity can be determined by considering a particular optical fibre length over which scattering occurs. A coupled light pulse travels along a fibre because of the total internal reflection at the core (refractive index n_o) cladding (n_1) boundary primarily in two main directions: forward down the fibre and backward towards the light source as shown in Figure 2.7. Forward Rayleigh scattered light is transmitted along with the input light, while the Rayleigh backscattered light forms the basis of operation for optical time-domain reflectometry (OTDR) as discussed in detail below (Agrawal, 2006).
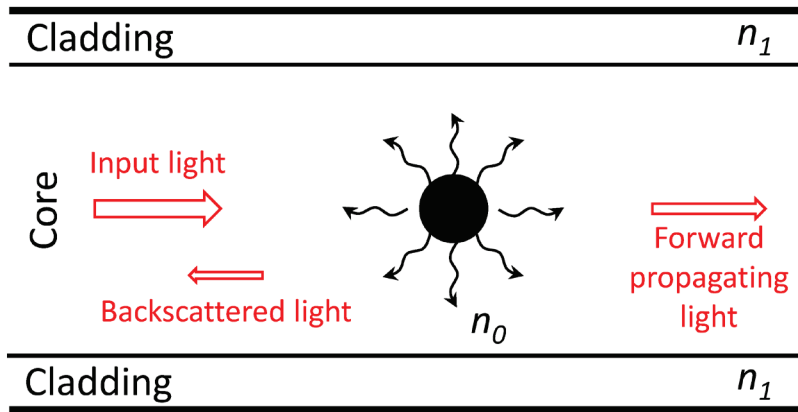
Figure 2.7: Schematic diagram of spontaneous Rayleigh scattering.

2.3.2   Optical time-domain reflectometry

The basic technology of all DOFS can be found in the development of optical time-domain reflectometry (OTDR). Barnoski and Jensen (Barnoski and Jensen, 1976; Barnoski *et al.*, 1977) proposed it for the first time in the late 1970s and demonstrated its ability for detecting malfunctions and faults in optical fibres. Nowadays, it is mainly used for monitoring the health of communication links and newly installed optical fibres.

Typically, an OTDR instrument launches a series of short high-power probe pulses (P_0) into the fibre under test (FUT) and the Rayleigh backscattered signal (P_B) is detected as a function of return time at the input end of the fibre (Figure 2.8). The distance *z* along the fibre can be calculated as follows:

$$z = \frac{c}{2n}t = \frac{v_g}{2}t$$

EQ 2.4

where v_g is the group velocity in the fibre and *t* the backscattered detection time.

The factor of 2 means a two-way propagation of the input pulse as it has to travel its way back to the launching end where a photodetector collects and converts the backscattered signal to an electrical current that is amplified and digitised. The data averaged over multiple probe

pulses is displayed on an optical power versus distance from the launching point plot as shown in Figure 2.8.
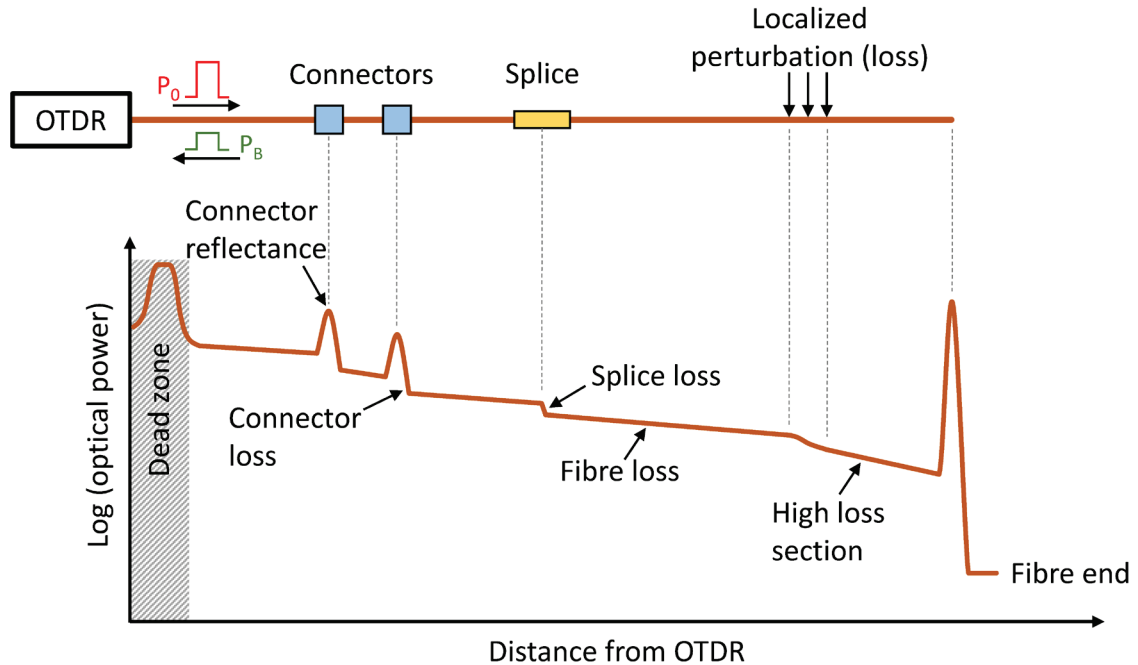
Figure 2.8: Schematic diagram of an OTDR trace output
(adapted from (Udd and Spillman Jr., 2011; Hartog, 2017)*).*

At the beginning of the OTDR, the high-power pulse may overload the instrument's receiver leading to strong back reflections of the signal and finally resulting in so-called event dead zones where no reliable measurements can be made. The minimum distance between the point where the signal enters the fibre and after which a signal reaches a normal backscattering level (~0.5 dB) is considered as the dead zone. Additionally, both peaks at the beginning and end of the optical fibre allow for the determination of the absolute fibre length. The strong spikes as shown in Figure 2.8 are caused by reflections and the slope of the straight lines is a measure of the fibre loss and thus the re-captured Rayleigh backscatter. Any abrupt change indicates a point loss, caused by a poor splice for instance (Santos and Farahi, 2014; Hartog, 2017).

Spatial resolution and measurement range are two important parameters that highly influence the performance of DOFSs. The maximum measuring length of the sensing fibre is called the measurement range and is related to the pulse repetition rate. An interrogation unit must wait until one pulse has travelled from the beginning of the fibre to its end, and until its backscatter

has returned to pulse entry. After that time the interrogator can send the next pulse. The spatial resolution is the minimum distinguishable distance between two sensing points along the fibre. Consequently, it is a function of the pulse duration corresponding to a distance:

$$\Delta z = \frac{v_g}{2} \tau \qquad\qquad EQ\ 2.5$$

where τ is the pulse duration. A backscattered pulse can only be distinguishable as long as the time between two pulses is longer than $\tau/2$. Otherwise, the backscattered pulses would overlap. EQ 2.5 shows that narrower pulses lead to a better spatial resolution. However, narrower optical pulses are received with lower optical power and result in shorter sensing distances. A pulse duration of 10 ns and a fibre group refractive index of 1.5 corresponds to a 1 m spatial resolution (Laferrière *et al.*, 2007).

In conclusion, in any OTDR system Rayleigh backscatter is the main scattering process.

2.3.2.1 *Coherent optical time-domain reflectometry – COTDR*

A traditional OTDR system uses an incoherent light source ending in a signal with a smooth trace. The progress in both laser technology and science, as well as the shift from multimode to single-mode fibre, led to lasers with narrower linewidth which have been applied to traditional OTDR systems. The exploration of coherent detection extended the range of OTD (Healey and Malyon, 1982; Healey *et al.*, 1984) and is realised by the optical mixing of the backscattered light and reference light. Healey (Healey, 1984) proved that light sources with better coherence could lead to a degradation of OTDR measurements. Instead of a smoothed line as shown in Figure 2.8, a rather jagged signal shape is obtained. What initially was considered as a nuisance (Izumita *et al.*, 1992, 1997), has later been proven to be the phase response of the Rayleigh backscattered light and in contrast to other methods, coherent backscatter cannot be averaged out (Shimizu, Horiguchi and Koyamada, 1992) because it arises from random effects. As the phase of coherent incident light is consistent for all the dipoles within a resolution cell so it is for scattered light also. As a result, the scattered light consists of the summation of electric fields that have a stable and random phase relationship. It was Dakin and Lamb (Lamb and Dakin, 1990) and later Taylor

and Lee (Taylor and Lee, 1993) who discovered the applicability of Rayleigh backscatter for distributed disturbance measurements. The practical demonstration of the sensitivity of backscatter intensity in COTDR followed in 1994 (Juškaitis *et al.*, 1994).

Digression – Coherence of light

The coherence of light is one of the most important light properties. If the phases of a light source at different locations or times have a fixed relationship, such light is considered as coherent. Hence, the correlation of the phase at different points (either time or distance) quantifies the degree of coherence and corresponds to temporal and spatial coherence. Consequently, there is a strong relationship between coherence and the spectral width of a light source; the narrower the optical spectrum the higher the coherence.

"Coherent light or light waves: Light where all parameters are predictable and correlated at any point into time or space, particularly over an area perpendicular to the direction of propagation or over time at particular point in space" (Tricker, 2002)*.*

2.4 Distributed acoustic/vibration sensing – DAS/DVS

While the effects of coherence are unwanted in conventional OTDR, Rayleigh-based distributed vibration sensors exploit exactly these effects. The phase of the incident light consistent for using a coherent probe changes the character of the Rayleigh backscatter and becomes extremely sensitive to temperature and strain. Thus, two types of DOFS based on Rayleigh scattering were developed: 1) dynamic strain and 2) static strain and temperature sensing. For the latter, data are collected at fine intervals of the source frequency due to a wide range frequency variation of the probe pulse. Hence, the pattern of the backscattered signal is processed as a function of probe frequency. In the case of dynamic sensing, the DOFS collects fast changes of the measurand due to dynamic variations of strain which are collected as a function of position along a fibre. This provides a distributed sensor detecting mechanical vibrations. In contrast to static strain and temperature sensing, the frequency of the probe pulse stays constant in case of vibration measurements. The connection between time and distance along the fibre is determined by the speed of light *c*, which is modified due to two conditions: 1) a two-way propagation of the light and 2) the group refractive index of the medium N_g.

Therefore, the longest that a fibre can be measured at a certain pulse repetition rate f_R can be calculated as follows (Liokumovich *et al.*, 2015; Hartog, 2017):

$$L_{max} \; = \; \frac{1}{f_R} \, \frac{c}{2N_g}.$$

EQ 2.6

Furthermore, the highest frequency that can be detected in the measurand is dictated by Nyquist frequency *f_R/2* (Shannon, 1949).

Distributed Acoustic Sensors are mainly used in applications when a long observation time is required and an indication of vibrational energy at each location is sufficient. Fields of application include 1) seismic monitoring; 2) security perimeter and pipeline surveillance; 3) energy cables; 4) production and integrity applications in boreholes and 5) transportation.

Active seismic monitoring applications include surface seismic acquisition (Lumley, 2001) and borehole seismic surveying (Martinez Pereira and Jones, 2010). Approaches using DAS for security purposes were reported by (Taylor and Lee, 1993; Park and Taylor, 2003; Owen, Duckworth and Worsley, 2012; Qin, Chen and Bao, 2012; Wu *et al.*, 2015). Wuttke (Wuttke, Krummrich and Rösch, 2003) proposed a methodology to utilise DAS as a reporting tool for vibration sensing in aerial fibres caused by wind. A promising application for DAS represents, for example, assuring the integrity of the well of boreholes by detecting sanding during production (Mullens, Lees and Duvivier, 2010). The brief overview, however, outlines the wide range of applications distributed sensors can be applied for. This also holds true for the transportation sector where DAS has been proposed as a means of monitoring traffic on highways (Crickmore and Hill, 2007) or railway tracks (Peng *et al.*, 2014; Wiesmeyr *et al.*, 2018).

Based on the papers published and research carried out, DAS has not been used for condition monitoring of railway infrastructure. Indeed, fibre optic strain sensing cables have been utilised to detect strain changes due to rail deformations. However, these fibres were laid specifically for this purpose in an experimental layout (Lienhart *et al.*, 2016).

3   SENSING PROPERTIES AND SIGNAL CHARACTERISTICS

3.1   Applied Technology

To understand how DAS works for condition monitoring of linear assets, the components of the applied system must first be described. In the course of the project, two OptaSense linear asset OLA 2.1-5000 interrogator units (IU) were installed in the telecommunication room in Münsingen. The deployed system comprises four main elements; an interrogator unit, a processing unit (PU), a control unit (CU) and a single-mode optical fibre.

The IU is the mandatory item in the system architecture and is not subject to any changes or model variations. DAS detects all events that occur on or next to an asset. Consequently, the technology has so far been used primarily as an around-the-clock monitoring and situation awareness system for critical assets and sites in the oil and gas industry, as well as in the transportation sector for rail or road traffic monitoring. Furthermore, additional aspects such as perimeter surveillance or border monitoring and protection are increasingly gaining in importance (Owen, Duckworth and Worsley, 2012). In theory, the IU is capable of monitoring linear assets with an extension of up to 50 km. The minimum sampling rate of the system is 1 kiloHertz (kHz) and can be gradually increased up to 20 kHz, although it was 2.5 kHz (2,500 samples per second) in the course of the project. The same applies to the spatial resolution; starting with a rather rough resolution of 20 m the system is able to operate with a resolution of 7.5 m. This corresponds to a segment length or "channel" of 7.5 m. Each channel or segment length corresponds to a spatial resolution. The nomenclature "channel" is adopted and will be used in the further course of the thesis. However, within the project, a spatial resolution of 10 m was chosen. In conclusion, considering all the theoretical sensing capabilities of the system, a 1,000 m optical fibre with a resolution of 10 m leads to 100 channels. As well as the resolution, the maximum number of channels that an IU can process is also limited by 5,000 channels (OLA 2.1-*5000*). If the events were sampled at a rate of 2.5 kHz, then the IU will deliver an averaged intensity over the chosen section length for each time sample and channel.

As already stated in Chapter 2.4, DAS relies on the natural effect of Rayleigh scattering caused by the reflection of light at minuscule impurities present in an optical fibre. Such a scattering process shows the lowest attenuation at a wavelength of 1,550 nm (cf. Figure 2.4) which also is

the operating wavelength of the IU. Based on the OTDR technology (cf. Chapter 2.3.2) the system utilises COTDR and processes the backscattered signal as already discussed. The data gathered by the IU is passed further to the processing unit (PU) where it is interpreted and converted for visual representation, which will be presented in Chapter 5.1. The PU is co-located with the IU and utilises a software specially designed for analysing this type of data. A control unit (CU), similar in size and performance requirements to an industrial personnel computer (PC), is used to monitor the system. The PC provides user access to the control unit where one has control of the system's settings in case of malfunctions or necessary adjustments. Neither the IU nor the PU has internal memory. Thus, they are not able to store the recorded data. This can only be accomplished via the computer itself and several external hard disks. The sensitive element within the architecture is a conventional single-mode optical fibre, which is already deployed alongside the track. Over 9,000 km of fibre-optic cables have now been laid in the SBB network (SBB, 2020) connecting the individual stations.

Two DAS systems are installed in the telecommunications room in *Münsingen* (Figure 3.1). The IU OPS1 unit runs along the *Münsingen–Bern* route and records events there on a total of 1,440 channels. The route section between *Münsingen–Thun–Spiez* is monitored with the interrogator unit OPS0 on a total of 2,724 channels. Considering a 10 m spatial resolution the total length of the optical fibre between *Bern* and *Spiez* is 41.640 km at which the track length from *Bern* to *Spiez* is 39.080 km. The discrepancy of 2.560 km is due to both cable routing and track layout. Firstly, an optical fibre is not always routed parallel to the track, crosses the track or, for example, leads into railway station buildings and runs parallel to the track again afterwards. Secondly, fibre optic cables are wound at certain intervals to have reserves in case of defects in the fibre. This obviates the need for a complete replacement and reinstallation of the fibre in such case.

Usually, a map window as depicted in Figure 3.1 displays the train stations as well as the real-time train traffic and fibre route and track layout. The automatic detection of train movements is already implemented in the system and works very well. Figure 3.1 on the left highlights three trains present on the track. The first one travels between *Ostermundigen* and *Gümligen*, the second between *Gümligen* and *Rubigen* and the third is approaching *Münsingen station*. On the right-hand side in Figure 3.1 four trains are visible whereby one has arrived in *Thun station*. In

addition to train detection, an algorithm for detecting people/animals on the track has already been implemented but was switched off within this figure.
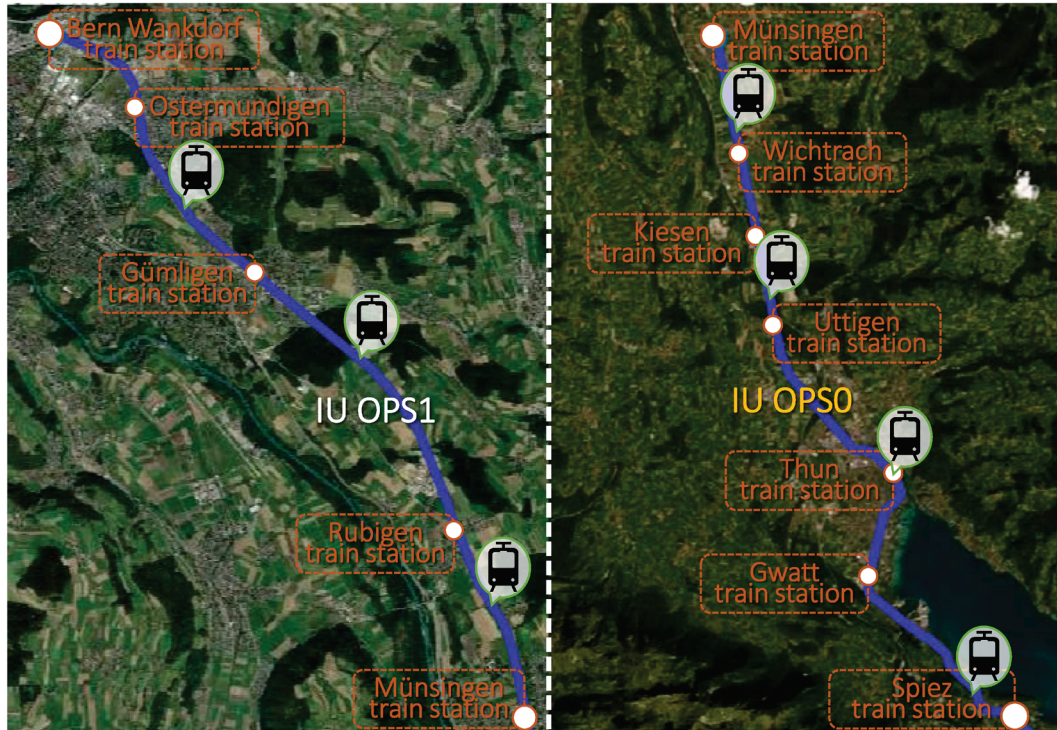
Figure 3.1: Adapted map window displaying fibre route, track layout and real-time train traffic.

However, there are two circumstances to consider here: 1) automatic pattern recognition was not yet mature enough for distinguishing between people and animals. 2) The system produced false-positive alarms. Consequently, the system often triggers an alarm due to the detection of vibrations and sound. These two points are currently being intensively analysed by both suppliers and customers. The aim is to develop an algorithm that can distinguish between people and animals on the track and thus reduce the number of false positives. Furthermore, it is of immense importance that the system can recognise the location of the sound source and thus enable an unambiguous track identification. A considerable amount of R&D is also currently being carried out in this area and work is underway to remedy this problem. The OLA generation is a qualitative sensing system operating in an intensity mode only. The implications and constraints of this technology are discussed in detail in the following chapters as well as the benefits of newly developed quantitative systems. In the concluding Chapter 9, a section is devoted to the latter.

Note that the deployed sensing technology is a qualitative system and relative measurement showing the amount of intensity to a predetermined reference measurement. Such relative units of measurements are always expressed in arbitrary units (a.u.).

Due to the sensing properties of the deployed system, there are only limited possibilities to draw accurate conclusions regarding the amplitude of the measured signal. In such a system, coherent detection is realised by optical mixing of the backscattered light and the reference light. Furthermore, one must be aware that a phenomenon called *fading* is ubiquitous in the field of DFOS characterised by a random attenuation of the signal. The received backscatter is the sum of all the signals and when they interfere with each other and are out of phase, the fading phenomenon appears. Such a phenomenon may lead to a temporary failure or dead detection zones (Hartog, 2017). This is especially true for COTDR. In contrast, phase-sensitive OTDR enables direct detection of both amplitude and phase with limited fading occurrence only and high performance (Juarez and Taylor, 2005). The advantages and shortcomings of both technologies will be discussed thoroughly in chapters 8 and 9.

3.2 Signal characteristics/pattern over the whole distance

As shown, OTDR is mainly used for both performance and health monitoring and the identification of fibre losses of network infrastructures. Thereby, the system itself and the optical fibre can be optimised for further operation. However, the scope of this thesis is neither the development/optimisation of an OTDR system nor the identification of fibre losses, but rather an examination of the system for its application as additional railway infrastructure condition monitoring technology and to which extent it is able to contribute to sustainable railway asset management.

In theory, in Rayleigh scattering based systems the backscattered intensity and signal characteristic changes mainly due to external perturbations. In terms of railways, the altered backscatter of optical fibres deployed alongside railway tracks rises primarily due to train movements, third party intrusion and natural events or disasters. Even though the latter two are of considerable importance for railway operations, they are of minor interest in asset condition monitoring and thus for this work. Hence, this subchapter is dedicated to signal analysis and its variation caused by train movements. The question arises whether the altered

backscatter shows the same signal pattern along the optical fibre or rather changes due to local conditions/boundaries and/or train movements. Naturally, minor changes in the signal pattern along the fibre are to be expected due to fibre properties (see also section 2.3.1 of Chapter 2), but it is necessary to analyse to what extent this takes place and what the reason for it is. To address this issue, Figure 3.2 illustrates 60 seconds of the raw signal of five channels recorded with interrogator unit 1. These five channels were randomly selected from a segment of 100 consecutive channels representing a one km long track section. The x-axis represents the time in seconds, at which the y-axis represents the intensity of the backscattered signal in arbitrary unit (a.u). The train depicted moves from the right to the left and crosses channel 300 (grey) first and channel 399 (turquoise) last. As illustrated, the signal pattern of each channel changes immediately as the train approaches the specific point and alters the backscatter significantly. The dot-dashed lines represent the mean value for each specific channel. Although a certain jagged shape appears in each channel, caused by both the travelling train and the local conditions, the peaks, as well as the mean values, differ from each other enormously. While channel 375 shows the most distinct signal pattern and the highest peak dispersion, it also has the second-lowest mean value (dot-dashed line). Some statistical values for each channel are depicted in Table 3.1.
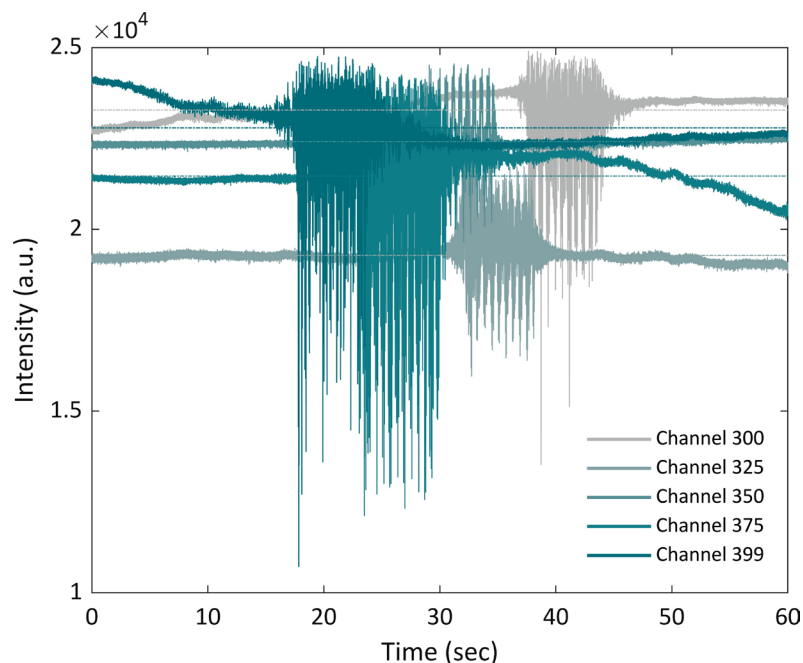
Figure 3.2: Rayleigh backscatter of the same train movement

in 5 consecutive channels distributed equidistantly.

	Raw signal				
	300	325	350	375	399
Min (a.u.)	13,518	15,949	19,649	12,111	10,709
Max (a.u.)	24,915	23,556	24,561	24,473	24,768
Mean (a.u.)	23,281	19,283	22,411	21,465	22,791
SD[4] (a.u.)	474	354	317	796	688

Table 3.1: Statistical values of the measurement as a train passes through channels 300, 325, 350, 375 and 399.

On the contrary, channel 300 has not only the highest mean value but also shows a significant scattering pattern. Furthermore, the levels of the unaffected signals, i.e. before and after the train approaches a certain point, differ significantly for each channel. This also results in notably varying means. A respective correlation between all channels is unambiguous even though differing signal patterns are observed.

Such differences as displayed above arise due to various reasons. An example of categorising the different factors and impacts on the signal can be as follows:

The location, position and the type of fixation of the optical fibre certainly influence the sensing properties as well as the fibre's properties. While these parameters are closely linked to the fibre itself, further ones are assigned to both infrastructure and trains. In the case of the latter to be more specific, a train's wheel condition, the train composition, loading status and speed certainly influence the backscattered intensity and therefore affect the signal pattern too. In the case of infrastructure, its condition, superstructure and substructure certainly have an impact on the signal. Further factors regarding the signal characteristics emerge due to random effects (phase in the sinus wave) and sensor effects (especially sensor noise).

From the results above, two further issues are identified to be covered in this work, because they are decisive for condition monitoring and asset management. The signal pattern changes from channel to channel, this is evident, but may remain stable within a channel and for the same train composition. Hence, the signal should show the same properties and behaviour in the same position where the time difference between the two train journeys differs slightly.

---

[4] SD = standard deviation.

What seems indeed highly theoretical at a first glance, is proved by the results depicted in Figure 3.3. The raw backscatter for the same train composition obtained at three random channels where the time difference between the two train rides is one hour reveals a completely different behaviour even though the speed at all three locations is almost equal.

The comparative analysis reveals a completely different scattering process taking place in all channels displayed in Figure 3.3. While the pattern seems to correlate for at least both train rides in the same train composition in the respective channel, it differs among the channels significantly even though the travelling speeds do not vary much. The scatterings taking place in Figure 3.3a are almost congruent for both trains having a similar impact on the signal. The same applies, in diluted form also to the train journeys in Figure 3.3b and Figure 3.3c, regardless of the contrasting signal pattern between the channels.

| (a)   Channel 300 | (b)   Channel 325 | (c)   Channel 350 |
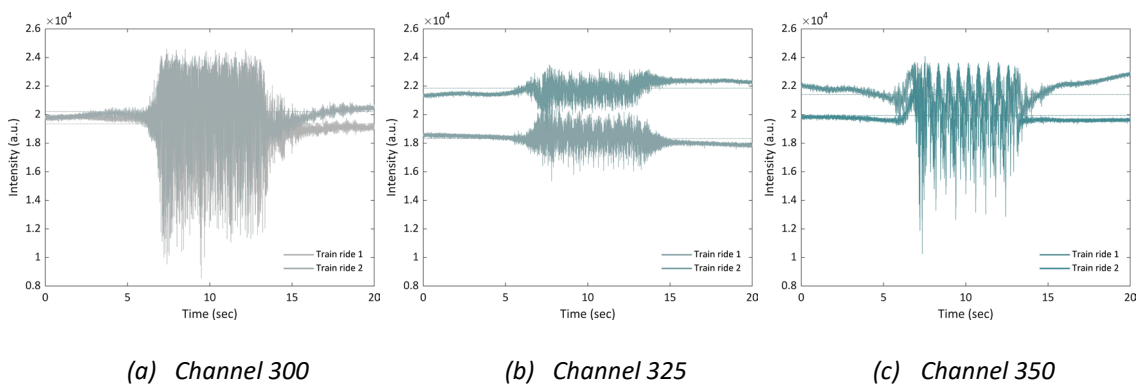
Figure 3.3: Rayleigh backscatter of two train rides in the same train composition

on the same day in different channels or rather at different locations

	Raw signal					
	Train ride 1			Train ride 2		
	300	325	350	300	325	350
Min (a.u.)	8,546	15,346	10,245	9,521	18,949	11,869
Max (a.u.)	24,299	20,910	23,683	24,578	23,491	24,093
Mean (a.u.)	19,355	18,316	21,407	20,206	21,845	19,930
SD (a.u.)	1,496	509	1,392	1,344	525	1,128

Table 3.2: Statistical values of the measurement as two trains in the same composition pass

through channels 300, 325, and 350 on the same day.

Nevertheless, railway infrastructure is subject to wear and tear and deteriorates more or less rapidly over time. Consequently, if the scattering is an indicator of the current condition, the pattern shall change after a certain time. The upcoming three figures show the backscattered intensity for 1.5 years of train rides in a specific train composition. The measurement data given are unadjusted and raw. In other words, this implies that the measurements have been checked neither for plausibility nor for outliers, and thus may also include incorrect measurements due to a malfunctioning measurement system. The first recording started in October 2017 (measurement M1), the last one took place in April 2019 (measurement M34). Details on the recording routine can be found later in Chapter 4.3.

It is evident that the signal changes at all three locations over the particular time, but the causes remain equivocal. The most considerable change is observed in channel 300 (i.e. Figure 3.4) whereby the signal scatters similarly for the first 17 measurements (M1-M17, Figure 3.4a). The subsequent measurements show a much more prominent scattering pattern, which is particularly reflected in the peak values and a noticeable jagged shape (Figure 3.4b).

(a) *(b)*
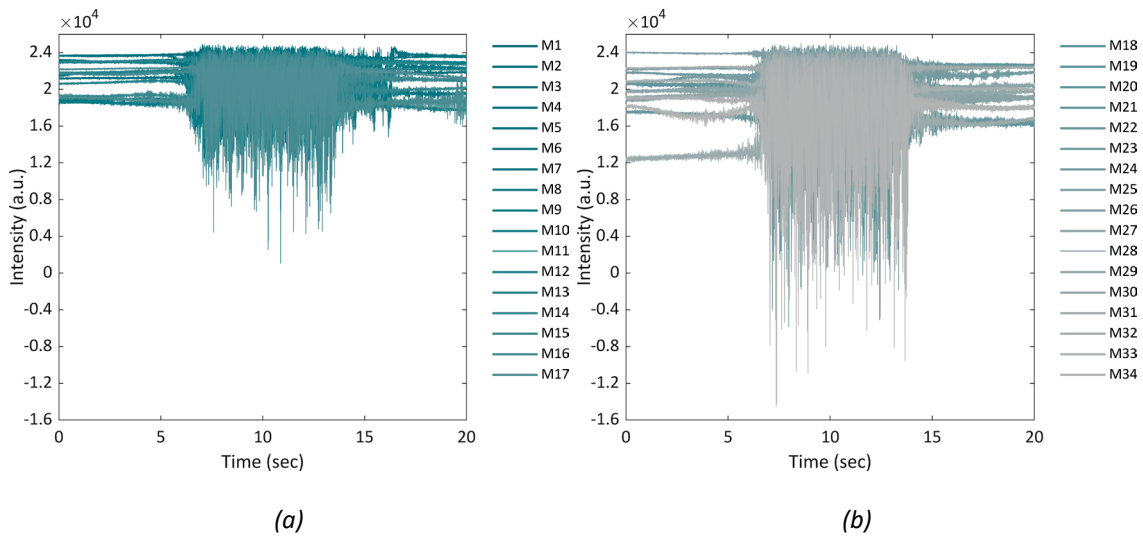
Figure 3.4: Time series of Rayleigh backscatter caused by train rides in channel 300.

The formerly considerably changing scattering pattern does not appear in channel 325 (see Figure 3.5), in particular. Especially the latest measurements in Figure 3.5b show a pattern without a distinctive scattering appearance. Contrastingly, in Figure 3.5b one measurement deviates from the others showing a diverging signal pattern.

(a)   *(b)*
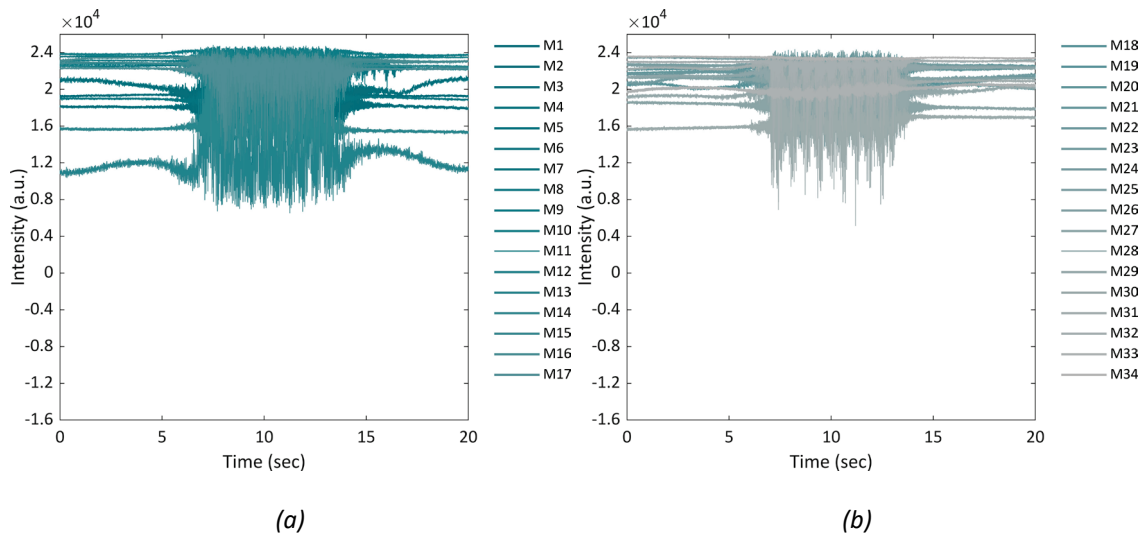
Figure 3.5: Time series of Rayleigh backscatter caused by train rides in channel 325.

While the train rides in channel 350 displayed in Figure 3.6a have a similar impact on the backscattered intensity it changes for at least one measurement in Figure 3.6b. Thereby one train journey influences the signal occurrence significantly, resulting in a characteristic scattering pattern and a high peak dispersion.

(a)   *(b)*
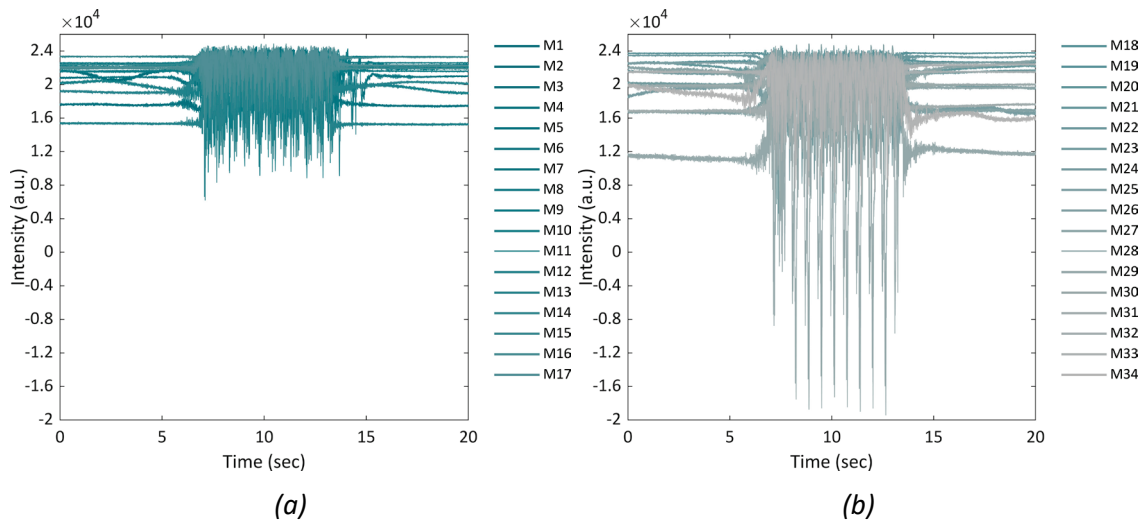
Figure 3.6: Time series of Rayleigh backscatter caused by train rides in channel 350.

The anomalies in the time series analyses mentioned may occur due to the various circumstances discussed before but and at least for one measurement, a system malfunction is assumed.

The results have shown that approaching trains, regardless of type, composition, speed and condition, have an immediate impact on the scattering process taking place in the fibre resulting in a changed signal pattern in the time-domain. The uncertainties with regard to the significance of the raw signal nevertheless remain for the stated reasons (e.g. *fading*, see previous subchapter). To determine whether the frequency response of the signal is also changing due to the impact of a train, spectrograms are generated for result visualisation. In general, a spectrogram is an intensity plot of the Short-Time Fourier Transform (STFT). In basic terms, this is a histogram in a power-frequency space where a specific frequency appears brighter and "hotter" for as long as it persists in the signal while the signal is evolving. Based on the Nyquist Theorem (Shannon, 1949) the sampling rate of a signal must be at least two times the highest analogue frequency component. The utilised system has a sampling rate of 2,500 samples per second, which means that the highest detectable frequency is 1.25 kHz. Such spectrograms are shown in Figure 3.7 for the first measurement M1 for the same channels given in Figure 3.3. The y-axis represents the frequency of the signal and the x-axis represents the time.

Firstly, frequencies up to approximately 40 Hz are steadily present even without a train movement as is clearly visible and thus frequencies up to 0.04 kHz can be classified as noisy (continuously present over the entire time). This confirms Hartog's statements (Hartog, 2017) that such dynamic sensors measuring rapid changes of the measurand are not able to perform a zero frequency measurement. When a train approaches and passes the specific channel, as displayed in Figure 3.7a between second five and 15, higher frequencies are also present and emerge due to the train's sound and vibrations.

(a) *Channel 300*   (b) *Channel 325*   (c) *Channel 350*
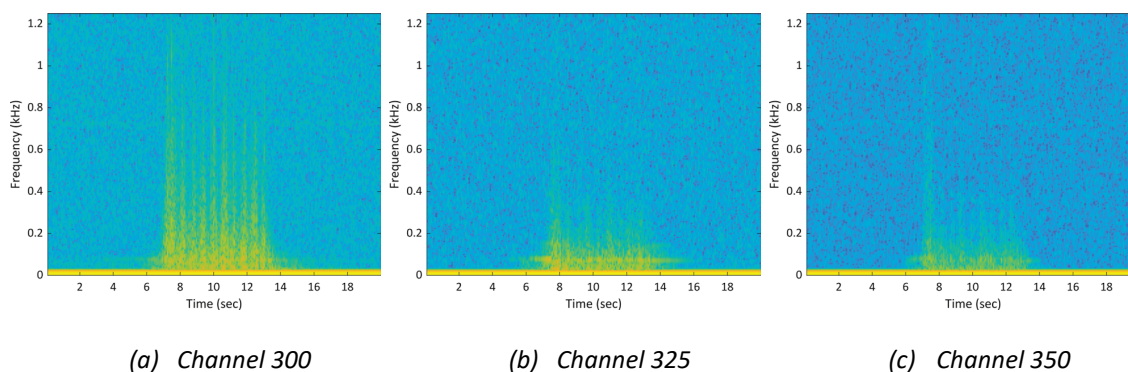
Figure 3.7: Spectrograms of three channels of measurement M1.

Taking a closer look at the frequency spectrum reveals the impact of at least each bogie emphasised by the "yellowish" peaks. On the contrary, even though it is the same train ride, a similar effect cannot be observed for the other channels (see Figure 3.7a & Figure 3.7b) which is startling because some impact is observed in the raw backscattered signal (see Figure 3.5 & Figure 3.6).

Another very interesting result relates to the time-series analyses of the backscattered intensity (see Figure 3.4, Figure 3.5 & Figure 3.6) and the frequency content of the respective channels. The signal seems to be rather more stable in the frequency domain than in the time domain which is underpinned by the results illustrated in Figure 3.8a and Figure 3.8c. These only minor changes in the frequency properties, of course, can occur because of no asset deterioration or due to executed maintenance and therefore an improved condition. However, the signal seems to be more reliable in the frequency domain. The result in Figure 3.8b confirms the previously raised assumption that at least one of the measurements is not fully correct as it shows no frequency response at all (except the continuously present noise up to 0.04 kHz).

(a) Channel 300 *(b) Channel 325* *(c) Channel 350*
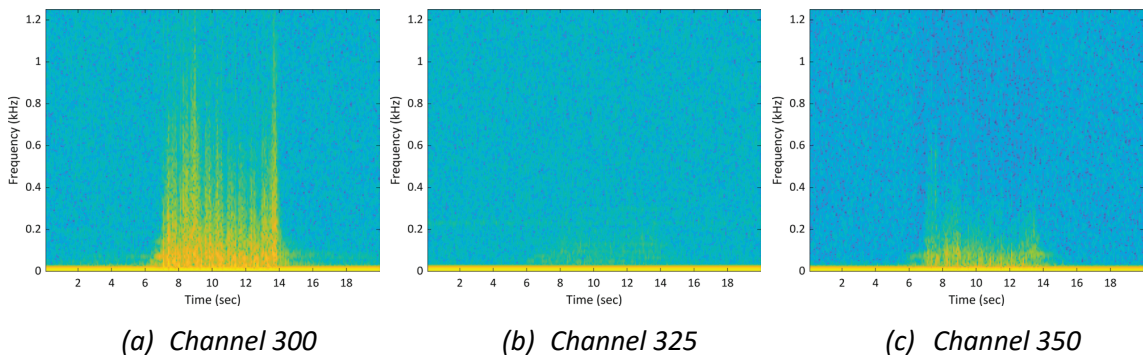
Figure 3.8: Spectrograms of three channels of the last measurement M34.

The results above show that the fibre is highly sensitive to external perturbations leading to significantly different scatterings taking place within the cable. This shows that it is of crucial importance to know the root cause of the changed scattering processes and where they occurred along the track. Therefore, the identification of the optical fibre cable layout and its link to the track is mandatory.

3.3 Identification of cable layout and linking to track

Generally, optical fibres are deployed in bundles together in combination with other cables within cable conduits alongside railway tracks. An overview of the cable duct location provides SBB's *DfA (Datenbank fester Anlagen, database for fixed installations)*. In this database, which is more like a data warehouse, all track related assets are documented. For instance, it provides information about track ID, superstructure and position and location of the asset. Chapter 4.1 gives a more detailed review of the content and data of this database.

The map window illustrated in Figure 3.1 is sufficiently accurate for a general view for both the layout of the optical fibre and track, as well as for a visualisation of the actual traffic. Yet, when it comes to in-depth signal analyses as shown in the results previously, knowledge about the exact fibre and track layout is decisive. This is not only because both track and cable layout vary but also due to divergence in the length of fibre and track. As already noted, the difference in length is more than 2.5 km, the over-length being on the fibre side. The points where excess lengths occur must be identified and subsequently taken into account in the analyses. DAS is a truly intrinsic distributed measurement technology where light beam never leaves the fibre and is divided into equidistant measurement points. The measurement takes place in the fibre itself, therefore the fibre length and the position of the fibre are significant. Sections with unclear fibre path must be identified and documented. Otherwise, this can lead to incorrect results interpretations and subsequently result in erroneous conclusions regarding the applicability of the system for railway condition monitoring and asset management.
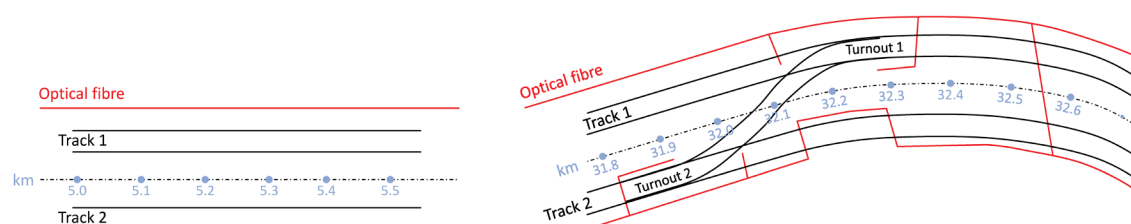
Figure 3.9: Schematic layout of track and optical fibre.

For the predominant part, the concrete duct protecting the cables inside is located on the left or right side, parallel to the track as shown in Figure 3.9 on the left. This represents the ideal case, as the fibre runs parallel to the railway track and is at a constant distance from the track. Railways tracks are linear structures with both straight sections and sharp curves with very short

radii and this may change the distance between the conduit as well as its routing. Furthermore, components such as rails, sleepers, ballast and turnouts are subject to wear and tear and must be maintained in order to obtain a certain track quality. Finally, at the end of their service life, they have to be replaced. For operational reasons, it may be necessary to install new turnouts, construct new stations or install new signalling systems. Each new installation needs power and must be linked to and integrated within existing system architectures. These circumstances may result in the need for new conduit and cable routing affecting the layout of optical fibres. Thus, not only the superstructure changes. The illustration on the right in Figure 3.9 shows a schematic track and fibre layout at which the fibre's layout is not unambiguous. While one optical fibre runs on the left side of track 1 another one is deployed next to track 2 on the right. The FUT and its layout must be identified for any application or testing that DAS is used for.

It may also be the case that previous cable lines have not been dismantled or a cable even changes trackside for various reasons resulting in extra cable lengths. All these circumstances highlight why it is vital to identify the exact cable layout that has been carried out in a first step. The route was followed at neuralgic points, such as stations, locations with spools and bridges, resulting in a rough estimate of the fibre location. These points, also called calibration points, where the fibre makes a significant change in both routing and position and length compared to the track, were stationed, documented and referenced by GPS using longitude and latitude data. While 19 calibration points were referenced for the track section between *Bern–Münsingen*, there were 32 calibration points for the section *Münsingen–Spiez*. For the remaining points and fibre lengths, it was interpolated with a spatial resolution of 10 m. This process enables identification of sections to be discarded because of bad signal quality and unfavourable fibre layout. If there is a failure to identify such sections, this may lead to false assumptions and concluding remarks on signal quality, as well as the reason for signal anomalies and faulty measurement.

Many IMs have already deployed optical fibres alongside tracks, predominantly at main routes. In the case of existing lines, fibre optic cables have been laid afterwards in cable ducts when needed for signalling and telecommunication purposes. When laying these cables, it was never intended to apply those cables safety-relevant applications, train tracking or even infrastructure condition monitoring. Since the use of DOFS techniques has become prominent and offers considerable benefits covering wide application areas, it becomes obvious that the current cable position affects the performance of the sensing system. In this context, FOS experts and *Fiber Optic Sensing Association (FOSA)* members have made recommendations for the installation of fibre optic cables utilised for 1) train tracking; 2) train condition monitoring; 3) monitoring of rail defects; 4) natural hazards and 5) trackside works. These recommendations are the culmination of countless projects and provide an overview of the current state of knowledge.

The *cable selection* should be according to the proposed use. In railways, they are often used for communications, fibre optic sensing and railway operations. Therefore, optical fibres should conform to the recommendations of the International Telecommunication Union (ITU) ITU-T G652 or 655. So far, best practice is utilising a standard SMF which are already used for telecommunication whereby the fibre requires a good coupling between the fibre, the cable and consequently the environment. In the case of the railways, the environment refers to the track. DAS systems perform best when operating with wavelengths between 1,540–1,552 nm (c.f. Figure 2.4).

In addition to the cable selection, the *cable position* also highly affects the sensing abilities of DAS systems. For example, too great a distance between the source and the fibre leads to non-detection of certain events, such as people on the track, but may be sufficient for train tracking. Furthermore, the cable route, as well as the possibility of maintaining the system, should be considered.

For *cable deployment,* it shall be considered that on the one hand the fibre is able to detect the event of interest but prevents the fibre as well as possible from unwanted noise sources. On the other hand, the chosen installation method must protect the cable and sensing fibre from accidental or malevolent damage. The best performance is to be expected with a cable directly

buried at a depth between 30–60 cm from the surface and 1–5 m from the centreline of the track. Furthermore, it should be avoided to bury the fibre unprotected in the ballast or the ground. A good sensing performance can be accomplished by deploying the cable in a cable trough, which is also the most common case in railways. A rather poor performance for track condition monitoring is accomplished by fibres mounted on walls or fences. Such installation may be the case for bridges without ballast bed and thus needs to be considered when utilising DAS for condition monitoring of bridges. On the contrary, this deployment method shows good performance when detecting e.g. rock falls. Another method is clipping the fibre to rail foot. This installation type has advantages when monitoring natural hazards but shows rather poor performance for track condition monitoring and train tracking. The proximity of the signal source (vibrations of the train ride) and the sensor (fibre) leads to an increased noise level, causing an immense effort for signal analysis and interpretation.

4   DATA ACQUISITION

As mentioned, this research was part of a pilot project of SBB and OptaSense examining the potential of distributed optical fibre sensing in railways. It is therefore only a matter of fact that some of the results presented here also reflect the results of the pilot project. This chapter will give a brief insight into the characteristics and properties of the monitored track and the conclusive steps of data processing and positioning.

4.1   The monitored route

The section between *Bern–Spiez* was chosen as the pilot route including lines of both SBB and BLS. The total length of the pilot line is 39.080 km, including 29.048 km of SBB's network and 10.032 km of the BLS network. The way matters stand, IMs are not completely oblivious to their assets and their condition. They already have a variety of different databases, applications and tools that can be used to retrieve and document the condition of their assets. In the course of the project, access was granted by SBB to several applications providing a vast amount of information about the track to be monitored. The following will give insight into the ones utilised and the information provided.

The application most used and perhaps the most important is one named *Datenbank der festen Anlagen* (*DfA*). This inventory database stores information on all assets and provides an overview of the current and planned status of the assets. In the case of infrastructure, for example, information can be retrieved about the type of sleepers and rails, their age, radii, cant, type and thickness of ballast, as well as track category and kilometre. For example, 60 % of the installed sleepers are concrete sleepers with an average age of just under 14 years, while a further 30 % are wooden and 10 % steel sleepers with an average age of almost 22 and 39 years, respectively. Furthermore, detailed information about (insulated) rail joints (IRJ) and turnouts can be obtained, which will be examined in detail in Chapter 6.3. This refers only to the vast amount of information available. One way to distinguish turnouts is to refer to their basic form whether if it is a single or a double turnout, representing the majority of turnouts. Further types are special forms such as crossing turnouts or diamond crossings with slips. In the case of the pilot line, the distribution of the turnouts for the main tracks is as shown in Figure 4.1. Almost

87 % of the overall 302 turnouts on the main tracks between *Bern* and *Spiez* are single turnouts, followed by double-crossing turnouts (~12 %) and double turnouts (~2 %). Besides the form of turnouts, another distinction is made based on the curve radius – also referred to as the radius of the branch track. In the case of the single turnouts, the predominant radius of the branch track is 185 m followed by those with 300 m and 500 m. The smallest part is made up by turnouts with a greater branch track radius, whereby only four turnouts with a branch radius of 10,000 m are installed. Regarding the sleeper type, wooden sleepers are the predominant type for turnouts with 185 m branch radius. The average age of these wooden sleeper turnouts is slightly higher than 18 years. In general, the average age of wooden sleepers for all represented turnout forms and branch radii ranges between 15–21 years. A similar picture appears when looking at steel sleepers. These are now rarely installed, but they are the second most common type for single turnouts with a branch track radius of 185 m on the considered route. This is also apparent in the average age ranging from 26–47 years. An opposite scenario emerges when looking at concrete sleepers. A change in the strategy moving from wooden to concrete sleepers can be obtained in the number of installed concrete sleepers and thus the average age of this sleeper and turnout type. The average age here is 3–14 years.
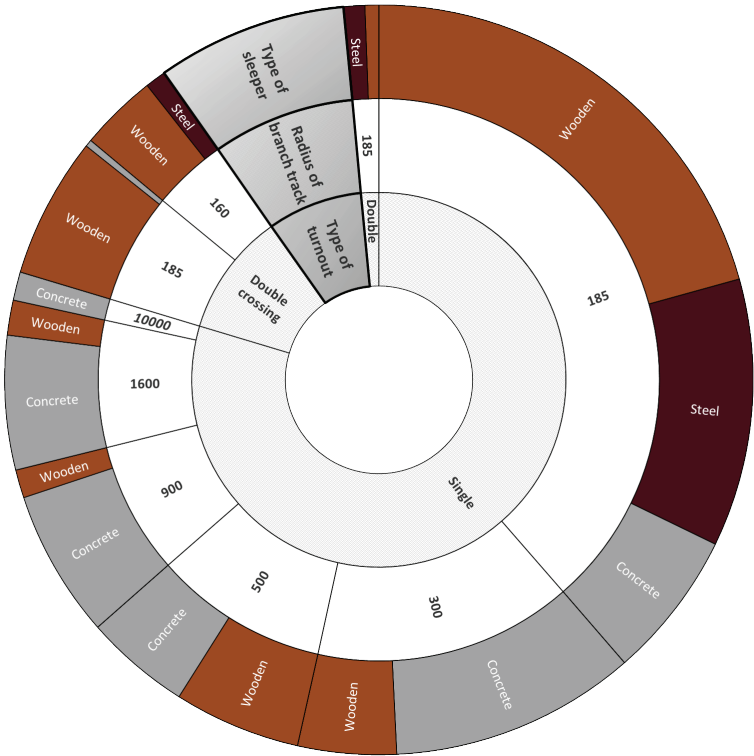
Figure 4.1: Distribution of turnouts from Bern to Spiez.

A second tool named *Anabel (Analyse und Auswertung Belastungsdaten,* analysis and evaluation of stress data*)* enables monitoring of all train paths taken by each vehicle and train individually. Based on this, it is not only possible to calculate the loading of specific tracks but rather to predict and forecast wear and tear of assets and the behaviour of a track in general (Holzfeind, Nerlich and Kull, 2016). Results of a data sample, which is also available[5] freely, as shown in Figure 4.2 enables one, for example, to not only calculate the number of trains that crossed specific stations per year and direction but also to distinguish passenger and freight traffic. With more than 75 % – it is true for both the 2018 and 2019 periods – that passenger traffic accounts for the majority of trains on the entire route from *Bern—Thun* although the train numbers decrease slightly in 2019. As the main part of the route is double-tracked, the loading varies between 84,000–106,000 gross-tonnes (GT) per day and track.
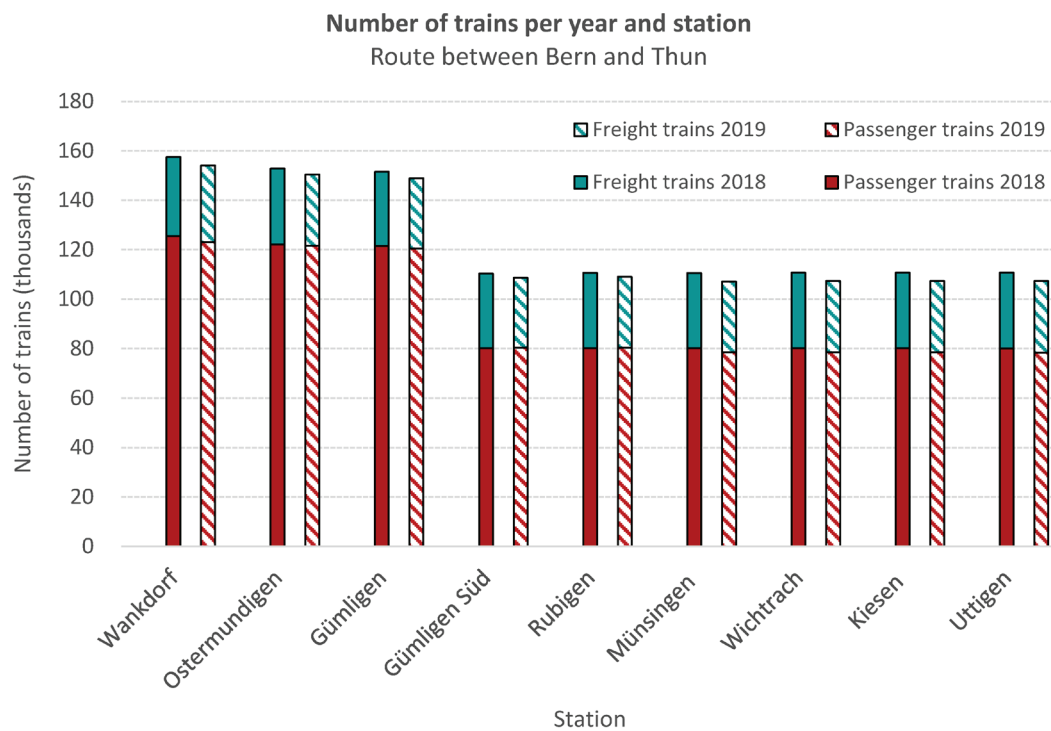
Figure 4.2: Number of trains.

---

[5] https://sbb.opendatasoft.com

While for the first three stations *Wankdorf*, *Ostermundigen* and *Gümligen* the loading per day and track are almost at the same level of 106,000 GT it decreases with every further station resulting in 84,000 gross-tonnes per day and track in *Uttigen*. From *Wankdorf—Gümligen* 55 % of the loading is assigned to passenger and 45 % to freight services. This distribution inverts beginning in *Gümligen Süd* and as of here 49 % of the loading per day and track are assigned to passenger and 51 % to freight services.

The composition of the transport-collective becomes so critical because different traffic types also change the wear and tear of assets due to different vehicle properties (Railway Group Standard, 2019). Higher speed with lower axle loads, usually assigned to passenger traffic, induces more dynamic forces and thus causes more damage to the infrastructure. This impact is described in (ORE, 1987; Railway Group Standard, 2019). For example, the costs of wear and tear of a track due to a train run can be calculated by taking the network-wide costs and dividing this figure by the number of train-kilometres or gross-tonne-kilometres. This approach, currently the most commonly used one, covers the loading of a track as the only parameter shifting maintenance costs from low loaded tracks to high loaded tracks. A somehow more sophisticated approach presented by Marschnig in his postdoctoral thesis "iTAC – innovative Track Access Charges" elaborates not only on various principles of track access charging in general but rather highlights the effect of different approaches which pricing schemes can be based on (Marschnig, 2016).

What appears to be very simple and self-evident is, in reality, a substantial contribution to sustainable asset management. *Anabel* is a key application for the *Swiss track wear factor* implemented in 2017 (Marschnig and Holzfeind, 2013; Holzfeind *et al.*, 2015; Marschnig, 2016). It classifies individual vehicles based on their properties and thus their impact and/or effect on the track deterioration. The vehicle-specific calculation of train path prices results in a costs-by-cause principle leading to both incentives for railway undertakings (RU) to buy and to develop more track-friendly vehicles in the medium to long run.

Further but not less important applications are *ZMON (Zustandsmonitoring,* condition monitoring*)* and *AMGT (Auftragsmanagement,* task management*)*. While in the former, asset condition deviations from the target state are documented and tracked, the latter manages both maintenance work and their costs.

The last tool utilised is *swissTAMP (Track Analysis and Maintenance Planning)*. This application links data from various applications and visualises and analyses the condition of the infrastructure. Further maintenance actions are predicted and planned on this basis (Wilczek *et al.*, 2017).

All these applications and databases provide a countless amount of information about the condition of infrastructure and assets. In Chapter 6 the information on track and turnout condition based on the information from the mentioned sources will be used.

This approach differs significantly compared to other methodologies and is somehow reverse engineering. In contrast to other approaches, here information about already known track failures and defects are taken, analysed and examined to determine whether the signal pattern and characteristic changes because of the different condition or due to other effects. This ensures that, on the one hand, the key issues of asset management are dealt with and, on the other hand, the random detection of signal anomalies is avoided which is a different approach. This includes signal analyses as well as finding pattern and characteristic anomalies. Afterwards, the reason for the changed signal has to be ascertained.

4.2 The process of positioning and stationing

Condition monitoring and sustainable asset management as defined in the introductory remarks require a component-specific condition assessment in a first step. This also makes it necessary that, regardless of the measuring method or technology, a failure pattern or signal anomaly can be assigned to the root cause and thus the component condition can be assessed. Given this, and taking into account the constraints, namely that 1) the spatial resolution is 10 m; 2) the channels are georeferenced and 3) railway lines are however expressed in line kilometres, the following obstacle must be overcome: Occurring signal anomalies due to track failures or rather changing asset conditions shall be assigned to the root cause. In other words, it must be possible to differentiate whether the signal anomaly emerged due to an isolated track defect or a worn-out insulated rail joint for instance. Otherwise, a signal pattern and changes in this would not be assigned to the causative location, which could lead to wrong conclusions. This burden can only be overcome and resolved by linking channel to asset data. This process – in this thesis referred to as *positioning* and *stationing* – takes place in two steps: 1) geo-positioning and linking of fibre

to track including documentation of fibre position as described in Chapter 3.3 and 2) linking of channels to asset data and hence track kilometre. A prerequisite for the latter is a profound asset data-warehouse like SBB's *DfA*. This application provides both information on asset type and position. Utilising this tool and using the available data enables a linking of the asset position such as the starting and ending point of a bridge or turnout with the corresponding channel of the DAS system. As a result, a file of the entire track including track kilometre, asset type and position and the corresponding channel is obtained. This approach is the sole key to conducting condition assessments of specific assets.

It is worth mentioning that the spatial resolution of the system varies now and then. This makes it necessary to carry out track visits and check whether the respective channel was assigned to the track km correctly. Such a process was especially necessary for the assessment of turnouts which will be dealt with in-depth in Chapter 6.3.

4.3 Data processing cycle – the initial stage

In order to start recordings of the pilot line and gathering data, access to the CU and the IUs was granted via a remote desktop connection. As an automated recording start was not possible this process had to be done manually each time a recording had to be started. This may not be a major obstacle during the week and at normal working hours but given that maintenance work is only carried out at night, it is very cumbersome and involves considerable extra work. This issue must be resolved in further product generations and releases. It must be feasible to define a time interval in which the system switches on and measures data. Be that as it may, the aim of the project was not the development of a measuring technology nor is it in the scope of this thesis.

Given the fact that two IUs were installed, gathering data second for second for each channel results in a raw data amount of some 180 GB data in *"*.dat format"*. This is valid for a sampling rate of 2.5 kHz and 4,164 channels but varies, of course, when the sampling rate and the number of channels (fibre length) are changed. The recorded data files are automatically split into 10.2 GB parts and stored in separate folders with time and date stamps. While a 10.2 GB file of IU1 (1,440 channels) contains slightly less than 20 minutes of a recording, a 10.2 GB file of IU0 (2,724 channels) contains about ten minutes of a recording. A two-hour recording is split up into

ten files gathered by IU1 and twelve files from IU0. These are standard settings of the manufacturer and are not changed during the entire project phase. After the recording session, it is necessary to convert the *"*.dat"* files into a readable format using the specific OptaSense DxS browser. For this, the hierarchical data format (HDF5) *"*.hdf5-format"* was chosen since this has proved to be particularly suitable for storage and processing of heterogeneous, large and complex data structures. Furthermore, it can also be processed with Matlab used for further data processing and analysis. After the conversion, approx. 80 GB of data in *"*.hdf5-format"* are created for a two-hour recording. This is still a considerable amount of data, which conventional computers cannot handle immediately making it difficult to analyse the data efficiently.

Based on the amount of data described, a recording interval is selected that generates enough data but keeps the storage requirement within acceptable limits. A measuring interval of one week fulfils these requirements optimally whereupon the entire pilot line was recorded every Thursday between 7 a.m. and 9 a.m. On the one hand, this methodology ensures that the data amount processed is at an acceptable level and on the other side it enables times series analyses because access to the CU was granted for ~1.5 years. Also, all maintenance work is recorded and partially analysed. In order to avoid producing more data, SBB provides the maintenance schedule for the years 2017 and 2018. This ensures that the data is only recorded during the nights when maintenance work takes place. In the period between October 2017 and March 2019, two hours on 33 days were recorded.

5 DATA ANALYSIS & METHODOLOGY

5.1 Waterfall diagram

The most common DAS systems deployed are for monitoring events along linear assets. Those are visualised by using so-called waterfall diagrams as shown in Figure 5.2. In terms of railways, a waterfall diagram is more or less a graphic timetable as depicted in Figure 5.1. Generally, a graphic timetable like the one below visualises scheduled train paths; in this case those ones of route 323 from *Bern–Thun* for the timetable period 2019 (*Offizielles Kursbuch: Grafische Fahrpläne*, 2020). Note that this is only an excerpt of a daily timetable showing all passenger train rides throughout a day. Further information on different timetables can be found in (Walter, 2016) who elaborated on integrated timetables and their link to long term infrastructure development. The timetable referred to shows the train runs of the respective line between 8 a.m. and 9 a.m. at which on the vertical the time is increasing downwards and on the horizontal the space is increasing to the right. In addition to train numbers (for instance Intercity (IC) 959 departing from *Bern (BN)* at 8:04 a.m. and arriving at *Thun (TH)* at 8:22 a.m.) and train types, a timetable highlights station stops, crossings and overtakings, in particular. It should be noted that the trajectories shown are simplified and the speeds during a train ride vary including situational acceleration and braking processes.
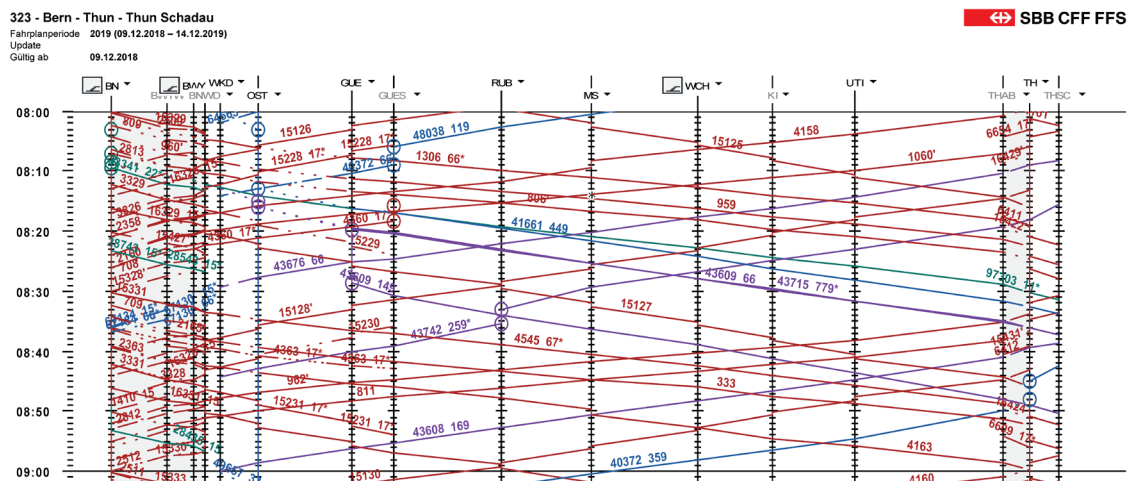
Figure 5.1: Train graphs (excerpt of (Offizielles Kursbuch: Grafische Fahrpläne, 2020)).

The analysis of stored DAS data provides a corresponding situation. In terms of signal analysis, a waterfall diagram is generated by applying a bandpass filter (BPF). For the illustration, in Figure 5.2 the BPF only allows frequencies between 43–201 Hz to pass and rejects the remaining ones.

The diagram in Figure 5.2 shows a one-hour recording of route 323. It is worth mentioning that the monitored track has its start in *Bern Wankdorf (BNWKD)* and ends in *Spiez (SP)*. On the contrary, the respective timetable in Figure 5.1 shows the train traffic from *Bern (BN)* to *Thun (TH)* and *Thun Schadau (THSC)*. This means that the train traffic presented in Figure 5.2 has its start after *Bern (BN)* and ends in *Spiez (SP)* located several kilometres after *Thun (TH)*. The channels plotted on the horizontal increase to the right. While the first 1,440 channels are monitored by IU1 the remaining 2,724 ones are by IU0. The ordinate shows the time increasing upwards. The colour scheme in the waterfall diagram indicates the level of acoustic intensity of an occurring event. While blue represents the noise of the signal or no detected event, the colour red indicates a particularly dominant event on this channel.

The train mentioned previously departs from *Bern Wankdorf* at 8:10 a.m. and arrives at *Thun* at 8:22 a.m. As the signal intensity varies along the monitored track the train trajectories change pattern too. This is due to several reasons: Firstly, the fibre position and location change along the track and therefore the signal intensity too. Secondly, external noise sources have a significant influence on signal characteristics. This is especially true for the section between *Kiesen* and *Uttigen* where a highway runs parallel to the railway track inserting a constant interference noise. Thirdly, previously installed fibres are used whereby no changes were made regarding layout and routing meaning that in *Münsingen* where the interrogator units are located several channels of both IUs overlap. This is why trains seem to travel back in time in this area. Furthermore, utilising previously installed fibres also entails coils of fibres usually used as reserves in case of broken fibres. Such coils lead to discrepancies between optical distance measured in the cable and the true distance a train has travelled in a certain time. This can be seen for example between *Thun* and *Spiez* as the signal of a train ride vanishes in the middle resulting in a total loss of intensity appearing now in blue only. It is worth mentioning that a total of 980 m of fibre optical cables are coiled between *Bern Wankdorf* and *Spiez* and are not considered for further analyses.

Additionally, interruptions in trajectory can also indicate a stop at a station as shown in Figure 5.2. Furthermore, signal patterns vary because of the different train types and travelling speeds. While passenger trains appear as thin trajectories which usually have a higher operating speed like the one of the IC mentioned, those of freight trains are brighter with a lower travelling speed too. Finally, signal patterns and characteristics significantly change because of boundary conditions like the asset condition affecting both the observed intensity and the pattern.
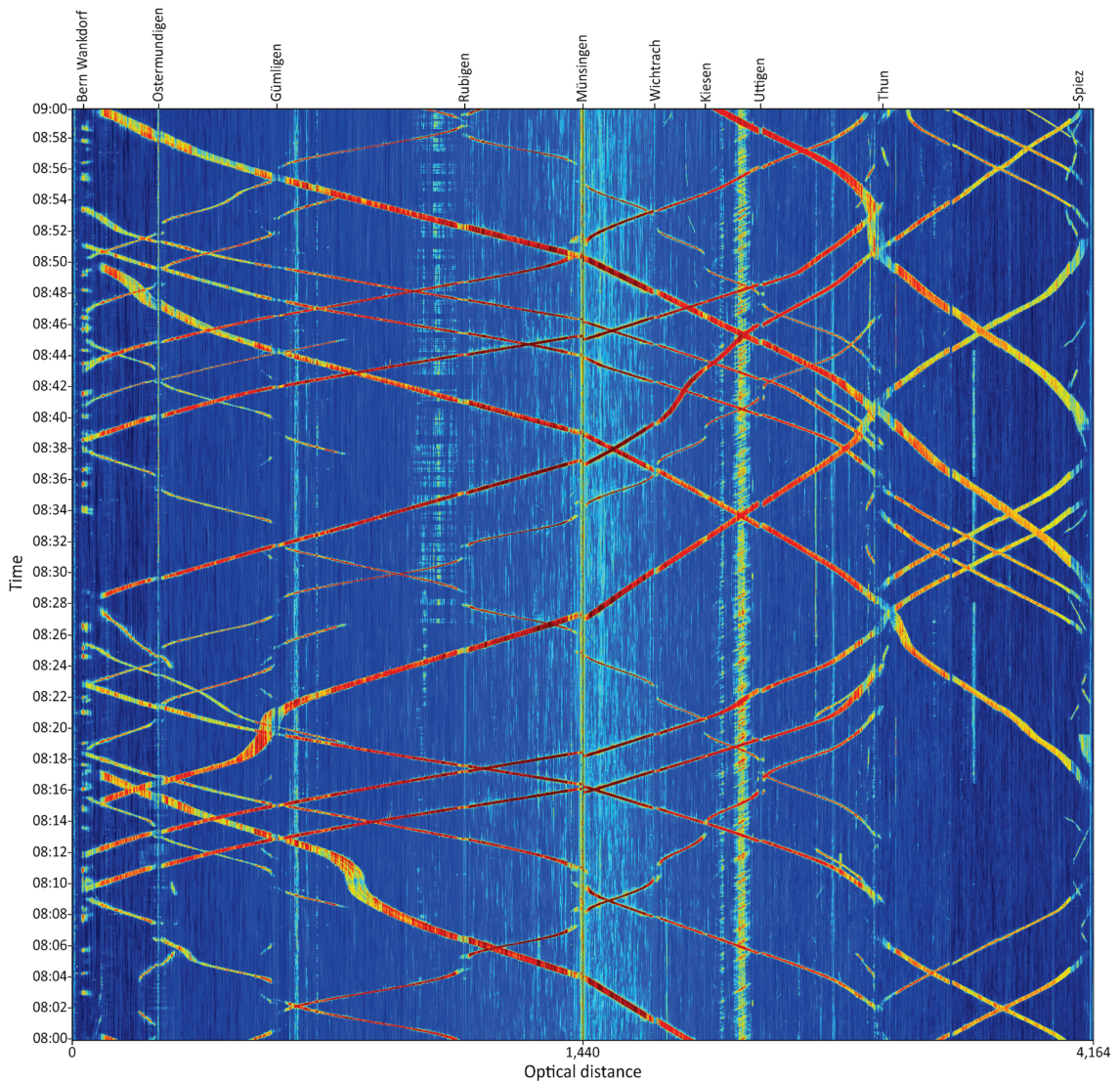
Figure 5.2: Train graphs in a waterfall diagram form.

While the system provides real-time monitoring of events along assets of interest (with a certain latency less than 1 second) a waterfall diagram as shown above can only be accomplished by analysing historical data according to the described data processing cycle. However, similarities, as well as differences between the two illustrations, are obvious. In both cases, train traffic is shown, but the latter shows the actual train movements of both passenger and freight traffic and all occurring events on or beside the track of interest. Therefore, the system provides information about the actual status of train operations and enables an immediate reaction in the case of occurring deviations from the scheduled train operation.

Kowarik (Kowarik *et al.*, 2020), working in close collaboration with Deutsche Bahn, examined a commercially available DAS system for near real-time train tracking utilising artificial neural networks with quite promising results.

5.2 Condition monitoring

In railways, infrastructure managers have several data sources for condition monitoring and assessment of both infrastructure assets and rolling stock. The focus here is the infrastructure and its condition monitoring over time.

Analysing the condition and hence reaction of the asset as a consequence of a train passing reveals the asset condition, although due to different train types. Therefore, looking at one specific point or asset the reaction of each train ride and passing due to a load becomes apparent. As shown, the signal is highly sensitive to train type and weight.

To sum up, the signal can be interpreted as a reaction of the infrastructure to the load and impact of train crossings. As the focus is on asset condition monitoring instead of train condition monitoring, a certain train type and train composition shall be chosen. Only this allows for time series analyses and comparing like with like. This is demonstrated by the following observations.

5.2.1 Influence of train composition

The frequency analyses reveal the signal's sensitivity and reaction due to the impact of various train types, different loads and weights and finally speeds in a more or less distinctive manner.

Railway operation, in general, is classified into freight and passenger services. The former carries a variety of commodities on national and international routes. A further distinction can be made with the market segments such as "*trains carrying dangerous goods versus other freight trains*" or "*block trains versus single wagon load trains*" (The European Parliament and the Council of the European Union, 2012). Additionally, depending on the kind of cargo myriad wagons exist and are utilised fulfilling the specific requirements. E.g. the Austrian Rail Cargo Group (RCG) classifies their fleet of different types of wagons into eight subcategories as they are 1) open wagons, 2) covered wagons, 3) flat wagons, 4) innowagon, 5) special wagon, 6) container wagon, 7) low floor wagon and 8) powder wagon (*Rail Cargo Group - Wagon equipment*, 2020). This is only the official wagon fleet of the Austrian freight undertaking and may be different for other countries. Especially since the free movement of goods and the liberalisation of the railway sector, almost every RU is allowed, after paying the track access charges, of course, to use the infrastructure in the specific country and to transport goods and passengers from one point to another. It is therefore no surprise that the number of wagon types is almost unlimited. Consequently, different wagon types make it necessary to use other types of bogies and thus the distance of axles varies too. Furthermore, the loading status of the wagons may differ within the same train and finally, each freight railway undertaking has locomotives tailored to their purpose and carried goods. The circumstances mentioned impede using signals altered by freight trains for infrastructure condition monitoring and assessment, ending in questionable results and compelling conclusions though.

According to (The European Parliament and the Council of the European Union, 2012) the latter shall be split into at least two segments: 1) passenger services within the framework of a public service contract and 2) other passenger services. Either way, a separation is made, passenger railway undertakings purchase train fleets specifically according to demand. E.g. in SBB's fleet strategy one parameter considered is the average journey time and another is the travelling speed. In the case of journeys taking longer than two hours, a passenger's comfort with customer-oriented zones and a 250 km/h maximum speed are decisive aspects. For such

international long-distance transport (Eurocity), SBB uses single-deck rolling stock like the *ElettroTrenoRapido (ETR 610)* or the *Giruno* only. Contrastingly, for regional transportation with an average travelling time of 20 minutes, high capacity is crucial and thus electric multiple units (EMU) are utilised (*SBB Fleet strategy*, 2020). Note that fleet strategies differ from country to country and even from RU to RU within the same country. However, SBB's strategy simplifies the identification of train type and composition and enables using the signal pattern of passenger trains for infrastructure condition monitoring.

The timetable described defines the plan case. However, train breakdowns or capacity bottlenecks can lead to a change in train disposition affecting, of course, the signal pattern significantly. In a normal case, the disposition changes will be documented in *Anabel*. Determining a reference train allows comparing like with like and delivers valid and plausible results. The reference train chosen in the course of the project is part of SBB's InterCity service and consists of one locomotive (Type Re460), eight double-deck coaches (Type IC 2000) and one driving trailer which is also a double-deck coach but with a reduced number of seats. The reference train has a total of 40 axles. Travelling from *Bern–Spiez* the coaches are pulled, and then pushed on the way back. This train always operates in the same composition and formation, even though the individual coaches are subject to changes. Therefore, minor speed variations at the same positions should not greatly affect the signal properties. The same applies to the weight and loading of the reference train. The tare weight of the locomotive and the coaches is always the same. Furthermore, the recording routines intention when set up was to monitor the track in the morning rush hours, ensuring that the number of passengers is almost constant. Of course, passenger numbers vary, especially within a day but, as the reference train travels each day at the same time the minor changes in passengers and thus loading are negligible. Even the track wear model, which is the basis for track access charging in Switzerland, adds a constant 30 % rate of occupation as an additional load to the tare weight of a coach for proper wear simulations. This assumption is certainly not 100 % correct, but it is assuredly more accurate than calculating and simulating with an empty or full train.

Under certain circumstances, the disposition of a train may change and is, for whatever reasons, not documented in *Anabel*. This will certainly be a hurdle initially but finding the particular train – the reference train – is possible anyway. This can be explained at best with Figure 5.3 showing a train crossing at a rail joint in an advanced state of wear. It is not accurate to claim that the rail

joint is already worn out and at the end of its service life and consequently needs to be maintained. While the backscattered intensity for the specific position is depicted on the left-hand side, the right-hand illustration shows the spectrogram – the frequency content – of the signal. The scattering is highly vigorous providing no further information about train type. This issue can be resolved by observing the frequency band. Before the train approaches and passes the channel, frequencies up to approximately 0.04 kHz are steadily present containing no valuable information. At the moment the train enters the channel, the backscattered signal is altered and the frequency content changes. In this specific case, higher frequencies are observed as a result of the infrastructure response to the train passing the worn-out rail joint.

(a)   *(b)*
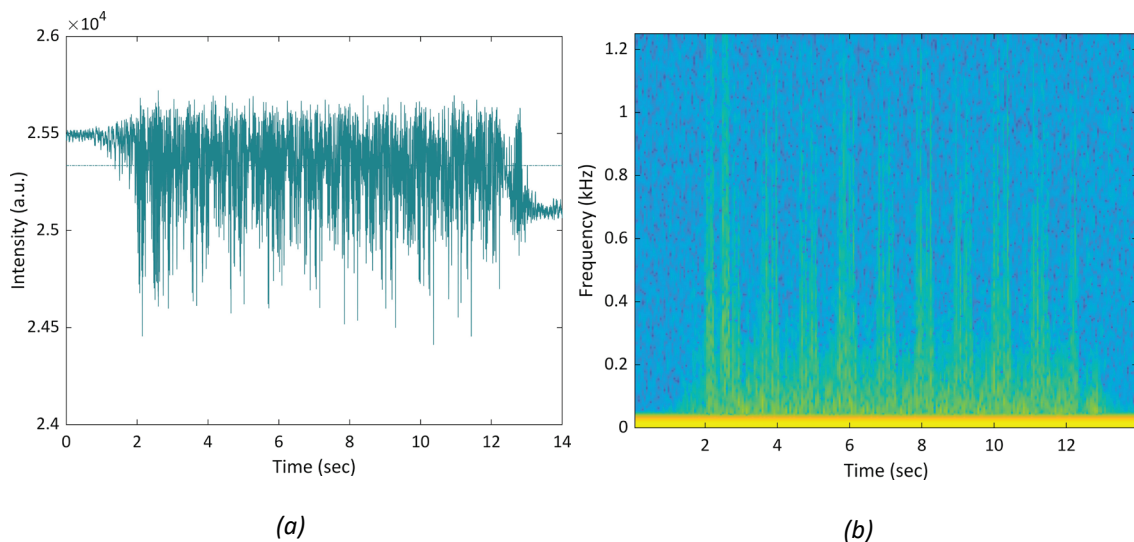
Figure 5.3: Rayleigh backscatter (a) and spectrogram (b) of the reference train
passing a rail joint in an advanced state of wear.

Each time an axle or at least the bogie passes the rail joint, the infrastructure reacts to the impact of the load. The yellowish peaks indicate this fact. The depicted train formation consists of a locomotive and nine coaches and is, in fact, the reference train. The first yellowish peaks arise due to the impact of the locomotive's bogies and axles followed by the pulled coaches. As the train travels further and no axle passes the specific point higher frequencies are no longer present. Consequently, only frequencies up to ~0.3 kHz are visible and can be considered as the train specific signature. As the next axle and bogie pass, the rail joint responds to the impact immediately and higher frequencies are present again. Additionally, knowing that the total length of the train that is passing is 259.7 m (9 coaches each 26.8 m long and a locomotive with

a length of 18.5 m) and the passage took slightly more than ten seconds, the travelling speed at this point can be calculated (~94 km/h).

Analysing the signal of another train, e.g. a *Rabe 503* in double traction, proves the results described (see Figure 5.4). In its original formation, the train is composed of 7 coaches and thus 28 axles. Operated in double traction as illustrated below this means a total of 56 axles and 14 coaches and a length of 374.8 m. The impact of almost every axle is apparent when passing the particular rail joint even if the peaks of the individual axles differ. This is no surprise because not all coaches carry the same load. However, the train passing lasts roughly 13 seconds which means that the travelling speed at this point is ~104 km/h. This corresponds very well with the previous observations.

(a)   *(b)*
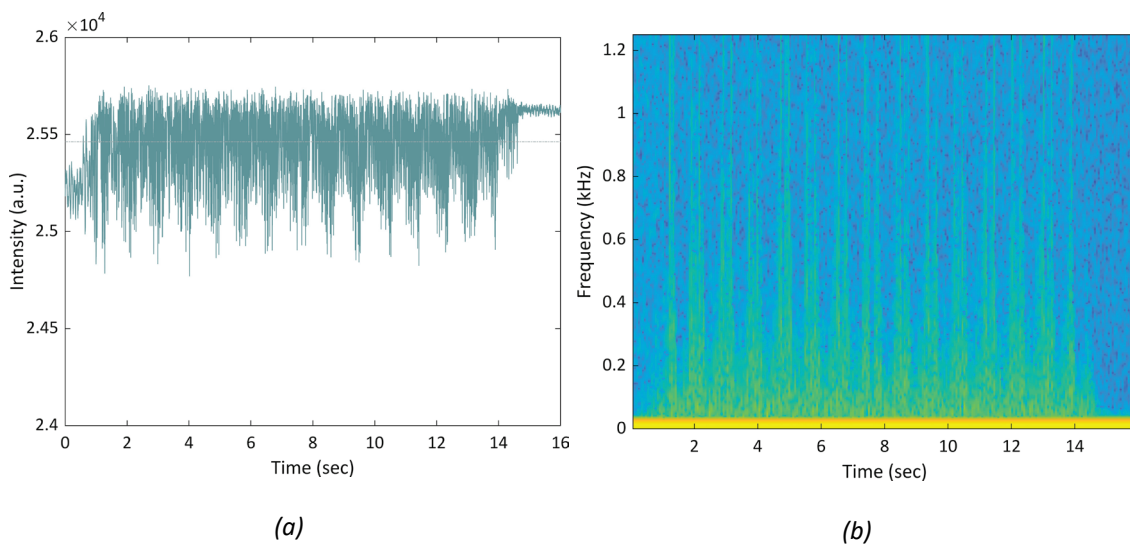
Figure 5.4: Rayleigh backscatter (a) and spectrogram (b) of the Rabe 503 in double traction passing a rail joint in an advanced state of wear.

The results reveal the technologies' potential for further applications such as wheel condition monitoring, detection of wheel flats or train integrity checks. At certain points where the impact of the train is striking in terms of dynamics the number of coaches, as well as the impact of axles, becomes apparent. In combination with information provided by tools like *Anabel,* it is possible to check whether the last coach/wagon is still part of the train formation and thus the integrity can be confirmed or negated. Additionally, the impact of wheels in whatever condition is quantifiable. Following the train path over a distance, periodically occurring anomalies in the signal pattern allow for identification and assessment of defects such as *wheels out-of-*

roundness or *wheel flats*. Yet, several sensors for train condition monitoring are nothing new and already exist and they are continuously being improved. Such wayside detectors, often referred to as WTMS, are deployed at points of interest or neuralgic points in an infrastructure manager's net. A brief overview given in the introductory remarks is examined in somewhat greater detail at this point.

WTMS can be classified for example either as reactive or predictive. The former is used for detecting actual faults on the vehicles, as many of these faults are hard to predict or have a very short failure to fault time. Mostly, the information provided by these systems is not suited for trend analyses. Nevertheless, they are of great importance to protect the infrastructure from further damage caused by the fault. Examples of reactive systems are 1) dragging equipment detector (DED) or 2) hot box/wheel detector (HBD/HWD). A DED is used to detect equipment that is hanging below the vehicle whereupon HBD/HWD are designed to detect overheated journals (hot boxes) or wheels (Barke and Chiu, 2005). The latter provide possibilities for a proactive maintenance approach. From the collected information it is possible to analyse the condition of the equipment to predict possible failures and faults that may occur in a near or distant future. This makes it easier to plan the maintenance activities ahead and also to utilise the equipment more efficiently. Some examples in use are 1) acoustic bearing detectors (ABD) and 2) vehicle performance monitoring/wheel condition monitoring. ABDs use microphones to record sounds from the passing vehicles focussing on the wheel bearings as bearing defects produce vibrations at frequencies that can be connected to the characteristics of the defect (Stack, Harley and Habetler, 2004; Barke and Chiu, 2005). A vehicle monitoring system is a general term for technologies used for monitoring the performance of vehicles, bogies and individual wheelsets. Systems are using the contact forces as well as non-contact monitoring systems. The contact systems are often based on strain gauges and/or accelerometers. The non-contact systems often use lasers and vision technology. To evaluate the wheel condition it is the status of the wheel surface and the wheel profile that are of interest (Barke and Chiu, 2005). Predictive technologies collect condition information over time and foresee a failure development in the near or distant future. In such a case, this information is sent to the particular RU to carry out the necessary maintenance task preventing both the infrastructure and the rolling stock from damage. This prolongs the service life and leads to lower life cycle

costs of both. The latest developments enable train performance measurements and wheel condition monitoring of vehicles at train speeds up to 250 km/h (Mittermayr *et al.*, 2019).

The brief review on WTMS sensors reveals the vast variety on systems existing, some as stand-alone applications developed by IMs in-house in close cooperation with suppliers (Mittermayr, Stephanides and Maicz, 2011; Bisang, Frey and Koller, 2017) and others as rather modular concepts (Vermeij, Venekamp and Boom, 2011; Arndt, 2015). However, DAS can contribute in combination with other sensors – in terms of sensor fusion – valuable data to both IM and RU. Some sensors can be removed and replaced by utilising FOS, at least in the near future as the technology is still not examined thoroughly for such purposes. Further research is necessary for enhancing the system and sensing properties. What sensors and trackside installations can be removed remains to be seen. However, the goal shall be reducing the number of sensors attached to the track.

5.2.2   Influence of track

Train type, condition and speed undoubtedly affect the signal pattern, scattering behaviour and consequently the frequency content. Equally important, though, is the influence of the infrastructure and its condition. External perturbations and local conditions change the signal properties providing the user with essential information on boundary conditions. Otherwise, the sensing system could not be used for condition monitoring, intrusion monitoring and many other applications. Ensuring pipeline integrity, immediate leakage detection and risk mitigation for example are very common applications for DAS, because pipelines are linear assets. The influence of the infrastructure on the signal properties can best be demonstrated by simply comparing the results depicted in the figures below (Figure 5.5–Figure 5.8). Each channel corresponds to a certain position of the monitored track. Channel 300, depicted in Figure 5.5, is linked to a straight section with concrete sleepers. The scattering (Figure 5.5a) is quite characteristic and shows a distinctive pattern. As mentioned previously, train-related signal content and noise are visible up to frequencies of 300–400 Hz (see Figure 5.3 and subchapter 3.2). Using a Butterworth high-pass filter (HPF) 3rd order with 400 Hz cut-off frequency removes all lower frequencies and hence reveals the single peaks of bogies and thus axles when passing this channel (Figure 5.5b). Noise is still present in the signal, but the impact of the vehicle and the response of the infrastructure are clearer than ever. The locomotive is the

heaviest vehicle in the train composition with heavier bogies inducing also more noise. This may be one reason making it difficult to identify the impact of each axle. Nevertheless, at least two high values are visible. For the coaches, the bogie distance is bigger, and they are thus easier to make out. The highest impact is introduced by the fourth axle of vehicle one, which is the second axle of the second bogie. Furthermore, the impact of the first axle of the driving trailer at the end of the train is also remarkable.

(a)   (b)
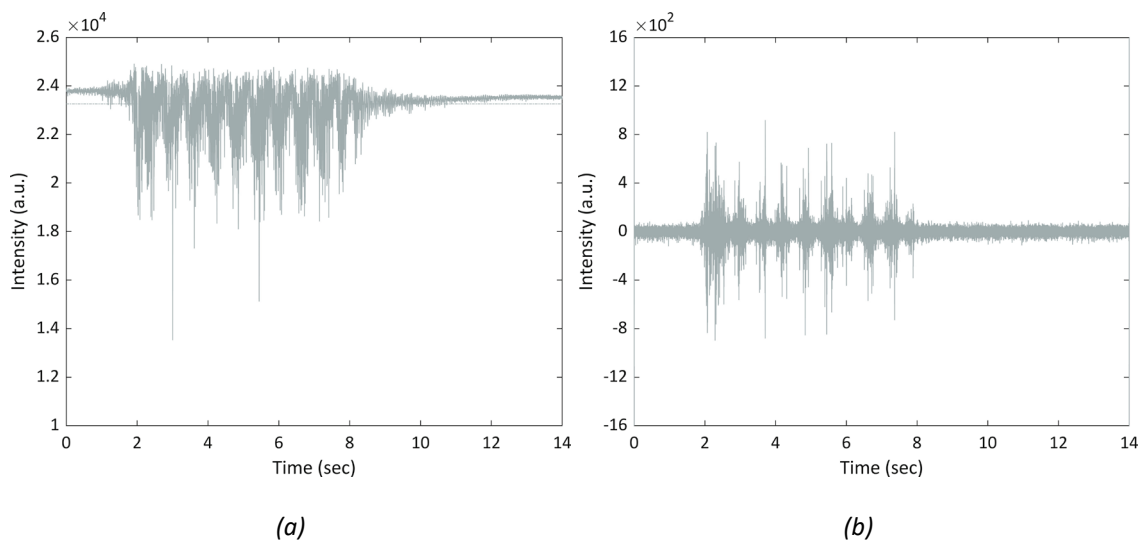
Figure 5.5: Rayleigh backscatter (a) and high-pass filtered signal (b)
of the reference train passing channel 300.

When compared to the results above, the scattering in channel 350 (Figure 5.6a) changes significantly. However, when only 500 m further away from channel 300 the two measurements show no correlation. The question then arises as to the reasons for the drastically changed measurement results. Once again, this issue can be resolved by linking asset data (*DfA*), both fibre and track layout and channel position. Channel 350 is in the middle of a coil and seems to have no sensing capabilities at all. This is also confirmed by the results illustrated in Figure 5.6b. After filtering out the signal content considered as noise, almost no information is left.

(a)   *(b)*
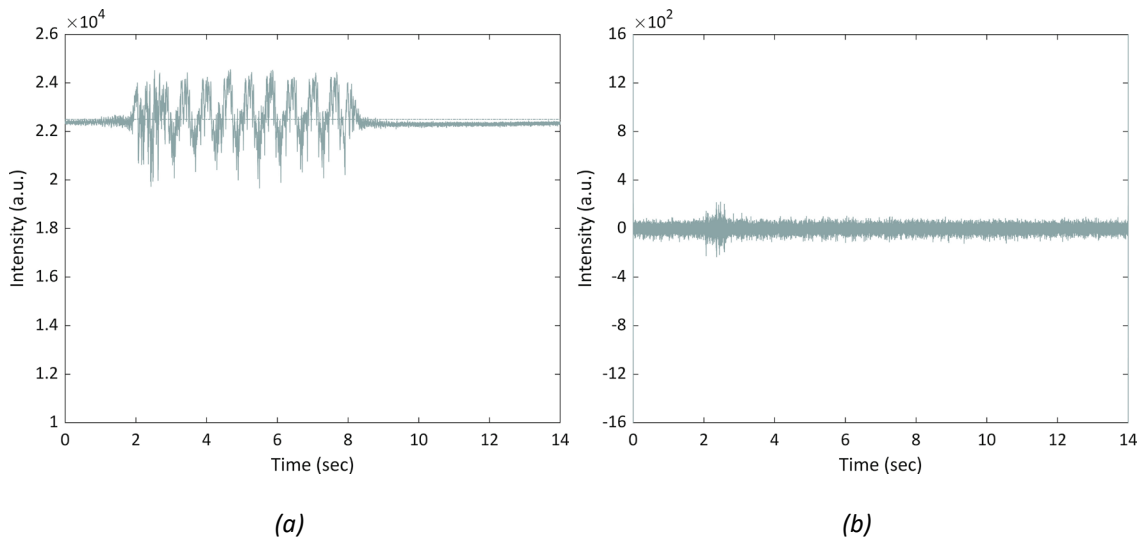
Figure 5.6: Rayleigh backscatter (a) and high-pass filtered signal (b)

of the reference train passing channel 350.

The scattering occurring at a position only 250 m further away once more delivers a completely different signal pattern (Figure 5.7a). This channel shows not only a very prominent peak dispersion, but also seems to be very noisy although frequencies below 400 Hz are filtered out and therefore neglected. (Figure 5.7b).

(a)   *(b)*
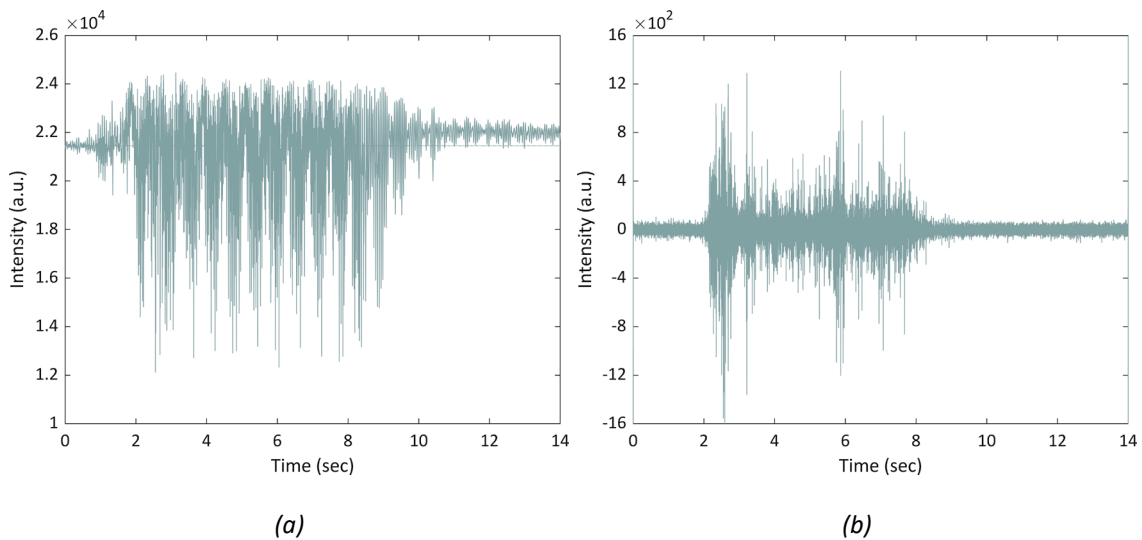
Figure 5.7: Rayleigh backscatter (a) and high-pass filtered signal (b)

of the reference train passing channel 375.

In contrast to Figure 5.5, neither the number of vehicles nor the impact of single bogies or axles can be identified. The signal still appears noisy, even though the HPF filter removed any lower frequencies.

However, the last position analysed in this chapter – channel 1,946 (rail joint) – reveals a scattering completely in contrast (Figure 5.8) to those analysed previously. Firstly, no extensive peaks can be observed when analysing the backscattered signal. In fact, the scattering shows no characteristic properties and the signal seems to be weak. While high peak values could previously be identified, this is no longer the case at this position. A reason could be that this is almost the 20th km of IU0. However, an already weakened signal only after 20 km does not seem very reasonable. While the backscattered intensity has a remarkable behaviour, the filtered signal exposes something different. Now the impact of not only each bogie but rather every single axle is unambiguously identifiable and the vehicles forming this train are countable. Compared to the peaks in Figure 5.5b these ones are significantly lower. Furthermore, it is quite evident that all noise has been removed by applying an HPF.

It must be noted that the travelling speed in the figure below is significantly lower (~93 km/h) than in the previous figures. However, the difference in speed may be a reason, but as the peaks even within the figures above vary it cannot be the only reason. This is proven by the fact that the same speed observed in Figure 5.3 delivers higher peak values.

(a) (b)
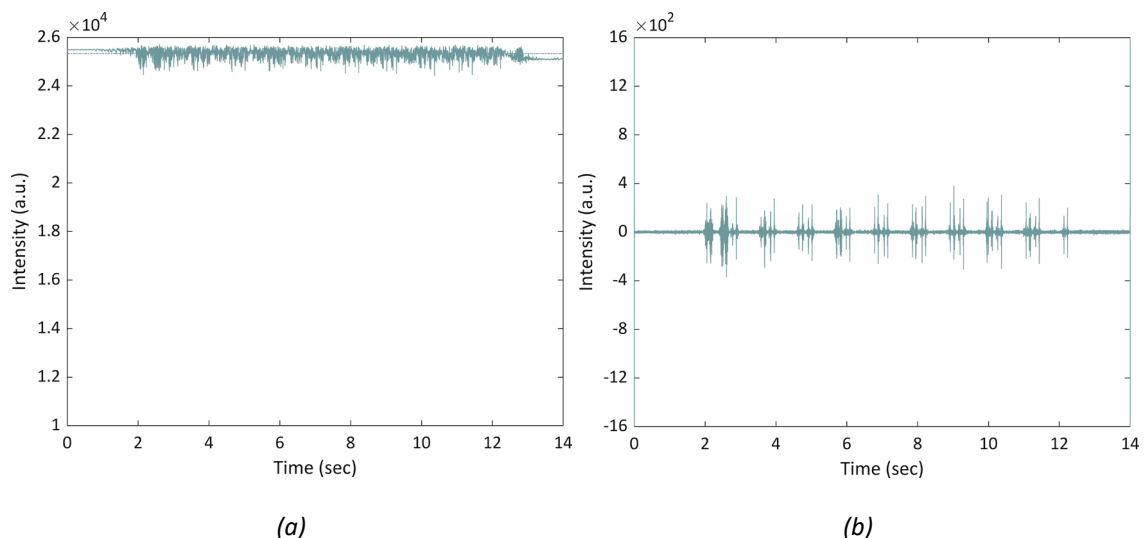
Figure 5.8: Rayleigh backscatter (a) and high-pass filtered signal (b)

of the reference train passing through channel 1,946.

As the train is kept constant and only the position is changed and therefore the condition of the infrastructure, the reason for the signal pattern must be infrastructure related, at least to a certain degree. The table below presents some statistical values of the figures discussed recently. The first four columns depict the backscattered intensity of the signal originally observed, the subsequent four columns show the values after applying for a Butterworth HPF 3rd order with a cut-off frequency of 400 Hz.

	Raw signal				HPF signal			
	300	350	375	1,946	300	350	375	1,946
Min (a.u.)	13,518	19,649	12,111	24,411	-3,949	-3,716	-3,653	-4,233
Max (a.u.)	24,915	24,561	24,473	25,722	3,581	3,395	3,305	3,830
Mean (a.u.)	23,260	22,494	21,448	25,335	-0.025	-0.024	-0.023	-0.027
SD (a.u.)	825	639	1,498	176	78	51	107	51

Table 5.1: Statistical values of the measurement as a train crosses the position.

In general, the results presented confirm the system's capability to track condition monitoring.

Another parameter that has to be considered and is track related concerns the path a train takes travelling from one location to another. This is somehow railway specific and needs further explanation. When utilising optical fibre for any application, the sensing fibre is attached to the specific asset of interest ensuring comprehensive asset protection. However, in railways and the course of this project, a dark fibre of existing cables laid in cable ducts is used. In general, only one cable duct exists protecting all cables from accidental or deliberate damage. What seems to be worth only a side note becomes more important in case of double-tracked or even multiple-tracked lines. Here, trains use one track for each direction, which means that e.g. a train travelling from A to B takes track 1 and, on its way, back takes track 2. Again, only one cable duct is present guiding all deployed cables. Furthermore, certain circumstances may make it necessary to allocate a changed path for the specific train journey. This is not a major obstacle in itself since it is a daily occurrence. If, however, FOS is used for condition monitoring, it must be ensured that the same track is always considered in the evaluations. For instance, if track 1 has a fault at a certain point and the signal is evaluated at the same point when a train passes over the other track, ambiguous conclusions may be drawn, and a previously conspicuous fault no longer appears to be present. Therefore, it must be ensured that the signal of a train is considered for both the same location and the same track. This hurdle is overcome with a two-

sided approach, as information provided by *Anabel* are used and the FOS data is cross-checked again afterwards.

As shown, each train type produces a different signal pattern leading to a peculiar signal characteristic. Furthermore, the FOS signal changes in a remarkable manner over a certain time as well as within a day of two train rides in the same train composition. This may happen due to several reasons/conditions where some of them can be overcome with a methodology enabling a constant comparison of like with like. An effort to classify these influences is made as follows:

1) infrastructure condition
2) location, position and fixation of optical fibre cable
3) properties of optical fibre cable
4) train condition/properties
5) random effects
6) sensing properties.

Some of the circumstances mentioned cannot be overcome or rather are not subject to change and most importantly not in the scope of the thesis. This holds true especially for optical fibre and sensing properties as well as effects occurring randomly. The position and location of the fibre are sorted out for most of the route. The influence of train properties is reduced to the maximum necessary by analysing the signal of a reference train in the same composition. Finally, the infrastructure condition is of major interest. In order to deliver additional valuable data for infrastructure condition monitoring only identified track faults are analysed.

This approach ensures that like with like is always compared and correct conclusions are derived.

5.3 Data processing cycle – the final stage

The concept of using DAS for infrastructure condition monitoring presented here and based on the results above requires an approach to be derived covering issues of both huge data amounts and the influence of train composition on the signal pattern. While the former can be tackled with data conversion as described, the latter can only be handled with additional information provided by SBB's application *Anabel*. This application displays both asset-specific loading and strain and enables tracking of each train path. Therefore, a reference train is chosen which always runs in the same formation. The selected train composition is a 40-axle train consisting of a locomotive of type Re460 (length = 18.5 m), 9 double-deck wagons of type IC2000 (length = 26.8 m), with the driving trailer at the end being the ninth wagon. This ensures not only the consistency of the data but also that like is compared with like. Consequently, each train in the described train composition is extracted from the prepared *hdf5* data and stored separately.

For the train selection, the data from *Anabel* is retrieved to 1) know the exact departure time of trains and especially that of the reference train from the station in *Bern* and the other stations along the line; and 2) to avoid the selection of the wrong train due to occasional delays. Afterwards, the data of the reference train run is extracted from the recorded data. However, this step is not carried out automatically due to the non-constant system offset in time. It is, therefore, necessary to first derive waterfall diagrams of the entire measurement series to identify the individual trains and consequently store the specific train run of the reference train separately. The same procedure was used for both interrogator units for all recordings. This step has another positive side-effect: The amount of data is reduced again, with only 1.5 GB of raw data for a single train run.

All further analyses are based on the selected train composition and thus allow a comparison of the results.

5.4 Conclusion

The FOS signal is affected by several circumstances changing both the sensing properties of the system and the scattering. One reason can be found in the sensing set up, because a dark fibre of already installed optical cables is utilised. A modified and customised experimental arrangement may lead to less random signal patterns and thus more precise measurements.

Nevertheless, some hurdles can be overcome by developing a methodology which allows a comparison of like with like and finally drawing consistent conclusions on the system's capability for infrastructure condition monitoring. An example of a feasible approach to tackle this issue is presented here.

The results presented so far proved that the measurement method can derive valuable information on areas of interest but also outlined the requirements for further research. The asset condition including the rolling stock has a certain impact on the signal reflected primarily in the frequency content.

There is a strong demand for further research, especially in the field of sensor fusion and the replacement of other technologies.

Deploying a methodology as discussed – reference train and known track failures – ensures that DAS is used for the right purpose and can deliver additional information for CM and AM.

6   CONDITION MONITORING

6.1   Introduction

Condition monitoring of railway infrastructure focusses mainly on track geometry/irregularity measurements. In general, track irregularities are considered as deviations from the design geometry within a 1–200 m wavelength range. For this purpose, measurements with the track recording vehicle are carried out and statistical values representing the actual track geometry are calculated. During the evaluation process the track data is filtered into different wavelength ranges (3–25 m denoted as D1 (most common), 25–70 m (D2) and 70–150 m vertically (D3)) and statistical values are calculated, the common one being the standard deviation (SD). Wavelengths shorter than 1 m are defined as roughness or corrugation of rails. Track irregularities and geometry standards for tracks and switches&crossings (S&C), as well as guidelines for maintenance machines, track construction and quality, are defined in the standards of the European Committee (European Committee for Standardization, 2010, 2012, 2014, 2017, 2018, 2019).

This thesis aims not to examine track geometry degradation, the reasons for the occurrence of rail surface defects and other issues closely related to this. Research on this has been published extensively upon which the following literature review provides a brief overview.

Hummitzsch and Holzfeind analysed track geometry behaviour on a large scale (Holzfeind, 2009; Hummitzsch, 2009) in the late 2000s, Vidovic examined track behaviour after substructure improvement (Vidovic, 2016; Vidovic, Landgraf and Marschnig, 2017), Marschnig and Neuper highlighted the positive effects of innovative components on track quality and behaviour (Veit and Marschnig, 2009; Neuper, Neuhold and Landgraf, 2018). Landgraf and Hansmann analysed the wavelengths D1 and D2 and outlined the possibility to determine the root cause for track geometry degradation whether it occurs due to bad ballast condition or malfunctioning substructure. Fractal analysis of vertical track geometry is well published and implemented by various IMs (Hansmann, 2018; Landgraf, 2018). Furthermore, while Audley (Audley and Andrews, 2013) elaborated on track degradation due to tamping measures An (An *et al.*, 2018), Caetano (Caetano and Teixeira, 2016) and Neuhold (Neuhold, 2020) developed, under different aspects, of course, models for an automated tamping demand prediction.

Track quality has been and is up to now thoroughly examined and matter of ongoing research. However, this is by no means less than efforts in the field of rolling contact fatigue defects. Increasing numbers of cracks close to the rail's running surface heightened the demand to understand such mechanisms. To undertake research in this field, the European Rail Research Institute (ERRI) formed a Rail Rolling Contact Fatigue Committee (ERRI D 173) 1987. Since then considerable efforts have been undertaken to examine the occurrence of rail surface defects (Clayton and Hill, 1987; Bogdański, Olzak and Stupnicki, 1996; Cannon and Pradier, 1996; Muster *et al.*, 1996). An overview of various rail defects can be found in (Cannon *et al.*, 2003). Nowadays, various models for the prediction of RCF exist based on finite element analysis and models exploiting empirical laws (Burstow, 2004; Bevan *et al.*, 2013; Goryacheva, Soshenkov and Torskaya, 2013; Dirks, Enblom and Berg, 2016).

The following results examine the ability of DAS for track and turnout condition monitoring. Based on this, it shall be possible to distinguish between different asset conditions. Additionally, time-series analyses reveal whether it is possible to monitor the degradation of an asset over time. As this approach strives not to describe the track geometry the focus is placed on isolated track defects.

This chapter tackles RQ1–4. While RQ1, RQ2 and RQ3 will be answered by the results presented in the following subchapters, RQ4 is rather theoretical and will be discussed in each chapter at least briefly.

6.2 Track

6.2.1 Isolated track defects

6.2.1.1 White spots in ballast bed

During an on-site inspection, two significant white spots in the ballast bed were detected at the monitored route (see Figure 6.1) and the certain track kilometre was linked to the channel showing the highest intensity. The results of only one section are discussed but can be considered as generally valid.

Such isolated track defects do not occur suddenly but rather develop over several weeks or months. Of course, this depends in particular on the load, the vehicle collective, the substructure and superstructure, but also on the condition of the track. In this particular case, the ballast has been crushed as a result of a malfunctioning weld and overstress. Presumably, there is already a very large amount of fine-grained material (crushed ballast) in the ballast bed and the bottom edge of the sleeper may be worn out resulting in an inadequate load transfer.

Figure 6.1: Section with characteristic wear pattern after ballast break-up.

In order to verify and validate the indication of the DAS signal, the time series of the standard deviation of the longitudinal level is considered for the relevant section (see Figure 6.2). Note that the y-axis represents does not show the standard deviation in mm but rather the limit value exhaustion level (LVEL) for the section. If the LVEL reaches 100 % a maintenance measure (in this case tamping) is necessary immediately.

The white spot occurs in the area of km 0.03 (to guarantee the anonymity of the data the track km has been modified). The most recent measurement run M9 is shown in dark turquoise while the remaining measurement runs are shown in increasingly darker colours from M1 (light grey) to M8 (greenish). The nine measurement runs took place within 14 months, resulting in a measurement interval of 1.5 months which is quite frequent as a TRV usually measures the same section a maximum of six times a year. The measuring campaign shown here outlines that this is a rather challenging area and needs to be monitored more often. At the depicted section the track situation deteriorates steadily between M1 and M4. The LVEL for M1 of track km 0.03 was 70 % and increases within four months to 85 % (M4). Between M4 and M5 (one month) the values appear at a stable level showing almost no deterioration. This seems not at all reasonable, considering the rapid deterioration previously.
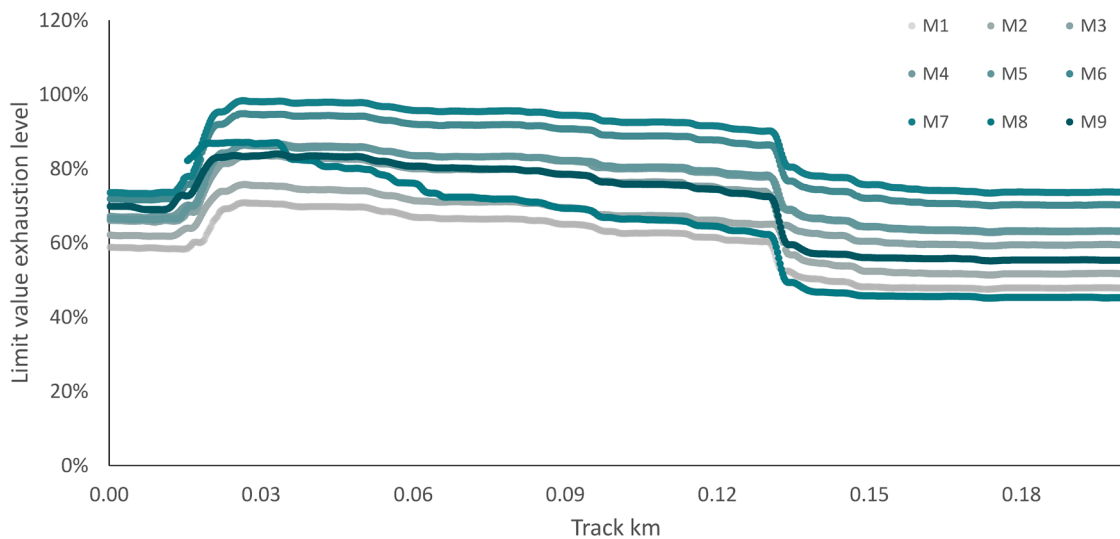
Figure 6.2: Limit value exhaustion level (LVEL) for the section with the white spot.

In fact, this section was maintained (tamped) between the two measurement runs and hence the geometry corrected. Afterwards, the deterioration process continues resulting in a LVEL of almost 100 % measured during the campaign of M7. Again, the section has to be tamped in order to guarantee a proper track quality and safety level. This maintenance task can be classified as a rather reactive measure. The executed maintenance leads to an improved track geometry for the entire depicted segment. In the area around track km 0.03, the LVEL is about 85 % captured during M8 which took place ten months after M1. Subsequently, this section

hardly deteriorates in the following months. This does not apply for the area after the white spot as the track geometry deteriorates continuously in the following months.

To compare the results of the track recording vehicle and FOS signal the time series of the original and filtered signal is depicted in the following illustrations. Some statistical values are shown in Table 6.1 too.

Since the recording days of the IU and the TRV are not congruent, the track geometry measurements of the TRV are compared with the results of the closest recording of the interrogator unit, but not all of the measurements are shown for reasons of clarity.

The development of the FOS signal M1–M4 (Figure 6.3 & Figure 6.4) follows a similar logic as those of the TRV. While the raw signal shows only slight deviations a significant deterioration in the form of higher peak values is observed in the filtered signal (Figure 6.3b–Figure 6.4b).

(a) *(b)*

Figure 6.3: Rayleigh backscatter (a) and high-pass filtered signal (b)
of the white spot at track km 0.03. Measurement M1.

	Raw signal					HPF signal				
	M1	M4	M7	M8	M9	M1	M4	M7	M8	M9
Min (a.u.)	13,278	13,388	18,259	7,602	11,306	-2,954	-3,942	-3,034	-4,843	-2,845
Max (a.u.)	25,188	25,313	25,377	24,972	25,085	5,619	5,990	5,771	5,663	5,446
Mean (a.u.)	23,229	23,804	23,915	22,504	21,725	0.130	0.139	0.134	0.131	0.121
SD (a.u.)	1,093	1,235	734	1,673	1,454	198	221	205	329	161

Table 6.1: Statistical values of measurements as a train crosses the white spot at track km 0.03.

(a)   *(b)*

Figure 6.4: Rayleigh backscatter (a) and high-pass filtered signal (b)

of the white spot at track km 0.03. Measurement M4.

Yet, the raw signal of both measurements demonstrates a similar pattern

The executed maintenance task after M6 leads to an improved track geometry which is also reflected in the FOS signal illustrated in the figure below. Noteworthy is the fact that the filtered signal after the maintenance work still appears noisy and the impact of the individual bogies or even axles is hardly recognisable.

(a)   *(b)*
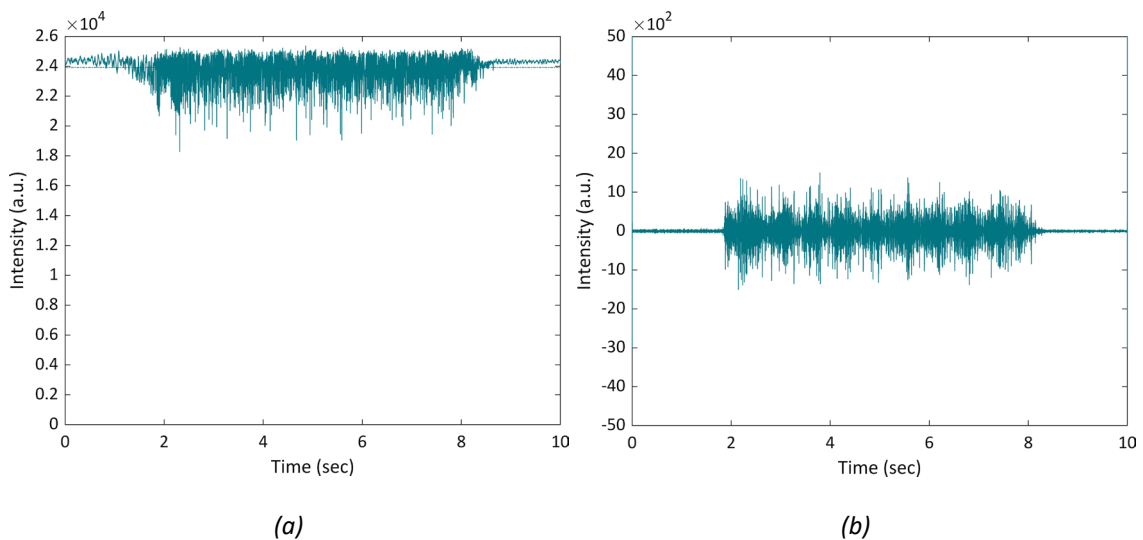
Figure 6.5: Rayleigh backscatter (a) and high-pass filtered signal (b)

of the white spot at track km 0.03. Measurement M7.

A reasonable explanation may be that the causative failure was removed totally and the characteristic impact of the vehicle as it passes the specific section is not present any more, also resulting in considerably lower peaks.

After the track quality has been improved again a deterioration within two months is observed in the FOS signal (see Figure 6.6, M8), although this is not visible in the limit value exhaustion level. Subsequently, in the period from M8–M9 (time difference two months) the FOS signal once again displays a changed pattern and differing properties. Both raw data and the filtered signal demonstrate improved values resulting in a substantially lower peak dispersion. The lowest values in the DAS data are observed for the latest measurement M9 indicating the best ballast condition and track geometry for this section. The values and peaks of the filtered signal outlined in Figure 6.7 confirm the discussed results.

(a)   *(b)*

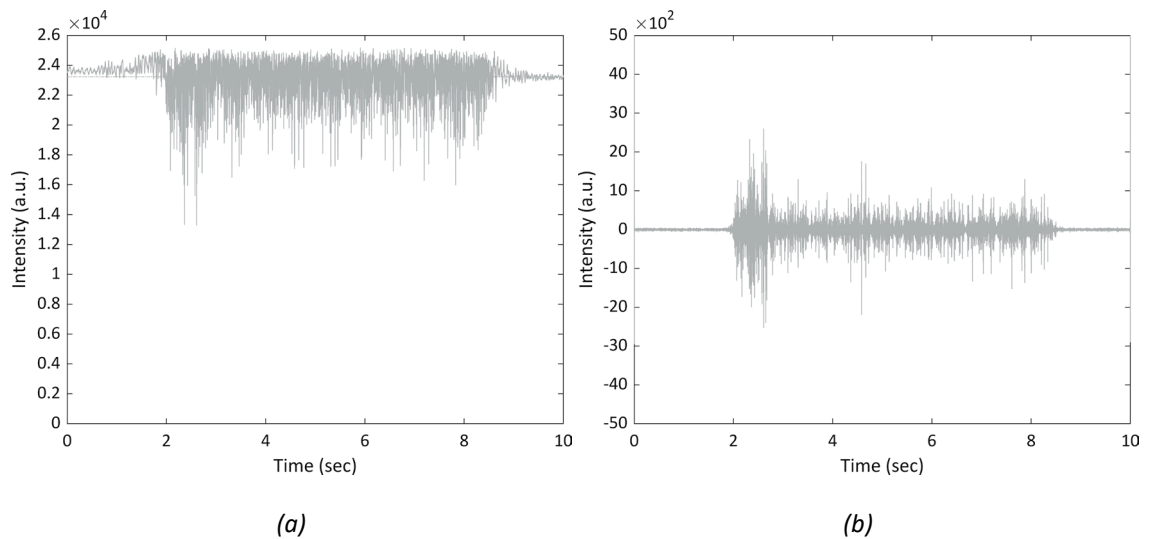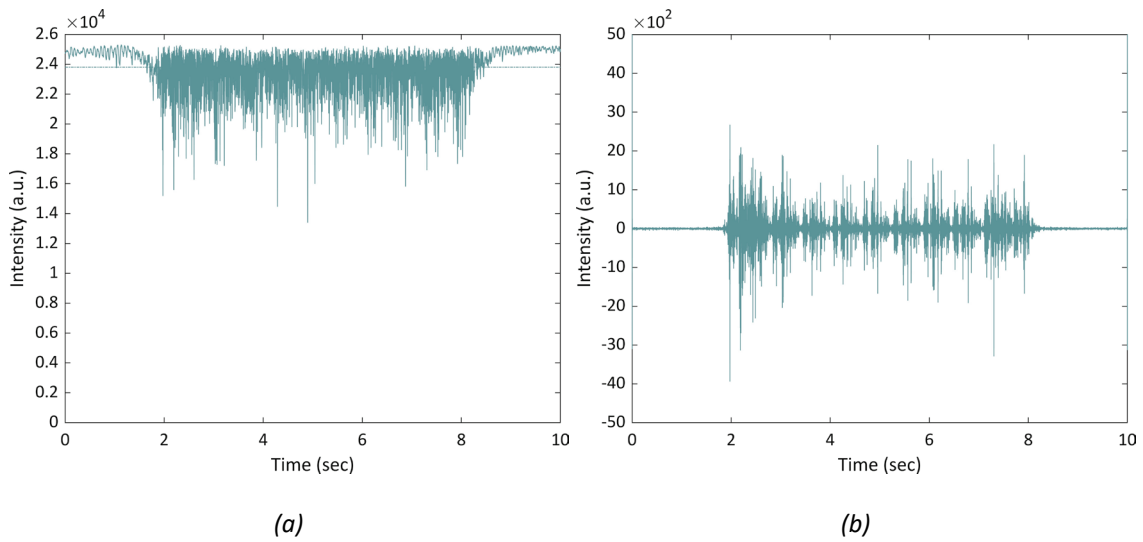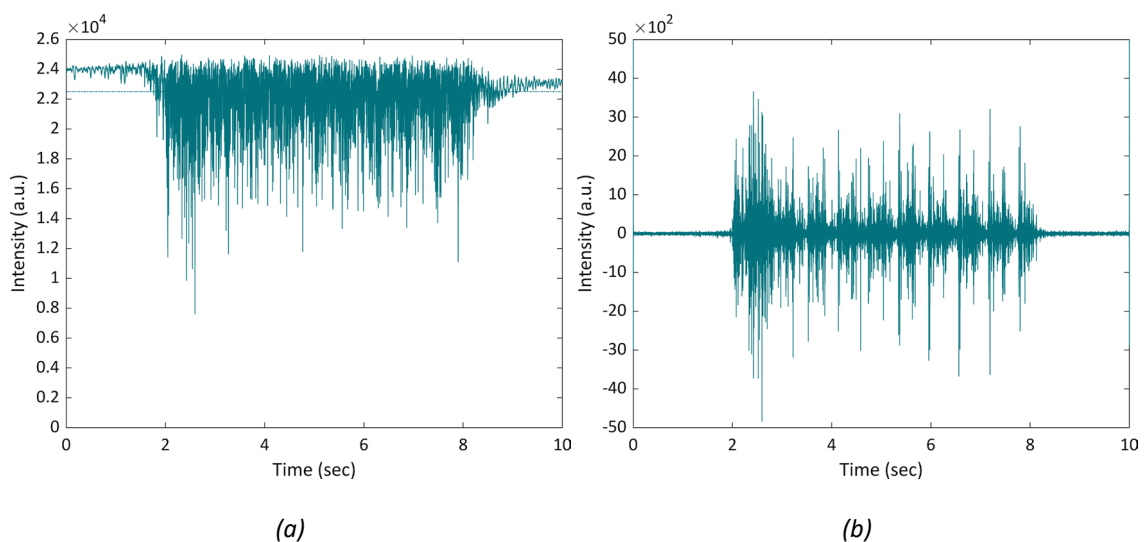*Figure 6.6: Rayleigh backscatter (a) and high-pass filtered signal (b)*

of the white spot at track km 0.03. Measurement M8.
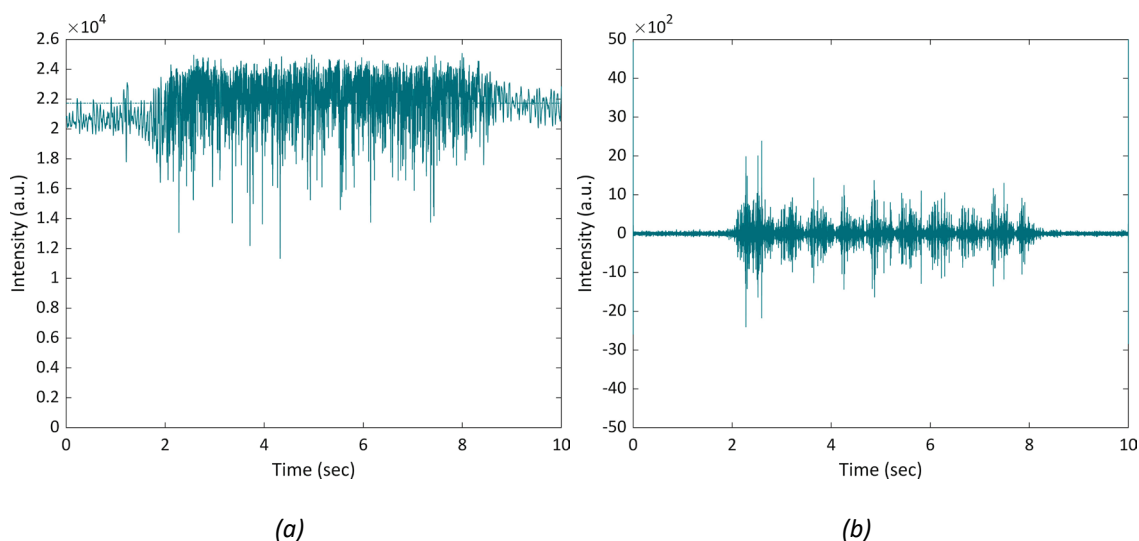
Figure 6.7: Rayleigh backscatter (a) and high-pass filtered signal (b)

of the white spot at track km 0.03. Measurement M9.

The difference between the results from the TRV and FOS is quite surprising but may arise due to two circumstances: 1) in the period from M8–M9 the track geometry was improved and is therefore again on a similar level as shown in Figure 6.5; 2) the vehicles of the train composition outlined in Figure 6.6 are not in faultless condition (flat spots, out-of-roundness) and this is consequently reflected in the signal.

The aforementioned issues are tackled by comparing the signal of a section in a better condition several channels further away (km 0.18) from those with the ballast break-up. The boundary conditions (substructure, superstructure, speed) of both areas are the same, with the track position being the only specific difference. Furthermore, the distance from the optical fibre guiding cable duct remains constant over the whole section in question, which means that this should not influence the signal transmission and sensing properties. Comparing like with like reduces the influence of the sub- und superstructure to a minimum and enables consistent conclusions and statements regarding the system's ability to identify isolated track defects.

The statistical values of track km 0.18 are set out below. Each measurement of the section with the white spot shows a higher SD in the filtered signal, in particular. Especially the difference within the measurements M8 is striking. Furthermore, while the SD of the white spot from measurement M8 to M9 decreases for track km 0.18 the inverse case is observed as the values increase. This effect is also observed in the limit value exhaustion level.

	Raw signal					HPF signal				
	M1	M4	M7	M8	M9	M1	M4	M7	M8	M9
Min (a.u.)	17,330	14,647	18,695	15,747	9,858	-2,681	-2,762	-2,956	-2,771	-3,399
Max (a.u.)	25,212	25,167	25,236	25,141	25,019	5,094	5,280	5,622	5,278	5,490
Mean (a.u.)	22,282	22,522	23,351	22,643	22,082	0.118	0.123	0.131	0.123	0.126
SD (a.u.)	1,148	1,042	715	994	1,533	99	146	98	123	148

Table 6.2: Statistical values of measurements as a train crosses at track km 0.18.

What seems surprising at a first glance is resolved after analysing the tamping records of the region. After measurement M8 a maintenance task was executed. More precisely, it was an instruction for spot tamping (tamping over a short length) in order to improve the track geometry in the area of the white spot. However, the exact date is unclear and not documented but discussions with the asset manager of the region in charge provided information about the executed maintenance task. In addition, the turnouts in this area were maintained explaining the rather unchanged track geometry at track km 0.03 on the one hand and the characteristics of the DAS signal on the other hand. In contrast to that, the deterioration of the section in the proximity of track km 0.18 appears reasonable as there was no maintenance work executed.

The following figures illustrate the results of the first measurement M1 and the last measurement M9 of track km 0.18. These reflect the trend of the track geometry discussed before.

(a) *(b)*
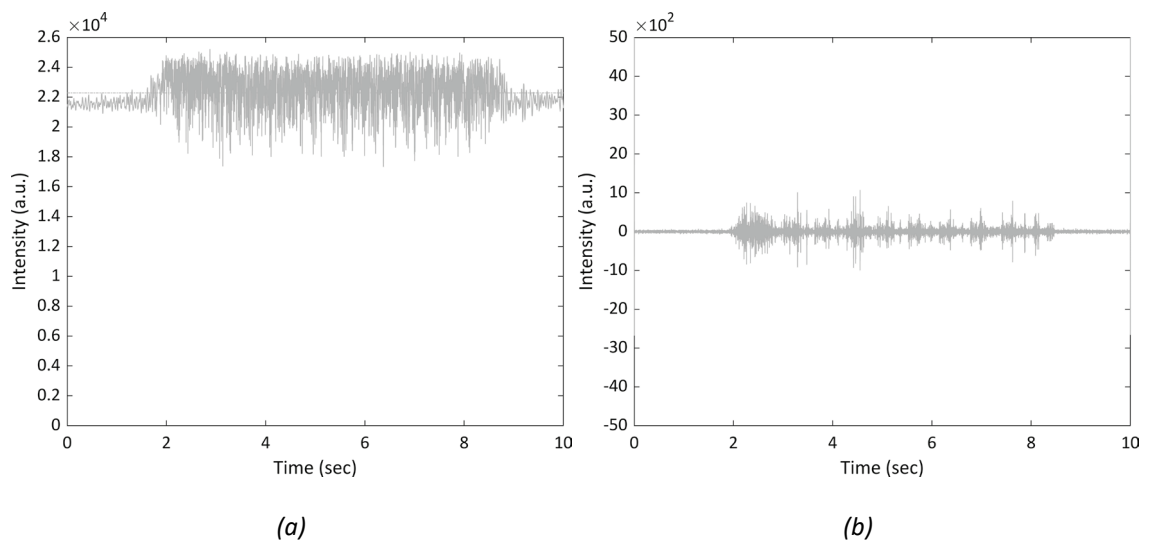
Figure 6.8: Rayleigh backscatter (a) and high-pass filtered signal (b)

at track km 0.18. Measurement M1.

While the peaks of each axle of the coaches are more or less at the same level, the impact of the locomotive, or more precisely of the first axle of the second bogie, is remarkable. This could indicate a faulty wheel but is subject to speculation as it was not further examined.

(a) *(b)*
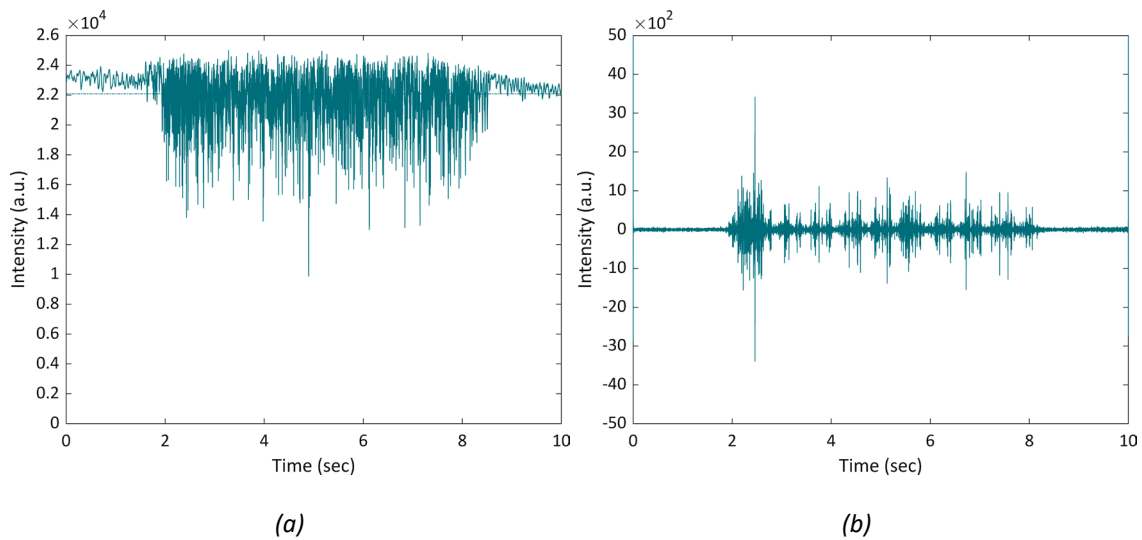
Figure 6.9: Rayleigh backscatter (a) and high-pass filtered signal (b)

at track km 0.18. Measurement M9.

Finally, the spectrograms of the two sections in question are depicted in the following graphics. Figure 6.10a shows the spectrogram of the area with the identified white spot. The mid-waved track failure leads to increased dynamics resulting in higher frequencies present in the signal. This does not apply for the section further away from the white spot where frequencies above 0.8 kHz are hardly determined.

(a)   *(b)*
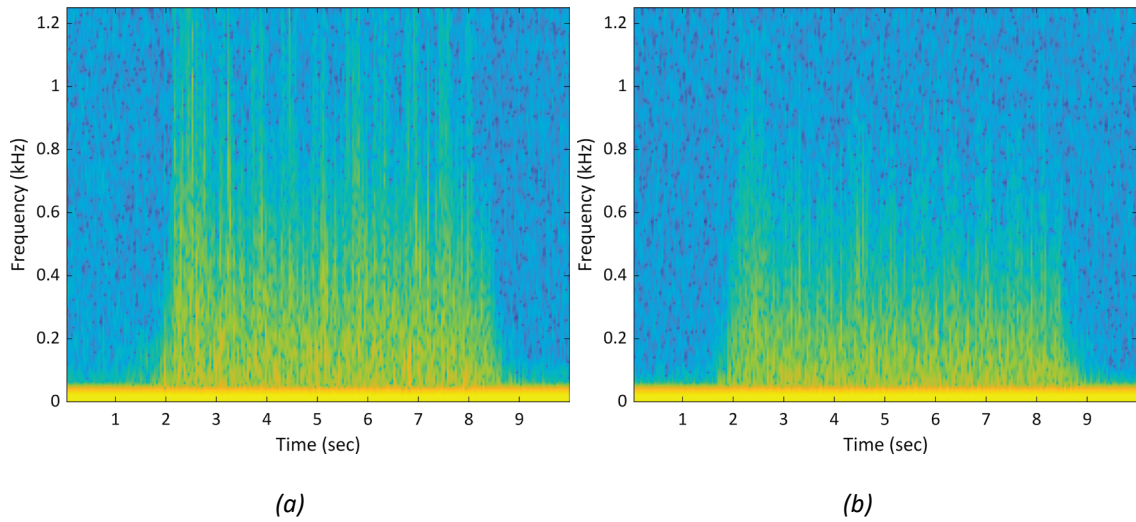
Figure 6.10: Spectrogram of measurement M1 at track km 0.03 (a) and track km 0.18 (b).

The tamping task executed ahead of measurement M9 leads to an improved track geometry which is also reflected in the frequency content of the DAS signal (Figure 6.11a). The spectrograms appear almost equal, although track km 0.18 seems to be in a better condition.

(a)   *(b)*
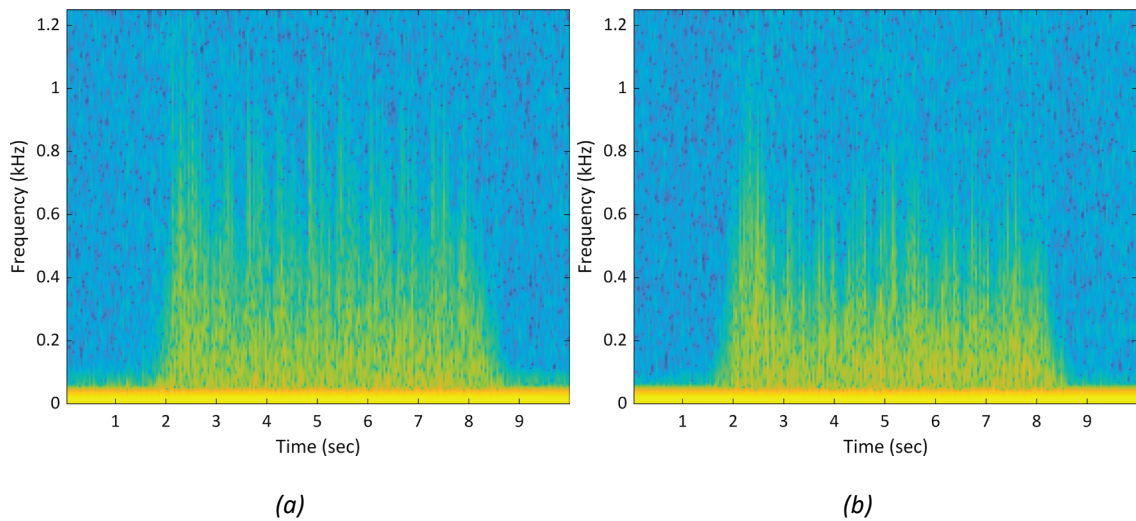
Figure 6.11: Spectrogram of measurement M9 at track km 0.03 (a) and track km 0.18 (b).

6.2.1.2   Insulated rail joint (IRJ)

During an on-site inspection, an insulated rail joint with crushed ballast in an advanced state of wear was identified (see Figure 6.12). The insulated joint is located in a straight section. The sensing conditions are considered to be well suited as the insulated joint is located next to the optical fibre guiding cable duct. Consequently, the sensing capability should not be impaired. Each time a train passes through this section and crosses the specific rail joint a distinctive impact is perceived.

Figure 6.12: Insulated rail joint with characteristic wear pattern after ballast break-up.

Since there is no measurement technology available up to now that can identify and monitor such a fault, DAS data is examined in order to verify the possibility of detecting the described defect. In general, worn-out IRJs are considered as isolated track defects and pose a field of application for DAS.

As there is no record of any maintenance work or deterioration of the IRJ, the time-series of the measurements are not in focus. Any statements regarding the degradation of the IRJ without further documentation would be highly theoretical and only an assumption. The determination of whether and to what extent the failure can be identified and detected is completely appropriate for the outset. Furthermore, the question arises as to how the defect can be assigned to one specific channel or whether the effect of *fading* described in Chapter 2 occurs.

Table 6.3 outlines the statistical values (raw and filtered) of the section in the proximity of the IRJ. The filtered values underline the premised theory that the highest values of the SD are observed at the point and consequently channel linked to the failure. The channels before and after the IRJ show similar standard deviations after applying a high-pass filter.

	Raw signal			HPF signal		
	Before IRJ	IRJ	After IRJ	Before IRJ	IRJ	After IRJ
Min (a.u.)	22,678	23,011	23,969	-3,771	-3,822	-3,842
Max (a.u.)	25,743	25,729	25,742	3,776	5,973	3,839
Mean (a.u.)	24,830	24,856	25,261	-0.051	-0.051	-0.052
SD (a.u.)	423	434	205	46	61	49

Table 6.3: Statistical values of measurements in the proximity of the IRJ.

The discussed results are underpinned by the following figures.

In Figure 6.13 the signal in front of the IRJ is illustrated whereby a distinctive scattering in the raw signal is recognisable. On the contrary, the values of the filtered data are not significant at all and the spectrogram shows no anomalies either.

(a) *(b)* *(c)*
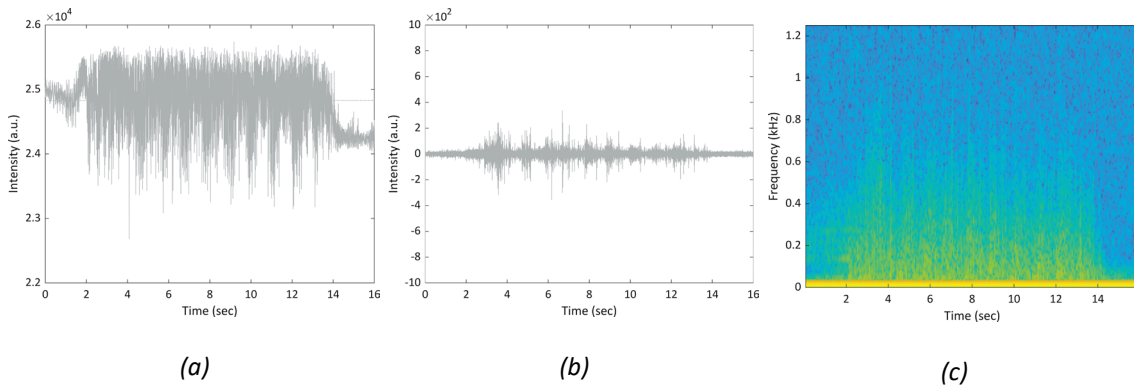
Figure 6.13: Rayleigh backscatter (a), high-pass filtered signal (b) and spectrogram (c) of the channel before the IRJ.

This situation changes for the next figure. While the raw signal of the channel before and the IRJ do not differ greatly, both the filtered signal and the spectrograms certainly do. The response of the infrastructure due to the load of the train is now clearly visible and the impact of the individual axles appear.

(a)   (b)   (c)
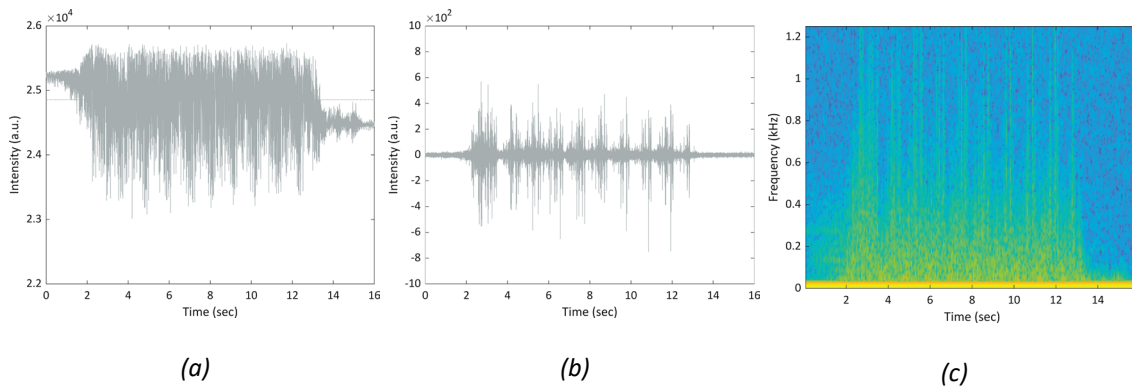
Figure 6.14: Rayleigh backscatter (a), high-pass filtered signal (b)

and spectrogram (c) of the channel linked to the IRJ.

Figure 6.15 shows the DAS signal of the channel next to the IRJ. The altered backscatter of this channel does not correlate with those before as the scattering looks completely different. This does not hold true for the frequency content. The spectrograms of the IRJ and the channel after appear similar, of course, with some limitations. Though the peaks of the filtered data vary significantly, the higher values are on the side of the channel linked to the IRJ.

(a)   (b)   (c)
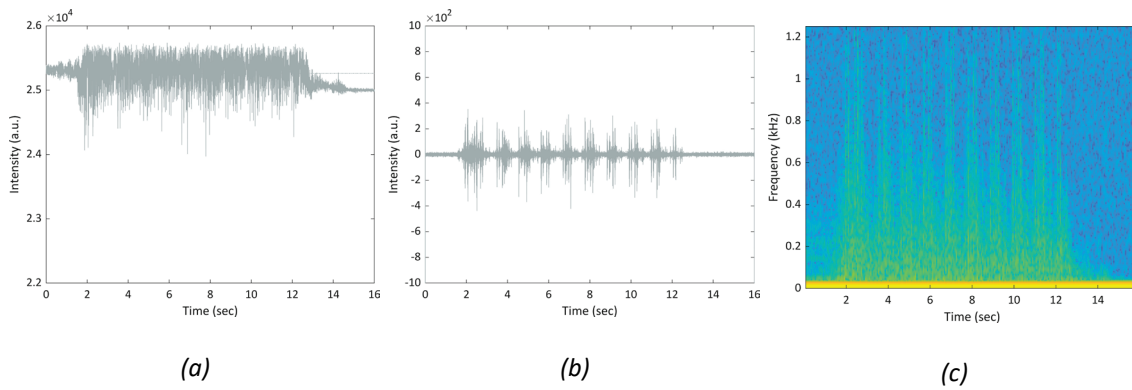
Figure 6.15: Rayleigh backscatter (a), high-pass filtered signal (b) and spectrogram (c) of the

channel after the IRJ.

Conclusively, three key points are particularly striking: 1) there is no fading of the signal into the preceding channel; 2) the spectrogram of the following channel is similar to that of the channel linked to the IRJ and 3) applying a filter reveals the point of failure and enables correct identification of such.

6.3 Turnouts (switches & crossings)

Turnouts are crucial parts of railway infrastructure transferring running vehicles from one track to another, hence raising the capacity of railway systems. Consequently, the success and efficiency of any train operation strongly depend on the performance of turnouts. While it is obvious that they are an integral component, they are also very costly, both in terms of investment and maintenance. Marschnig (Marschnig, 2016) stated that costs of maintenance and depreciation for turnouts – broken down to one track metre – exceed track costs up to eleven times. Reasons for higher cost are mainly the component complexity and moveable parts and more complex vehicle dynamics in turnouts. The graphic below depicts the main components of a turnout which is composed of three main elements: 1) switch panel; 2) closure panel and 3) crossing panel. The switch panel guides a moving vehicle in the desired direction and consists of two half sets of switches at which point the diverging track begins to diverge from the main track. A half set consists of a stock rail and a switching blade – a moveable part directing the vehicle towards the designated track. The beginning of the switch panel is marked by the first rail joint and ends at the switch heels (not plotted in the figure below). The second element – located in the middle – is called the closure panel and connects the switch panel and the crossing panel which separates the main track from the diverging track. The principal elements of the crossing panel are check rails, wing rails and crossing nose. The latter is the point at which two running edges converge. The first rail joint after the crossing panel marks the beginning and ending point of the crossing panel. There are two ways a vehicle can move through a turnout. Facing move if the switch panel is crossed first, trailing move if the crossing panel is entered first.
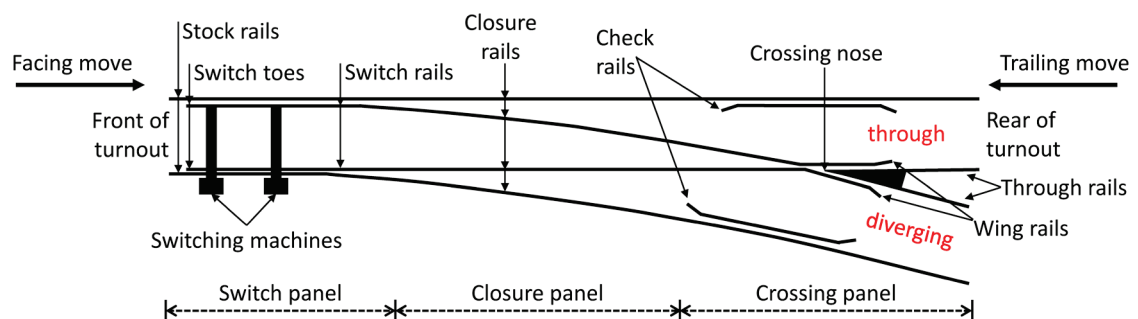
Figure 6.16: Schematic illustration of the components of a single turnout.

As stated, compared to trough-going tracks vehicles are exposed to different and higher dynamics when crossing the certain sections of a turnout. Kassa for instance (Kassa and Nielsen, 2008) reported that the highest lateral force in the switch panel was to be found when a train takes the diverging route (moving in the facing move). However, while no significant vertical force changes were recognised concerning the moving direction, taking the diverging route induces higher vertical contact forces. Some similar observations were also made by Nicklisch (Nicklisch *et al.*, 2010) who outlined that tremendous disruptions can be observed in the switch panel and the crossing panel. The former occurs when wheels move further from stock rail to switch rail resulting in lateral displacements and occasionally wheel flange contact. For the latter, severe impacts are mainly caused by the gap between the wing rail and the crossing nose. Thus, it is not at all surprising that, driven by high costs and the concomitant demand to acquire a deeper understanding of the turnout behaviour, great efforts have been made in recent years to gain knowledge and reduce costs.

One major issue in regard to turnout behaviour is data availability and reliability. For instance, track recording cars are used for the assessment of track geometry. Such measurement technology assessing turnouts under load is lacking in particular. Wilfling postulated (Wilfling, 2017) that among the variety of sensing and measuring technologies not one is able to inspect and capture all relevant parameters considered within a manual inspection. Yet, a combination of all examined systems would allow execution of almost 96 % of the required inspection tasks automatically. To counteract this situation two main approaches have been developed in the past two decades: 1) multi-body simulations of the dynamic train – turnout interaction, mainly for identification and prediction of wear and tear in turnouts and 2) using measurement data for turnout behaviour analysis and prediction of such. The former aim primarily to simulate degradation of rail profiles as a consequence of vehicle/track (turnout) interaction (Kassa, Andersson and Nielsen, 2006; Alfi and Bruni, 2009; Nicklisch *et al.*, 2010; Johansson *et al.*, 2011) in order to avoid severe damage and RCF. Besides the metal parts, it was found that ballast is the service life-limiting component for turnouts on concrete sleepers, upon which for turnouts on wooden sleepers it is the sleeper itself (age and condition) and the inadequate adhesion between rail and sleeper that trigger a replacement of the turnout (Dittmer, 2018). Aiming to describe and predict ballast degradation in turnouts, a study carried out in Denmark gathered acceleration measurements of the rail for two years

(Asadzadeh and Galeazzi, 2019). However, Fellinger (Fellinger, 2020) can rely on a considerably longer time series as he uses data of the Austrian track recording vehicle – usually used for track geometry measurements – for behaviour analysis of turnouts having set the main focus on ballast degradation and prediction of maintenance for such.

The brief literature review above reveals some ongoing research aiming to monitor the condition of turnouts, to analyse the behaviour and consequently to predict their behaviour and necessary maintenance tasks in future, in particular.

In order to examine whether FOS is suitable for turnout condition monitoring, data of 35 turnouts stationed along the monitored route is analysed. The table below gives an overview of the investigated turnouts and their main characteristics, although not all of them will be analysed in detail. All turnouts are single turnouts (ST), whereby rails, diverging radius, crossing angle and sleeper type change (IV = UIC54E; VI = UIC60; diverging radius 1,600 m; C = concrete sleeper; W = wooden sleeper). The average speed represents the speed a train passes through the respective turnout. It is a mean value of all recorded train movements. Additionally, information on the moving direction for every mentioned turnout is provided.

Nevertheless, there are some limitations to be considered. Firstly, data were collected within the project period (~1.5 years) only and no additional measurements were made especially for turnouts. Secondly, no modifications were made regarding the cable route in order to enhance the sensing capability. Thirdly, turnout condition was not assessed separately which means that data on the current condition only exists and is documented for few turnouts (data source *ZMON*, see Chapter 4.1). Also, the positioning process (see Chapter 4.2) had to be carried out for each turnout at which the decisive positions were linked to the channel with the highest intensity observed (e.g. rail joint, crossing nose, weld). Finally, due to the restrictions mentioned the system cannot deliver limit values or define a specific condition leading to decisions such as maintenance or renewal. The data basis for this is merely too deficient and insufficiently validated. In order to derive such conclusions, it would first be necessary to determine the condition of a particular turnout to be able to unambiguously assign signal anomalies and patterns to a fault. Yet based on the approach derived, it is possible to assess the condition of the individual components and compare them with each other. This enables a measurement data-based turnout condition description and provides information about which turnout is in a worse condition.

Turnout	Type	Year of installation	Average speed (km/h)	Moving direction	Turnout in
T1	ST-VI-1600-1:25-C	2006	125.5	Trailing movement	Straight
T2	ST-VI-900-1:19-C	2005	153.6	Trailing movement	Curve
T3	ST-VI-900-1:19-C	2005	148.9	Facing movement	Straight
T4	ST-VI-300-1:9-C	1999	153.8	Trailing movement	Straight
T5	ST-VI-900-1:19-C	2005	153.9	Trailing movement	Straight
T6	ST-VI-900-1:19-C	2012	154.3	Facing movement	Straight
T7	ST-VI-900-1:19-C	1997	148.4	Facing movement	Straight
T8	ST-VI-900-1:19-C	2002	138.8	Trailing movement	Straight
T9	ST-VI-300-1:12-C	2002	138.2	Facing movement	Straight
T10	ST-IV-900-1:19-C	2004	61.5	Trailing movement	Straight
T11	ST-VI-900-1:19-C	2015	88.9	Trailing movement	Straight
T12	ST-IV-300-1:9-C	2005	89.0	Facing movement	Straight
T13	ST-IV-900-1:19-W	1999	84.4	Facing movement	Curve
T14	ST-VI-1600-1:25-C	2005	89.1	Trailing movement	Straight
T15	ST-IV-1600-1:25-W	1999	86.3	Facing movement	Straight
T16	ST-VI-1600-1:25-C	2016	82.6	Facing movement	Curve
T17	ST-VI-1600-1:25-C	2006	130.5	Trailing movement	Straight
T18	ST-VI-1600-1:25-C	2006	122.1	Facing movement	Straight
T19	ST-VI-900-1:19-C	2005	149.4	Trailing movement	Straight
T20	ST-VI-900-G-1:19-C	2005	150.6	Facing movement	Straight
T21	ST-VI-300-1:9-C	2005	151.2	Facing movement	Straight
T22	ST-VI-900-G-1:19-C	2005	141.6	Trailing movement	Straight
T23	ST-VI-900-1:19-C	2012	152.6	Facing movement	Curve
T24	ST-VI-300-G-1:9-C	2009	152.2	Trailing movement	Straight
T25	ST-VI-900-1:19-C	1997	132.8	Facing movement	Straight
T26	ST-VI-900-1:19-C	2002	128.5	Trailing movement	Straight
T27	ST-IV-500-1:12-C	2004	67.4	Facing movement	Straight
T28	ST-IV-900-1:19-C	2007	66.9	Trailing movement	Straight
T29	ST-VI-900-1:19-C	2015	85.5	Trailing movement	Straight
T30	ST-IV-300-1:9-C	2005	88.1	Facing movement	Curve
T31	ST-IV-300-1:9-C	2005	83.6	Trailing movement	Curve
T32	ST-IV-900-1:19-W	1999	87.4	Facing movement	Straight
T33	ST-VI-1600-1:25-C	2005	89.5	Trailing movement	Straight
T34	ST-IV-1600-1:25-W	1999	85.7	Facing movement	Curve
T35	ST-VI-1600-1:25-C	2016	85.0	Facing movement	Curve

Table 6.4: Considered turnouts.

6.3.1 Basic condition analysis of the crossing nose

The approach is based on the results derived previously and, on the signal, obtained by the reference train when moving through a turnout. Applying an HPF considering frequencies higher than 400 Hz shall expose short to middle wavelength failures. As aforementioned, track related signal pattern and response is visible up to 300–350 Hz. With a somewhat more conservative approach, all frequencies below 400 Hz are neglected to let higher frequencies pass only. Afterwards, the standard deviation of each train ride for every single turnout is calculated. The present train passed through each turnout taking the main route. Figure 6.17 depicts the observed results for the crossing nose. The first 16 turnouts are located at track 1, the other ones at track 2. Apart from turnouts T13, T15, T32 and T34, all other turnouts are on concrete sleepers. The standard deviation varies for each single train ride within a turnout and between the various turnouts too. Turnouts T2, T4 and T5 show the highest values as well as the biggest scattering within the measurements. As the measurements are not post-processed in terms of data cleaning, there are several outliers to be identified. This holds true for turnouts T2, T8, T9, T20–T22 whereas the lower whiskers are almost zero.
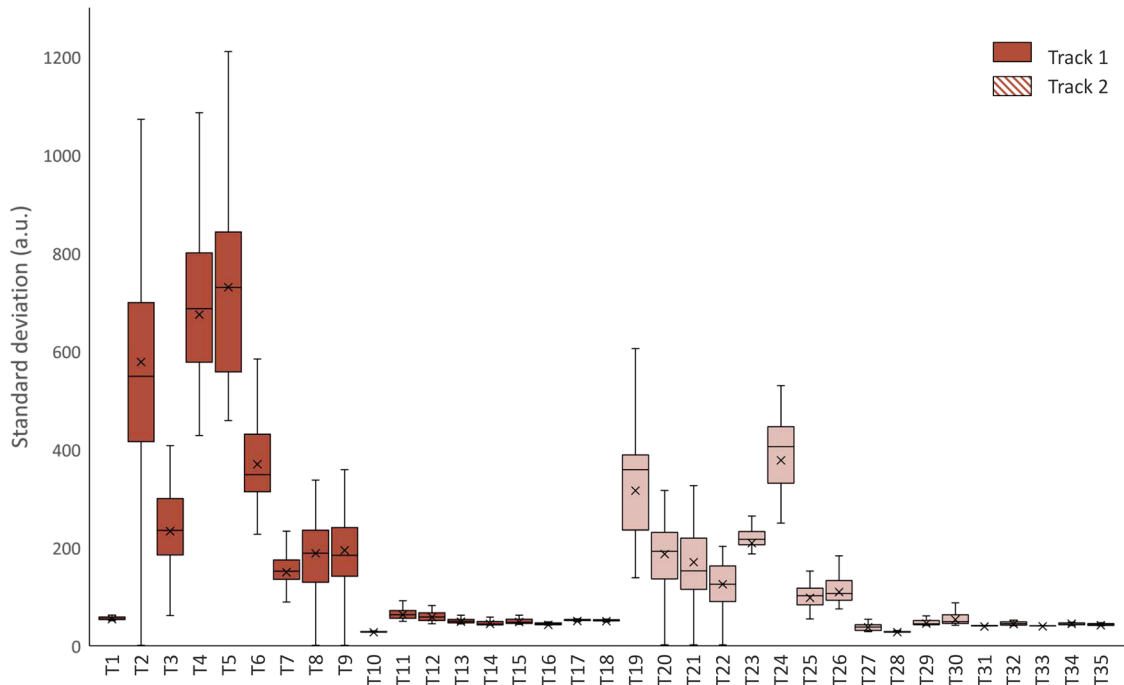
Figure 6.17: Standard deviation of each train ride of the reference train

when passed over the crossing nose of a turnout for track 1 and 2.

Reflecting on the scattering patterns mentioned in the previous chapters, the results below are considered as outliers or faulty measurements for these turnouts.

As stated, the only reliable data source for failures is *ZMON* where inspection staff documents deviations from the initial state of an asset which is indeed highly subjective. An extract from this tool gives the following findings.

For turnouts, T6–T20 and T26–T35 no severe failures or discrepancies were reported at all but there have been some prior to the start of the measurements. Even though T1 shows no suspicious values, reports document loosened welded parts and minor rail surface defects. According to *ZMON,* for turnout T2 (turnout in a curve) and T3, no failures were assigned to the crossing nose, although some minor rail surface defects (head checks) have been reported at stock rails. This does not apply for T4 which is one of the oldest turnouts along the examined route and has been in service for almost 21 years. Assuming an average daily load of 65,000 GT per day and track (currently more than 80,000 GT/day and track) results in a cumulated load of nearly 500 million GT hence it is no wonder several defects, as well as maintenance tasks, are documented in *ZMON* although these specifically only go back to the year 2014. Reported defects as a consequence of increased impact and dynamics include both broken and missing bolts and rail surface defects on the crossing nose or the close proximity. The graphic below confirms these statements. The impact of the vehicle (axles) and consequently the response of the crossing nose is visible, especially after applying an HPF (Figure 6.18b).

(a) (b) (c)
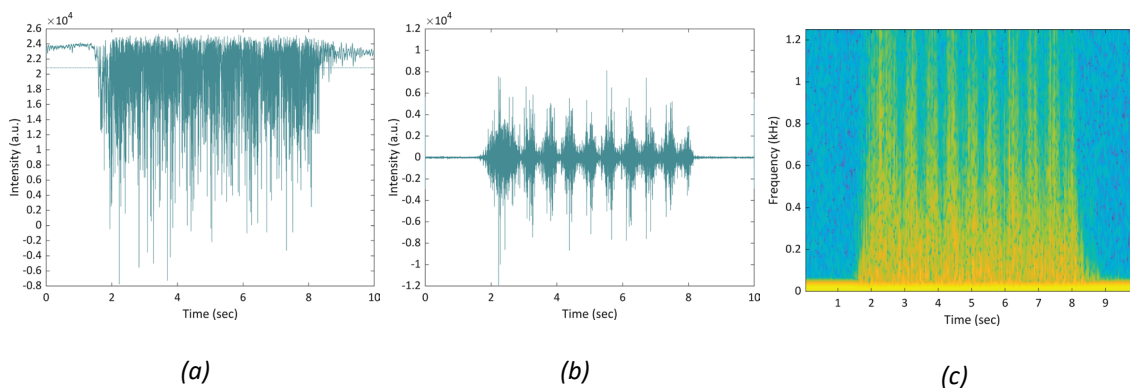
Figure 6.18: Rayleigh backscatter (a), high-pass filtered signal (b) and spectrogram (c) of the crossing nose of turnout T4.

T5 yields an unexpected result as no changed condition regarding the crossing nose was reported, in particular. Nevertheless, the highest values are found to be here. In contrast, corrugation at the stock and closure rails, as well as minor geometric position deviations, were reported. Apart from three missing fishplates at the stock rails, no further discrepancies are documented for turnout T6. Whether the results from Figure 6.17 are related to this cause is somewhat questionable. Reports for turnouts T7 (along with T25 the oldest turnout) and T8 show that there were some head checks in the past, but these were removed (ground) prior to the start of the FOS measurement campaign.

Another remarkable result is obtained by comparing the values for track 1 and 2. Even though turnouts T19–26 are located on track 2 (typically the track further away from the cable duct guiding the optical fibre) a higher standard deviation is noticed. This indicates on the one hand that the measurement has a certain relation to the condition of the crossing point and on the other hand it also applies to track 2. The first two turnouts considered on track 2, T17 and T18, show no severe damage, although minuscule rail surface defects were reported. The same applies to T19–T21 and T24 but are valid for stock rails only in the case of T19 and T20.

On account of the measuring principle, it is unlikely that such an error will be reflected in the signal. Besides, for T22 and T23 (one of the youngest) no defects were reported in the vicinity of the crossing nose, although major defects were noticed at the closure rails such as head checks and breakouts on the driving edge for T22. In contrast to the previous observations, T25 reveals several documented defects. In addition to exfoliations at the crossing nose and rail cracks at wing rails and the crossing nose, head checks were also reported. Given these observations, the results are surprising. However, this can probably be justified by the variety of maintenance carried out at this point, which will be discussed further in the next chapter.

Due to the results above the question arises regarding the influence of travelling speed on the values given. Figure 6.19 provides an answer to this issue. The x-axis represents the average travelling speed of all recorded train rides of the reference train when passing through a turnout. The y-axis, on the other hand, represents the average standard deviation of all train rides through a turnout for every single turnout.

Trains travelling at speeds slower than 80 km/h have less impact. That is scarcely surprising as lower speed leads to fewer vehicle dynamics and only matches up to three turnouts (T10, T27 and T28). Although this means that higher speeds lead to higher values, there are significant differences identifiable. Especially for speeds over 120 km/h, the standard deviations vary distinctively, whereupon the speed is equal for different turnouts, but the values are not. This implies that there is a correlation between the condition of the crossing nose and the standard deviation. For instance, T6 is passed through with the highest speed whereby the values are significantly lower than for T2, T4 and T5 and the average speeds differ only marginally. Furthermore, T1 is passed with average speeds over 125 km/h but shows no noticeable values and even at T3 the speed is almost 150 km/h, but the standard deviation is far below T2, T4 and T5. T19 has considerably higher values than T20 but the speed is almost the same. For T24 and T6 both the speed and values are nearly at the same level.
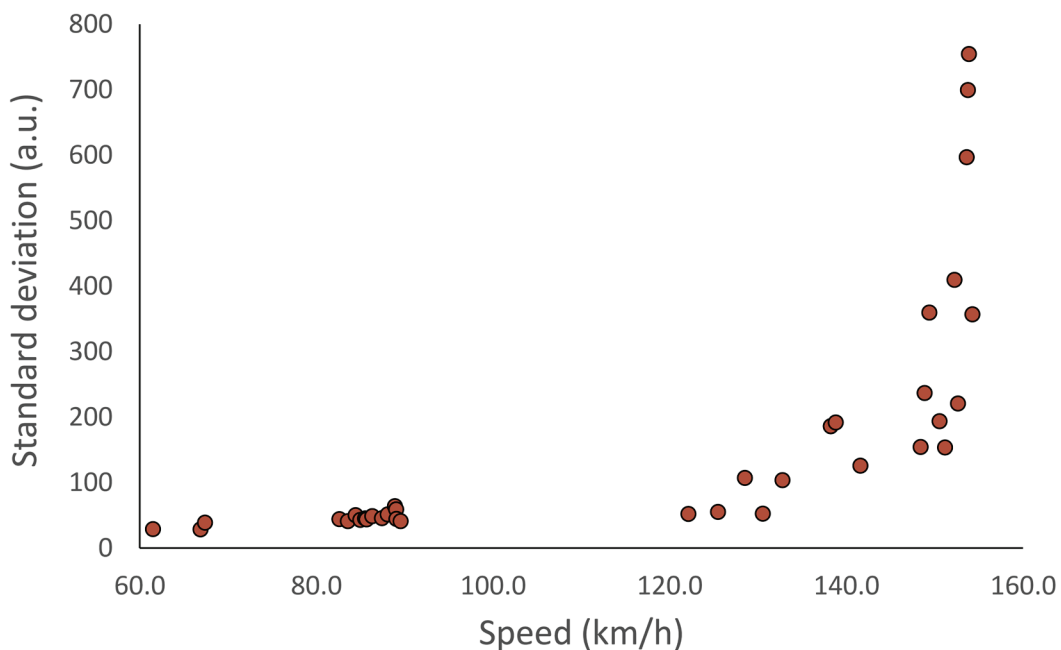
Figure 6.19: Mean standard deviation versus the average speed of a train

when passed over the crossing nose of a turnout on track 1 and 2.

A further noteworthy aspect becomes apparent when considering the direction of travel. For instance, the train passed through turnouts T1, T2, T4, T5, T8, T19, T22 and T24 in trailing move. T3, T6, T7, T9, T21 and T3 were passed through in facing move. Thus, no significant relationship between moving direction and track response due to train load and impact is identified. This

result is consistent with examinations carried out by Fellinger, who used measurement data from a track recording vehicle focussing on turnout behaviour analyses. Such data must be mirrored in the first step as a TRV does not always move through a turnout in the same direction. This is because of a measurement campaign planned and carried out. However, data mirroring according to the moving direction of the track recording vehicle does not influence the data quality and in particular the results.

The results discussed are also valid for the condition of the switch panel. The examinations show that it is possible – analogue to the observations derived for the crossing nose – to draw conclusions on the condition of this area.

In the subsequent chapter, the effects of component exchange and grinding on signal pattern and properties are examined. This will be shown on two separate turnouts and conclusions will be drawn upon this, which are valid for further turnouts.

6.3.2   The influence of maintenance tasks and component exchange

6.3.2.1   *Component exchange*

As aforementioned, for T24 – a turnout with almost 23 years in service and hence subject to high stress, several defects are documented in *ZMON*. Some of the pictures taken during the on-site inspection from SBB's inspection staff are shown in the figure below (© SBB) demonstrating exfoliations and a crack of the crossing nose.

Figure 6.20: Documented defects at T25 reported in ZMON.

Figure 6.21 displays the signal properties of the certain turnout before an executed component exchange. The spectrogram indicates that excitations indeed occur in the higher frequency range in the area of the crossing nose as a consequence of higher dynamics. The train passes through the turnout in facing move whereby the average speed slightly exceeds 130 km/h. Turnout 25 lays on track 2. Travelling in this direction, the formation of the reference train is changed at which the locomotive is located at the end pushing the coaches. This becomes apparent after applying an HPF (see Figure 6.21b). The distance between the bogies is constant between seconds two and eight and changes immediately as a response to the properties of the locomotive. It is additionally remarkable that the impact of the first axles of coaches three and

six are the highest, even higher than those of the locomotive. This can be on the hand due to load or wheel condition of the vehicle, or a consequence of the changing dynamics and running behaviour when passing through a turnout with such a defect.

(a) (b) (c)
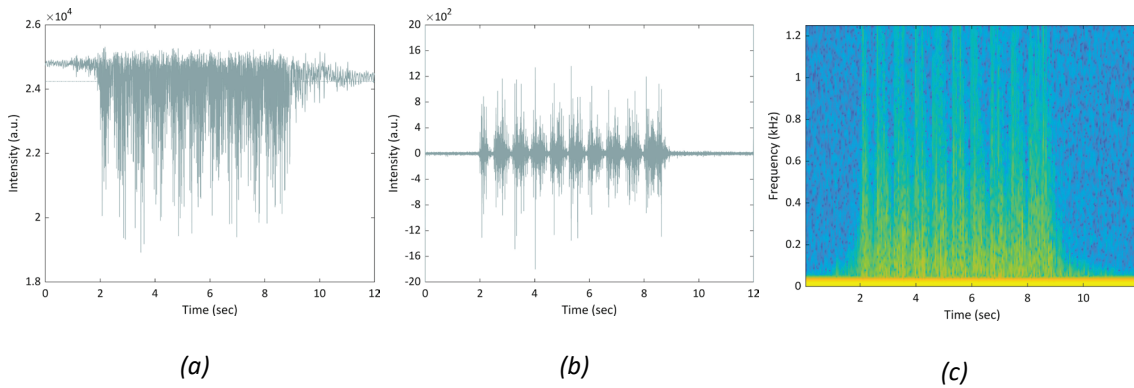
Figure 6.21: Rayleigh backscatter (a), high-pass filtered signal (b)

and spectrogram (c) of the crossing nose of turnout T25 before component exchange.

The maintenance plan envisages a component replacement, or more specifically an exchange of the crossing nose for this turnout. The plan was executed at the beginning of June 2018.

The time series of the obtained signal is illustrated in Figure 6.22.
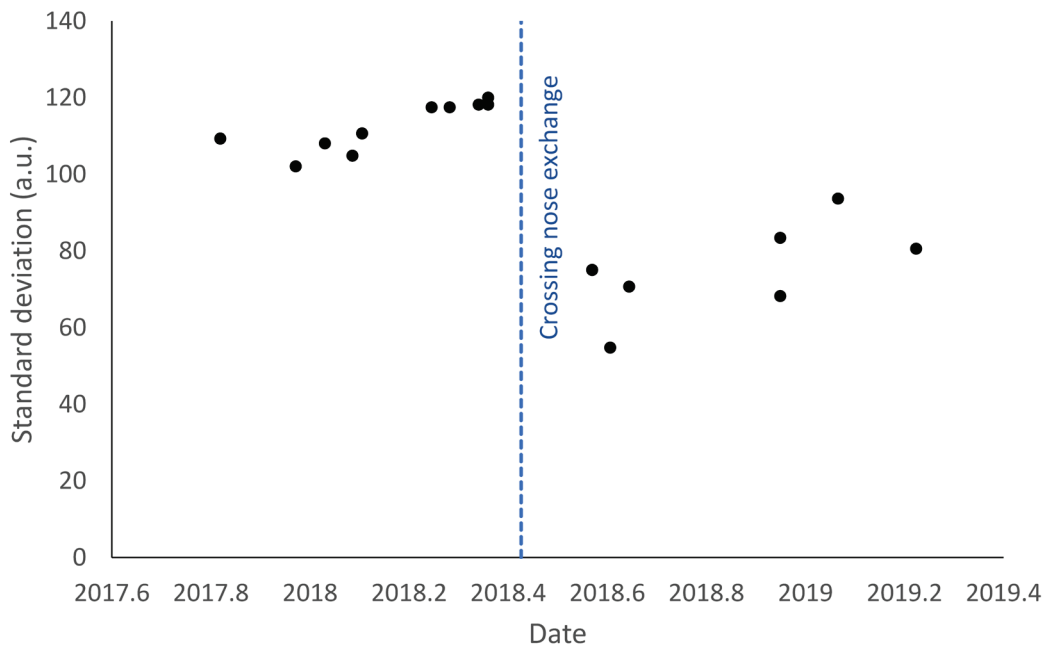
Figure 6.22: Time-series of the crossing nose of T4.

Again, an HPF is applied with 400 Hz cut-off frequency and the standard deviation (SD) is subsequently computed.

In general, the SD here is at a substantially lower level and the values scatter only slightly. The measurements seem to be stable here. In any case, after the maintenance, the values improved significantly thereupon all values are well below 100 (a.u.).

This is also confirmed when looking at the spectrogram computed after the maintenance task. In this case, the root cause of higher frequencies was eliminated after the component change and the amplitudes are now also considerably smaller and the deflections hardly noticeable (see figure below). Furthermore, the highest values are caused by the axles of the locomotive.

(a)   *(b)*   *(c)*
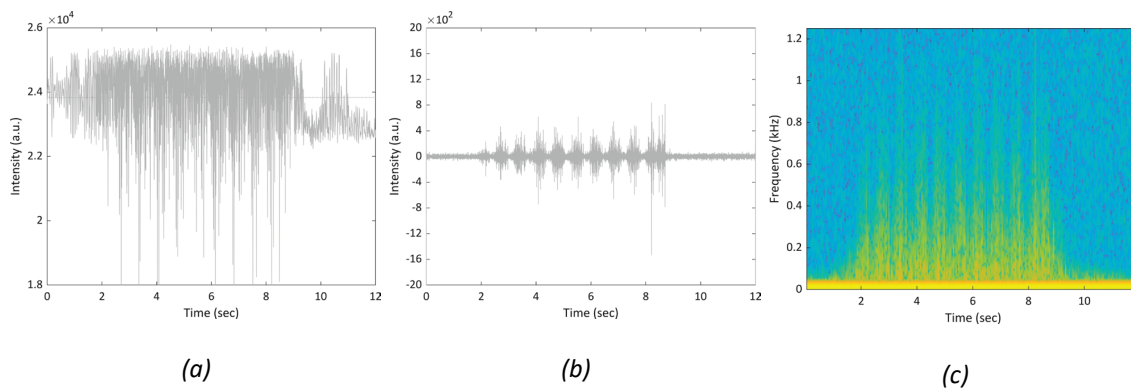
Figure 6.23: Rayleigh backscatter (a), high-pass filtered signal (b)

and spectrogram (c) of the crossing nose of turnout T25 after component exchange.

6.3.2.2   Grinding

For the crossing nose of turnout T3, periodically occurring cracks (head checks) and breakouts at the running edge are documented in *ZMON*. The corresponding pictures of the on-site inspection of the inspection staff are depicted in the graphic below.

Figure 6.24: Documented defects at T3 reported in ZMON.

Apart from the damage pattern mentioned, no further defects such as displacements of the crossing are documented for this turnout either. Although the average crossing speed through this turnout in through direction is among the highest, the standard deviation is way below that of other turnouts.

In April 2018, grinding as maintenance work was scheduled for this turnout and finally executed. The following figure shows the standard deviation of the filtered signal for the area in the vicinity of the switch toes (Figure 6.25a) and the crossing nose (Figure 6.25b). While the time series of the switch toes reveals no distinctive behaviour, that of the crossing nose is even more remarkable. The crossing nose shows higher values before and after the maintenance task than the area around the switch toes. However, the behaviour of the crossing nose after grinding is odd. After the maintenance was executed the values are immediately higher than before. Only after a few months and thus the passing of millions of tons do the figures return to similar levels as before the measure.

What initially appears to be more than questionable was confirmed by several discussions with SBB and DB asset managers. The phenomenon shown here has already been observed several

times. It is that after a grinding task the noise level of the rails increases and normalises only after a myriad of train crossings.

(a)

(b)
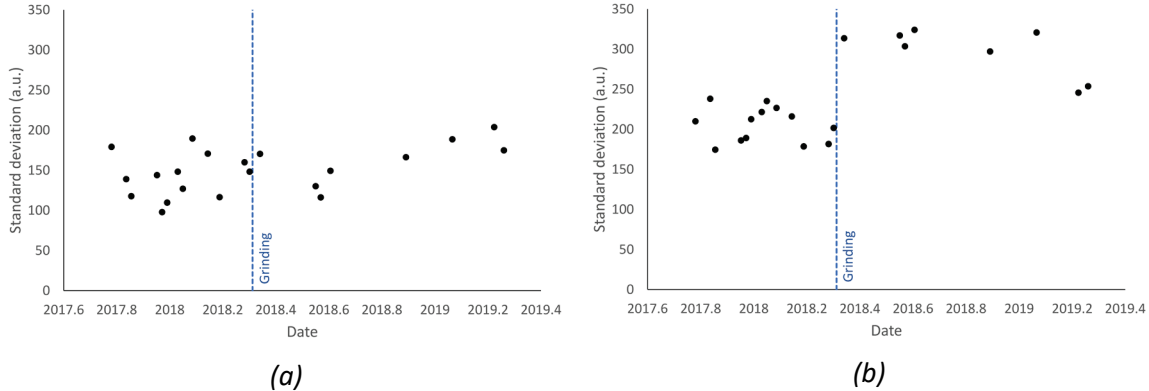
Figure 6.25: Time series of (a) the switch toes and (b) the crossing nose of T3.

In conclusion, the executed grinding work has led to significantly changed values in the crossing nose's proximity. However, this does not apply for the switch toes. Naturally, the further evolution of the signal would have been of enormous interest, but due to the completion of the project no description of this can be provided.

6.4 Conclusion

The observed results prove the system's ability for condition monitoring of various vital assets. While the raw data – originally observed backscatter – does not allow one to draw unequivocal conclusions, this issue can be tackled by applying an HPF with a specific cut-off frequency. This enables determining the condition of the track, IRJs and in particular the crossing noses.

Even if the system has some shortcomings – such as fading – the highest values appear at the position or rather in the channel assigned to the failure. This circumstance must be taken into account.

Furthermore, as the assets are in different states of wear, the measurements allow for a comparison in terms of which asset is in a more advanced wear condition and should be monitored more frequently. Furthermore, as demonstrated it is even possible to analyse the trend of the measurements and to monitor the deterioration process. After all, maintenance works performed on assets/positions are reflected in an improved signal pattern and scattering. This is particularly true if the previously much worse condition could be remedied by maintenance measures. In the case of assets not showing serious defects the improved condition cannot be determined unambiguously.

DAS delivers valuable information on the condition of sections/points degrading rapidly and where the measurement intervals of the TRV are not frequent enough. Such defects (white spots) require adjusted measurement campaigns as they show steeper deterioration rates and can lead to safety-relevant conditions.

FOS shall not aim to replace a TRV, which is anyhow not possible as the latter measures relative settlements and DAS delivers information on the vibrations and the reactions of the track due to the load caused by train movements. At the moment, the systems do not allow one to draw conclusions regarding the track quality in terms of limit values which are decisive for safety and track quality, but it gives an indication of where a certain failure is present.

7 ASSET MANAGEMENT – ADDITIONAL ASPECTS

7.1 Introduction

Sustainable asset management requires both an objective condition evaluation and decision making based on these evaluations. Such decision making shall not neglect the economical aspects of assets but rather must be included in such considerations. The renewal rate and the average service life are directly linked. In terms of maintenance, this is sometimes a somewhat challenging task. In theory, an asset has reached its economic service life when the cost decrease in depreciation is lower than the cost increase in maintenance (Veit, 2007). These relationships are beyond any doubt and are generally applicable. This is also valid for the correlation between maintenance quality and asset condition. The better the maintenance work carried out, the better the restored condition will be. As stated (see chapter Introduction) IM determine the state of their assets through a combination of inspections by experts, various measuring cars and sensors. Each of the mentioned activities assess the condition but neither surveys the quality of executed maintenance works. Based on this, the question arises: how to assess the quality and quantity of maintenance? This issue is directly related to *RQ5*.

As a consequence of loading and stress, railway infrastructure must be maintained several times during its service life. While the maintenance task tamping improves track geometry, rail grinding, rail milling and rail planing are used for removing rail surface defects. In general, tamping and grinding are the most common maintenance measures in terms of track maintenance machines. The overwhelming part of this work is carried out at night, whereby the documentation of the work carried out is often inadequate and incomplete. To date, the evaluation and documentation of the work carried out have been the responsibility of the maintenance company (contractor), while the IM can at best determine during the next measurement run whether and with what success the previous maintenance work was carried out. This circumstance applies above all to the evaluation of tamping work carried out. These matters are addressed in this chapter as it deals with the question of whether planned and executed maintenance tasks can be detected and evaluated with DAS. Furthermore, it outlines differences between scheduled and executed work and pursues the issue of whether the track

closure was long enough and in case it was too short, whether this became apparent in the working progress.

In the period during which the sensing system could be accessed, 22 maintenance tasks were planned on the monitored route, of which 14 were grinding actions and eight tamping works. The scheduled plan included works on both track and turnouts. Furthermore, information on the specific track and turnout as well as track km was available. Connecting this asset data with the specific channels (see Chapter 4.2) aims to determine whether and to what extent the individual works differ from each other in case they could be detected, while keeping the data amount at a reasonable level providing that information was mandatory.

In order to keep the extent of this thesis within acceptable limits, the measurements of several nights for both tamping and grinding are presented as examples. This is followed by a presentation of the other recorded tasks and a discussion of the results.

7.2 Tamping

7.2.1 Basic analysis

In the area of *Gümligen station* tamping actions for three tracks and twelve turnouts were scheduled on three consecutive nights (c. f. Table 7.1). On the first night tamping was planned for a section of more than two km (>200 channels) assigned to track 1 starting at channel 718 and ending at channel 923. Within the same shift, the maintenance of four turnouts is additionally intended. Further track tamping of sections of track 2 and 3 are planned on the third night, where the maintenance for four more turnouts is also scheduled. During the shift on night two, turnouts 51, 52, 55 and 56 are expected to be maintained.

As mentioned one shortcoming of the utilised technology is the inability to identify the specific track at which an event occurs. While this is a challenging task in the case of double-tracked lines it does not get easier for lines with even more tracks with complex track layouts. In principle, this means that train crossings, maintenance work and also access by unauthorised persons can be clearly assigned to a cross-section (channel) and consequently to the line kilometre but not to a specific track. This may be sufficient for third party intrusion detection and protection of malicious attempts, but track-specific allocation is necessary for condition monitoring.

Indeed, this can be handled rather easily in this case as the sections of all three tracks vary over the length and the starting and ending point also differ. Hence a clear assignment of the maintenance work to a specific track is only possible due to the different section lengths and starting points. Yet these statements are based on the assumption that the section in question will also be maintained at the intended length and that there will be no major deviations.

	Channel		Maintenance scheduled
	Start	End	
Track 1	718	923	Night 1 10 p.m. – 6 a.m.
Turnout 5	899	895	
Turnout 6	887	890	
Turnout 26	818	823	
Turnout 27	818	815	
Turnout 51	773	765	Night 2 10 p.m. – 6 a.m.
Turnout 52	754	762	
Turnout 55	741	732	
Turnout 56	719	728	
Track 2	888	936	Night 3 10 p.m. – 6 a.m.
Track 3	882	936	
Turnout 1	932	923	
Turnout 2	911	920	
Turnout 3	910	902	
Turnout 4	889	898	

Table 7.1: Scheduled tamping plan for area Gümligen station on three consecutive nights.

The maintenance plan above is naturally subject to certain variations. Such plans are made one year or even more in advance and require some flexibility. This may be necessary because of a changed path allocation for example. In addition, logistical constraints may result in changes in the machine transfer, which will defer the start of the work to another point. However, it is also possible that synergies may arise in the course of the work and other parts may be prioritised and others postponed, but at least the length to be maintained should be considered as constant.

In general, the backscattered intensity, scattering and signal properties as a result of maintenance work and machines do not differ too greatly from patterns discussed in previous chapters. Therefore, a waterfall diagram is generated in a first step to examine whether a maintenance task is detectable using FOS. As a waterfall displays all events taking place on and near a track, this process is just like the one described in subchapter 5.1.

Once again, a BPF with a bandwidth between 43–201 Hz is applied to reject all other frequencies outside this range, allowing a comparison of the results of Figure 5.2 and the upcoming ones. The train paths of these analyses of the three recorded nights are depicted in the following figures.

Gümligen lies on the route between *Bern* and *Münsingen*, which is why the recordings were made with IU1 only. All three figures show the train traffic operated between 10 p.m. and 5 a.m. but the train paths occur now as thin trajectories. This is of course due to the long period of over seven hours displayed. On the horizontal, the channels are plotted increasing to the right while the ordinate shows the time. The colour scheme in the waterfall diagram indicates the level of acoustic intensity of an occurring event at which blue represents noise or no detected event and red a very loud acoustic signal with strong vibrations. The bulk of the traffic handled can be assigned to the freight division. This is why hardly any stops can be discerned and the trains run through in a continuous flow. On the first night (c. f. Figure 7.1) in addition to the regular train operation, two more events, namely the planned tamping tasks, are observed between the channels 890 and 940.
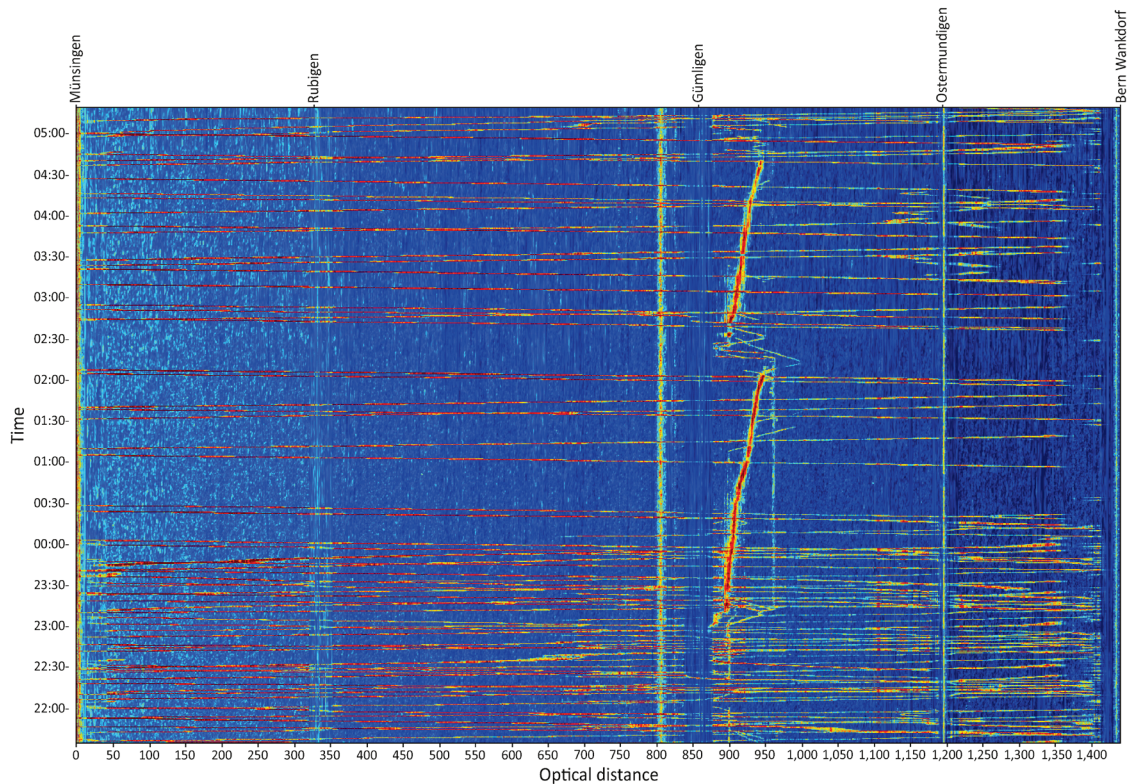
Figure 7.1: Waterfall diagram on the first night with detected tamping tasks.

While the first part started at ~11:15 p.m. and ended at ~2 a.m. (~3 hours) the second one lasted for somewhat more than two hours, starting at ~2:30 a.m. and ending at ~ 4:45 a.m.

A comparison of the recorded work with the scheduled plan of action reveals that this does not correspond entirely to the planned work from the first night.

Another point of interest is that within the night shift the line was closed entirely avoiding any train traffic (0:30 a.m.–1:10 a.m., 2:10 a.m.–2:45 a.m.). Furthermore, during this period only a few trains were approved to pass.

On the second night (see Figure 7.2) three separate tamping tasks are detected taking place mainly between the channels 740 and 800. In contrast to night one, these tasks were executed right in front of *Gümligen station*.
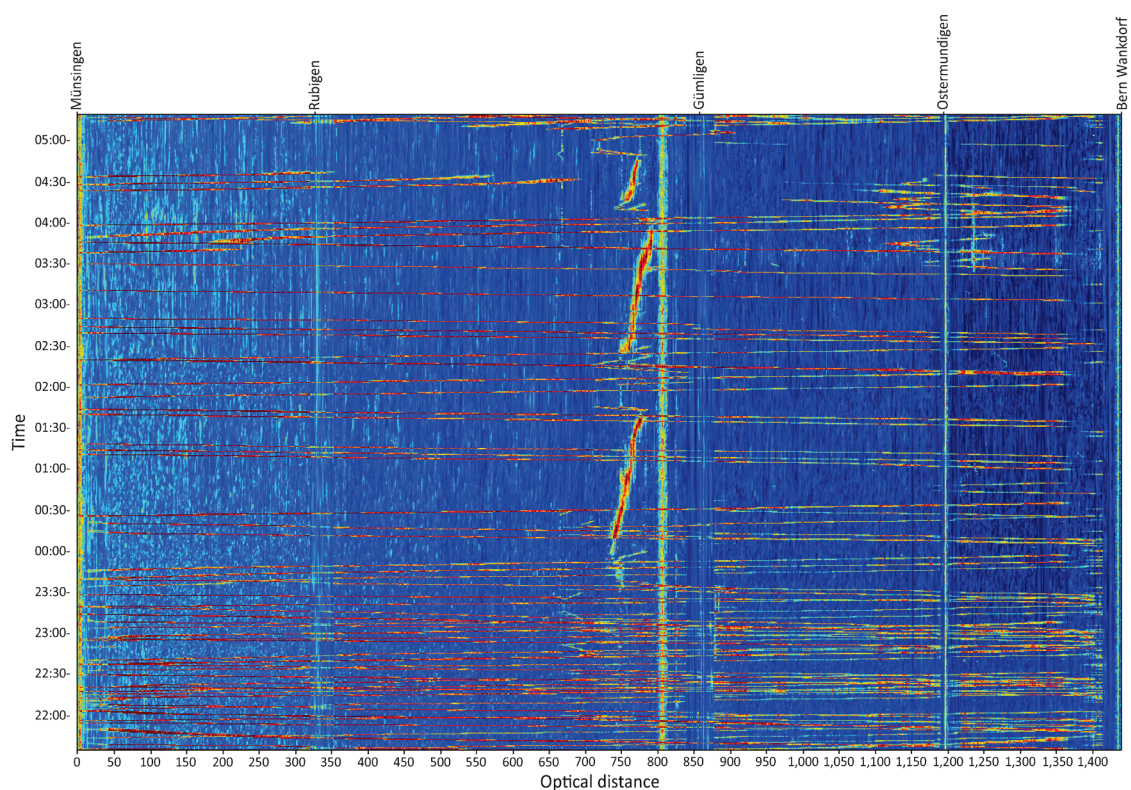
Figure 7.2: Waterfall diagram on the second night with detected tamping tasks.

Starting with the first tamping work at midnight the three tasks lasted all-in-all around four and a half hours. While the first two tasks were finished in less than two hours each, the third one did not even last an hour. It is remarkable that, in contrast to the first night, a total track closure

only took place once (~ 0:30 a.m.–1 a.m.). Towards the end of the shift, however, there were hardly any trains operating between 4 a.m. and 5:30 a.m. During the last night (see Figure 7.3) several shorter tamping tasks are observed. Starting before midnight at channel 900 the last maintenance detected was in front of *Gümligen station* at ~5 a.m. Again, the line was closed several times for at least 15 minutes to half an hour (0:45 a.m.–1:15 a.m., 3 a.m.–3:15 a.m.).

In addition to the maintenance work, another acoustic source is to be found around channel 800. Evaluations show that this is a municipal road that crosses the railway line.
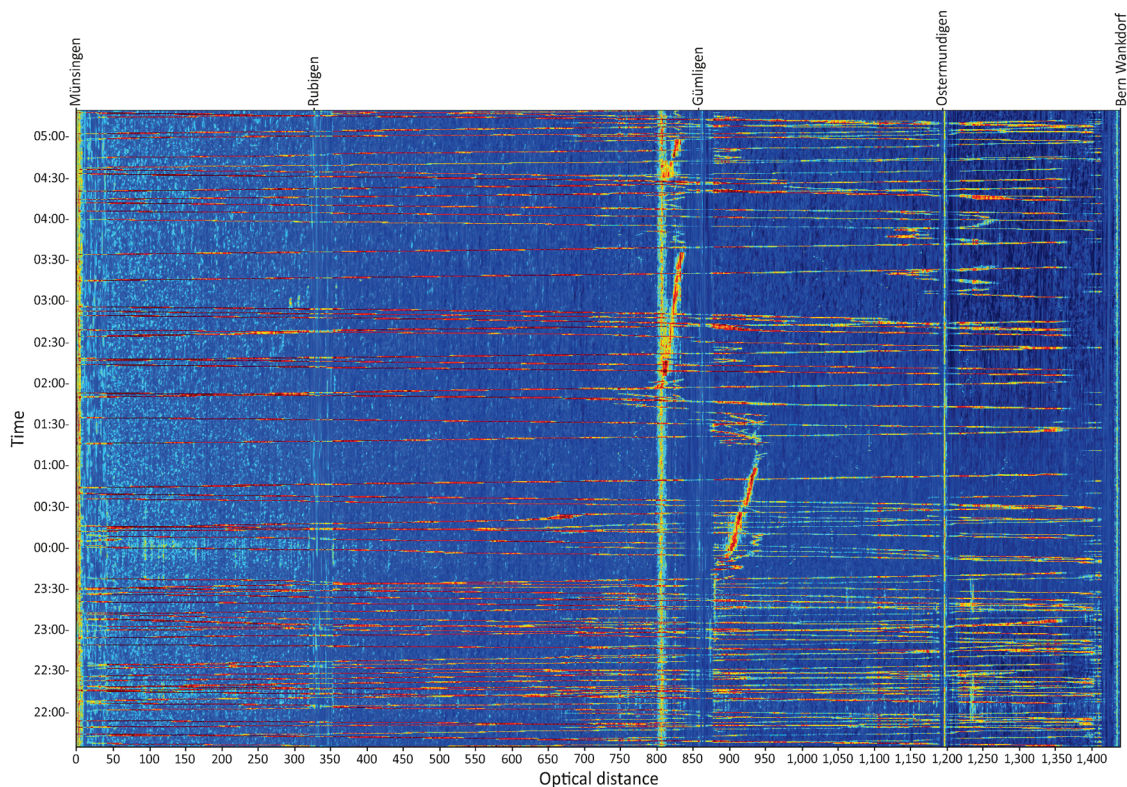
Figure 7.3: Waterfall diagram on the third night with detected tamping tasks.

In principle, it can be confirmed that the scheduled tamping plan was adhered to for the most part. The only exception is the area around channels 700–740 where no maintenance work can be detected during all three nights.

For a plausibility check of the recorded data, it was necessary to compare the results above with the execution reports (which are not owned by the asset manager).

Both turnouts 55 and 56 and the track section between the channels 718 and 740 have not been maintained according to the reports organised by SBB. The track closure seemed to have been too short. Another remarkable result is the accelerated working process on the third night visible for the tamping tasks executed after 2 a.m.

It must be additionally noted that the exact start and endpoints of the work cannot be clearly determined due to the system properties. Firstly, the spatial resolution of 10 m is a limiting factor and secondly, the acoustic intensity of a maintenance machine and the induced vibrations are much more intense compared to conventional freight and passenger trains. As a consequence, the signal scatters in several channels due to the excitation of the optical fibre caused by the working machine. This is reflected in the signal pattern of adjacent channels.

In the following section, detailed evaluations of the tamping work carried out are discussed. The aim is to investigate whether tamping work can be identified as such and whether the quality of the work can be inferred from this.

7.2.2 Tamping process analysis

The maintenance process tamping is nothing new and already well-published (Auer, Hauke and Wenty, 2015; Wenty, 2016; Auer *et al.*, 2018). While in the early years focus on tamping process enhancements was set, the latest developments in machinery technologies aim to assess the ballast condition during the maintenance task. For this purpose, tamping tines of tamping machines are equipped with multiple sensors measuring e.g. the compaction energy (Barbir *et al.*, 2019) or squeezing and tamping forces in order to carry out condition-based and therefore optimised maintenance (Offenbacher, 2019).

Note that this is not within the scope of the following analyses, although the sensing properties and results may allow for conclusions on ballast condition.

A tamping process begins with positioning of the tamping unit and aligning the track. Subsequently, one to three consecutive squeezing processes are performed; one squeezing process includes 1) ballast penetration; 2) squeezing movement and 3) lifting of the tamping unit. Modern machines used nowadays are multiple tamping machines moving forward continuously at a certain speed. This means that the machine does not have to stop during the tamping process. After the adjustment of the tamping unit, it is lowered, and the constantly

vibrating tamping tines start to penetrate the ballast bed. After reaching the final depth, the squeezing movement begins, and the ballast is compacted underneath the sleeper at a frequency of 35–42 Hz. These values, of course, differ from supplier to supplier and are related to machine properties. During the penetration of the ballast and lowering of tamping tines into the ballast, higher frequencies are sometimes reached. Ultimately, the tines are opened, and the tamping unit is lifted. The number of squeezing processes depends not only on the current track condition but also on the experience of the machine operator and may be repeated once or twice. However, the maximum number of squeezing processes should not exceed three and the squeezing time (squeezing movement) should be 0.8–1.2 seconds (Auer, Hauke and Wenty, 2015; Zaayman, 2017). These are, of course, theoretical values specified by manufacturers.

Infrastructure managers have no means of validating such parameters and must, therefore, rely on the information provided by the maintaining contractors. As these factors are quality and key parameters for tamping tasks, the question arises regarding the possibility of analysing executed tamping tasks utilising DAS.

In-depth analyses of the executed tasks are carried out based on the results shown in Figure 7.1–Figure 7.3. Although it is only an excerpt of a couple of channels, the results can be considered as generally valid.

Figure 7.4 depicts a detailed view of tamping processes between channels 920–924. The figure on top shows the intensity of the signal for each channel, with the dark red areas indicating a particularly high acoustic intensity (time on the x-axis, channels on the y-axis, power of the acoustic signal in dB on the right-hand side). The signal pattern suggests that the dark red areas are the respective squeezing processes. In the first 10 seconds, the tamping tines are closed three times, while the squeezing time appears constant. Afterwards, the tamping unit is moved forward to the next sleeper.

Between 4:10:40 a.m.–4:10:50 a.m., the ballast is penetrated and squeezed once at which the squeezing movement lasted slightly more than one second. The next tamping process, taking place between 4:10:20 a.m.–4:10:30 a.m. consists of one ballast penetration, two squeezing movements and finally, the lifting of the tamping unit. The results are generally in line with the manufacturer's specifications described above.

Another point of interest is, in particular, the current tamping frequency. Fischer has shown that frequencies permanently higher than 45 Hz set ballast in motion, somehow like a viscous state almost fluid, resulting in a less compacted ballast (Fischer, 1983). However, the latest in field tests have shown that increasing tamping frequency from 35 Hz to 42 Hz leads to improved tamping results (Grossniklaus, 2016). Applying an FFT reveals that the dominant frequency range of each tamping process and squeezing movement is between 35–45 Hz (see Figure 7.4, middle illustration, time on the x-axis, frequency band on the y-axis, power of the acoustic signal in dB on the right-hand side). Higher frequency ranges are only attained when the tamping unit is lowered, and the tamping tines start to vibrate, and when the tines and the unit are lifted. Utilising higher frequencies eases the insertion of tines and reduces the formation of fine particles to a minimum.

A more detailed examination of the individual squeezing movements and tamping processes indicate that the squeezing time never exceeds 1.2 seconds. This correlates with both the information provided by the tamping machine manufacturers and reports from the maintenance staff. The number of squeezing movements varies between one and three, which is particularly remarkable as this is a section with concrete sleepers and has to be maintained at a maximum of two squeezing movements per sleeper according to the instructions for tamping operations provided by the IM. Figure 7.4 is supplemented by the illustration of the backscattered signal at the lower end, which is only shown for the sake of completeness.
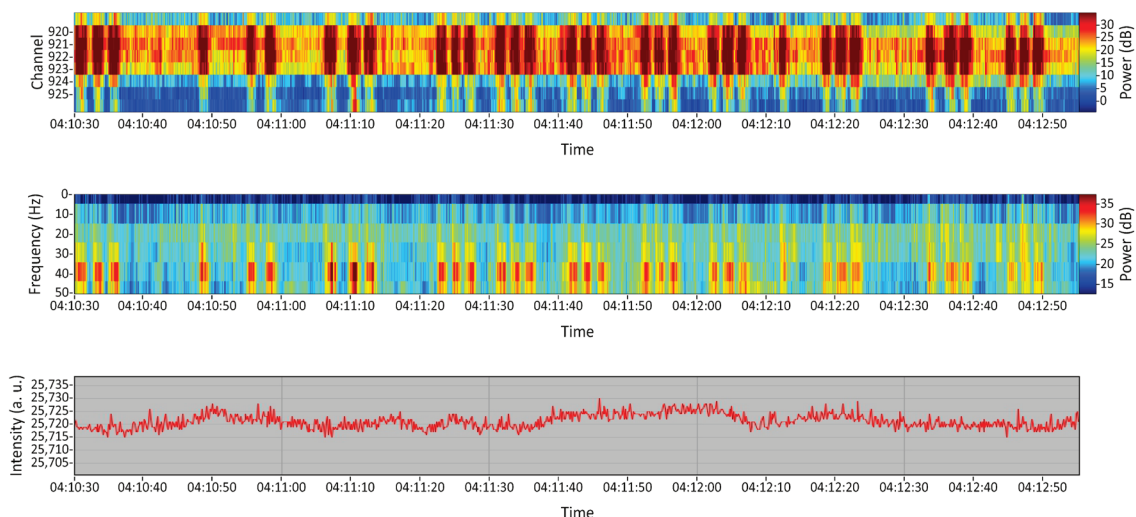
Figure 7.4: Detailed analysis of tamping processes of executed tamping measures.

7.3 Grinding

7.3.1 Basic analysis

Rail defects as a result of load and stress shall be removed in order to guarantee safe railway operation. The surface of rails can be treated in four different ways. The most common ones are rail grinding, rail milling and rail planing. Build-up welding as a maintenance measure is a special case and therefore exceptional. However, rail grinding is the most common measure for rail surface treatment and, depending on the type, can be classified into five groups (adapted from (Fendrich and Fengler, 2019)):

1) grinding of new rails
2) preventive grinding
3) maintenance/corrective grinding
4) grinding of welds
5) grinding to reduce noise.

The vital characteristics of the grinding types mentioned are described briefly below.

New rails are ground shortly after installation in order to remove micro-bumps and sinter as a result of the manufacturing process. Preventive grinding is carried out, on the one hand, to eliminate defects before they reach safety-relevant values, for example, and on the other hand, to maintain and achieve quality values defined individually by IMs. For a re-profiling of the rail, corrective grinding is used whereby, in contrast to preventive grinding, the measure is reactive and any damage to the rail surface that has already occurred is corrected. The grinding of welds takes place after the joint welding of two rails. Rail surface defects generate additional noise in interaction with the wheels and must, therefore, be corrected, especially in urban areas. A significant noise reduction can be achieved by utilising machines applying oscillating grinding processes.

In analogy to the scheduled maintenance plan in the area of *Gümligen station*, a plan for the grinding of track and turnouts was also set up (c. f. Table 7.2) for *Thun station*. What is striking in this case is that there is no explicit mention of the night in question. Merely the number of turnouts and tracks to be ground is given. The planned maintenance tasks are set to be performed on three consecutive nights.

	Channel		Maintenance scheduled
	Start	End	
Track 1	1,551	1,561	
Track 2	1,533	1,541	
Track 3	1,536	1,549	
Turnout 198	1,573	1,570	
Turnout 217	1,571	1,574	Night 1 – 3
Turnout 219	1,575	1,578	10 p.m. – 6 a.m.
Turnout 221	1,579	1,581	
Turnout 223	1,581	1,579	
Turnout 224	1,585	1,582	

Table 7.2: Scheduled grinding plan for area Thun station on three consecutive nights.

During the project period, several grinding measures were carried out. A selection of scheduled works from three nights in *Thun station* will be discussed in detail below. *Thun* lies on the route between *Münsingen* and *Spiez* which is why the recordings were made with IU0 only. All three figures (Figure 7.5–Figure 7.7) show the train traffic operated between 10:30 p.m.–4:40 a.m.

As before, the train paths occur now as thin trajectories with varying intensities of course. This is naturally due to the long period of over seven hours displayed. On the horizontal, the channels are plotted increasing to the right while the ordinate shows the time. Again, the colour scheme in the waterfall diagram indicates the level of acoustic. Blue represents noise or no detected event and red a very loud acoustic signal with strong vibrations. On the first of the three nights, maintenance work is detected between channels 1,575 and 1,650. In the case of the work depicted here, the zigzag pattern is particularly striking. On the one hand, this can be explained by the geometric properties of turnouts, because grinding of the main track as well as of the diverging track is necessary. On the other hand, when re-profiling a track or a turnout, the same spot is crossed several times resulting in the particular zigzag pattern. The first grinding work starts at 10:20 p.m. and ends at 10:50 p.m. This section is ground a total of eight times over a length of approximately 110 m. Both the length of the work and the number of overruns are visible in Figure 7.5 between channels 1,600–1,700 during.

The next section is maintained six times in two steps over a length of ~470 m starting at 10:50 p.m. and ending at 0:30 a.m. Additionally, the transfer of the machine to the beginning point of the following work can also be seen. Between 1:15 a.m. and 4 a.m., the turnouts 224, 223, 217 and a track section are ground. These activities can be partially seen very clearly in

Figure 7.5. In this case, the position of the optical fibre has a major influence on the sensing performance and hence the detected intensity. The layout of the optical fibre used for the recording is not clearly defined, especially in *Thun station*. The quality of the received signal and thus also the intensity depends on the position of the fibre optic cable. This occurrence is obvious in Figure 7.5 at 3:30 a.m. where the intensity of the maintaining machine is less than it was before.
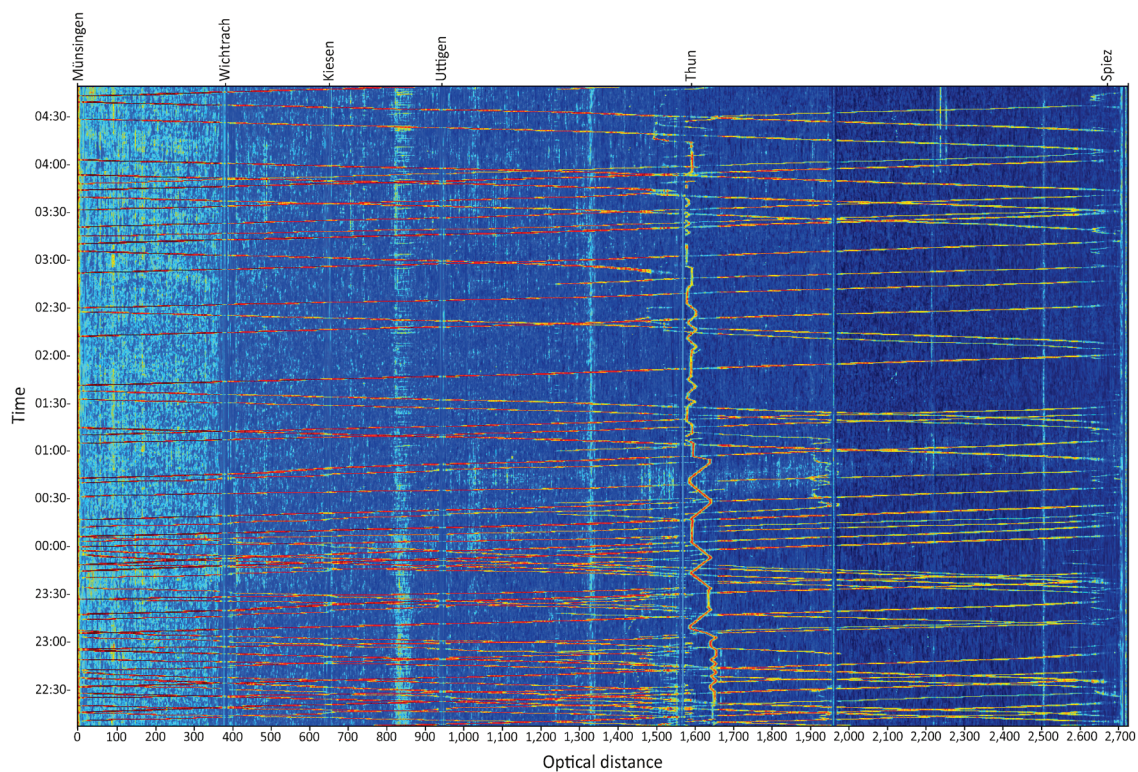
Figure 7.5 Waterfall diagram on the first night with scheduled grinding tasks.

The discussed circumstance is especially true for the maintenance executed on the second night, which only be scantly seen. The maintenance task is carried out in front of channel 1,600.

The linking of asset data and channels proves that this entails work on turnouts 198, 219, 221, 223, 224 and a track section as well. Furthermore, the measures started ahead of time which means that parts of the work have not been recorded. According to the execution report of the second night, the rails of turnouts 223, 224, 219, 198, 221 and track 216 were ground that night. Some of them can be seen in the previous graphic. It can also be seen that essential work is not

recorded or can only be guessed at. This is the case, e.g. in Figure 7.6 at 1:30 a.m. where work is taking place, but the intensity obtained is weak.
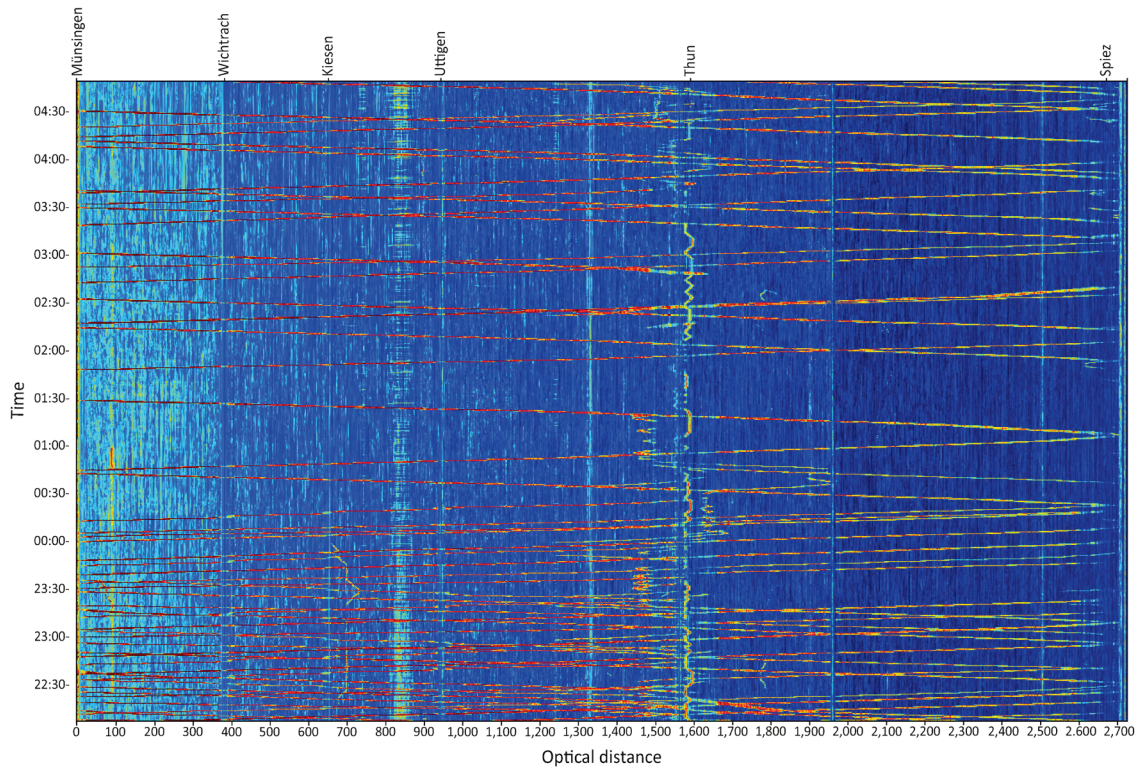
Figure 7.6 Waterfall diagram on the second night with scheduled tamping tasks.

On the third night, the system did not detect any maintenance work (see Figure 7.7). The only activities detected are caused by trains operated regularly. According to the execution report the work carried out took place outside the detectable area of the optical fibre and is therefore not detected.
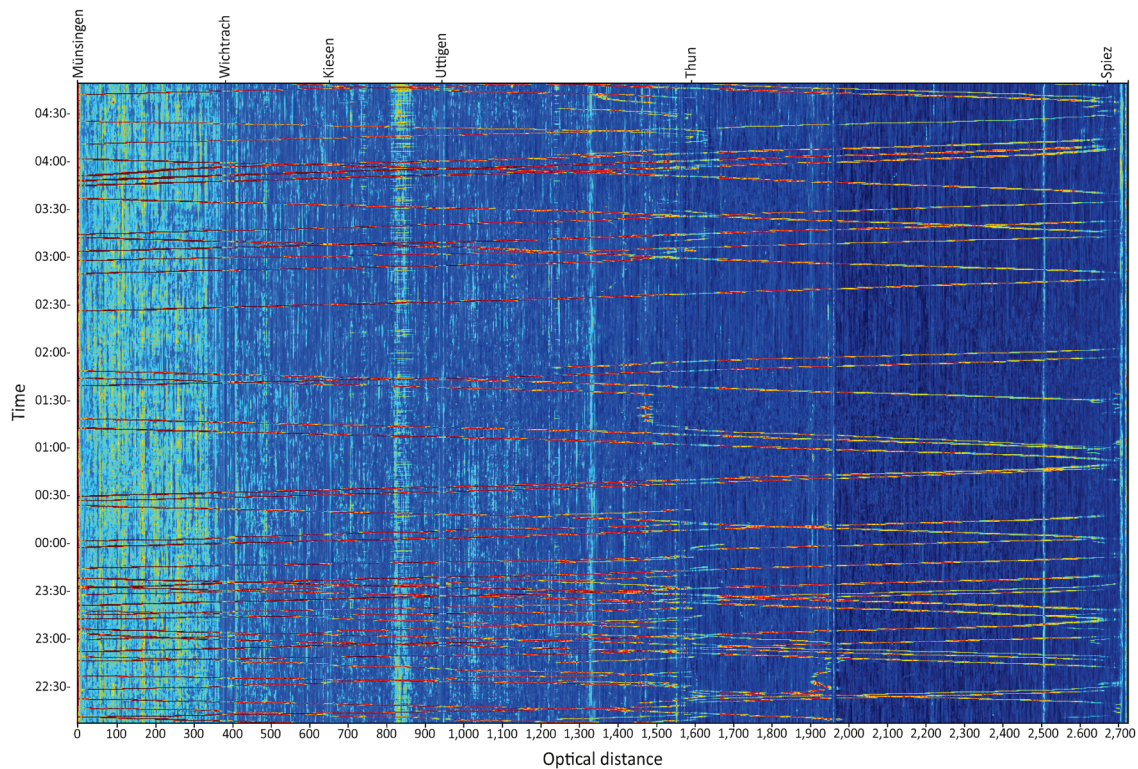
Figure 7.7 Waterfall diagram on the third night with scheduled tamping tasks.

In general, maintenance took place during the course of all three-night shifts but was detected on the first two nights only. A cross-check with the execution reports revealed that work took place in *Thun station* and maintenance was executed as scheduled for the turnouts. The opposite is true for the evaluation and interpretation of the grinding work on the track. The work carried out according to the execution reports and the planned activities according to Table 7.2 differ fundamentally from each other. Maintenance was executed at tracks other than the scheduled ones.

Furthermore, the comparison of Figure 7.5 and Figure 7.6 outlines the relationship between the position of the fibre and the quality and intensity of the signal. In the former illustration, the grinding work up to 1:30 a.m. is particularly intense and is therefore shown in red. The signal intensity drops afterwards. This is especially true and noticeable when analysing maintenance tasks of the second night depicted in Figure 7.6. In this case, entire work processes are sometimes undetectable.

7.3.2 Grinding process analysis

Compared to tamping, the characteristic signal for grinding work looks completely different. Figure 7.8 shows a detailed analysis of grinding work over nine channels and almost two minutes. As is clearly visible, grinding takes places between the channels 1,640 and 1,643 as the acoustic signal and vibrations are predominant at these channels.

Looking back to the tamping tasks the signal pattern occurs as a continuous process without any interruptions now. These results essentially confirm the process of grinding, as the machine only comes to a halt in exceptional cases and otherwise moves forward continuously while the tamping process repeatedly interrupts the work due to the lifting and lowering of the tamping unit, although the tamping machine moves forward continuously. During the grinding process, the material removal is actually kept constant and should be reflected in the signal, whereas if additional material is removed this may be reflected in a higher frequency and volume. The slightly varying volume at 0:28:00 a.m. and 0:28:40 a.m. would indicate this.
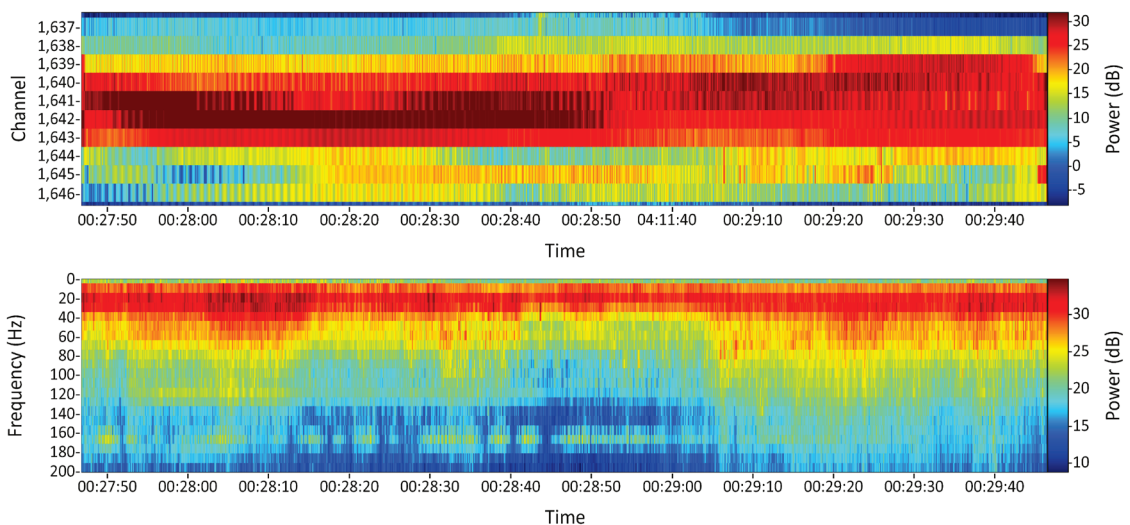
Figure 7.8: Detailed analysis of grinding processes of executed grinding measures.

These considerations are only theoretical and require further investigation but maybe a conceivable explanation. Here, the records of the companies carrying out the work could provide information and prove the plausibility of such a hypothesis.

The continuous working process and slight change in pressure are also reflected in the exciting frequency range. During grinding work, frequencies up to 80 Hz are excited with particularly high

intensity illustrated in Figure 7.8 at the bottom, showing the frequency and intensity band of a working grinding machine. The predominant frequency ranges excited are between 20–40 Hz with slight changes at the same time as the acoustic intensity in the upper illustration increases. However, higher frequencies are also present, but only to a negligible extent.

7.4 Conclusion

The presented results show Distributed Acoustic Sensing's capability to monitor all common maintenance works, assess and also evaluate these. It is not only possible to identify the start and endpoints of maintenance tasks but also to clarify the length of the processed section, despite the limiting factors namely spatial resolution and the transmission of the signal to adjacent channels.

Furthermore, it facilitates distinguishing between the two most important and common tasks of tamping and grinding, and identification of the dominant frequency ranges for all recorded maintenance activities. Additionally, the characteristic signal pattern can be displayed for each of these activities. Both recorded activities are continuous, track-bound work, but tamping with the individual lowering of the tamping tines and squeezing movements shows the most concise pattern. Also, for the first time, the working speeds of the activities become visible, establishing new ways of track work evaluations.

However, the limits of the system become apparent when the maintenance activities are assigned to the respective track or a specific turnout. For example, in a multi-track section it is not possible to localise the cross-section with the system used here. For this purpose, information on the planned work must first be obtained. The DAS system can then be used to check whether the planned section/turnout has been processed and afterwards compared with execution reports. It is only natural that planned work deviates considerably from executed tasks. Some of the reasons were already mentioned and must be identified by the IM in order to optimise future tasks, avoid failures made and ultimately to save money.

During the course of the project, several maintenance tasks were planned. Table 7.3 gives an overview of the nights on which recordings were made because maintenance work was planned. As can be seen, work could not be detected on all nights, which is mainly due to two reasons: 1) scheduled work was not executed or 2) maintenance carried out did not take place in the sensitive area of the optical fibre and was consequently not detected.

A waterfall diagram computed for all the nights listed in the table below makes it possible to determine whether the scheduled task was detected or rather executed.

On the 23rd of October 2017, planned maintenance work did not take place and was thus not detected. This also applies for the 6th December 2017. The tasks were finished ahead of schedule. On the 18th of January 2018, grinding took place beyond the fibre's sensitive area. The same holds true for the work in April while the works scheduled for October 2018 did not take place.

Scheduled date	Work type	Component	Detected
13 October 2017	Grinding	Turnout	Yes
14 October 2017	Grinding	Turnout	Yes
23 October 2017	Grinding	Track	No
03 December 2017	Grinding	Turnout	Yes
04 December 2017	Grinding	Turnout	Yes
05 December 2017	Grinding	Turnout	Yes
06 December 2017	Grinding	Turnout	No
16 January 2018	Grinding	Track & Turnout	Yes
17 January 2018	Grinding	Track & Turnout	Yes
18 January 2018	Grinding	Track & Turnout	No
05 March 2018	Tamping	Track & Turnout	Yes
06 March 2018	Tamping	Track & Turnout	Yes
07 March 2018	Tamping	Track & Turnout	Yes
04 April 2018	Tamping	Track & Turnout	Yes
09 April 2018	Tamping	Track	Yes
10 April 2018	Tamping	Track	Yes
11 April 2018	Grinding	Track	Yes
18 April 2018	Grinding	Turnout	No
19 April 2018	Grinding	Turnout	Yes
25 October 2018	Grinding	Track	Yes
26 October 2018	Tamping	Turnout	No
28 October 2018	Tamping	Track	Yes

Table 7.3: Recorded maintenance tasks according to the scheduled maintenance plan

including the type of work, component and if the certain task was detected with the system.

8   CONCLUSION & DISCUSSION

The rising mobility demand all over the world should be handled primarily by public transportation and is particularly more important considering the ecological and environmental aspects. An increasing number of trains and less time for necessary maintenance and renewal tasks naturally result in increased wear and tear and stress of railway infrastructure. Additionally, budget cutbacks and consequently less money put immense pressure on infrastructure managers all over the world to ensure the availability and required infrastructure quality despite the constraints. New approaches therefore have to be adopted, in order to determine and assess the condition of the infrastructure adequately although without additional trackside sensors or measuring equipment, which may result in track closures necessary for measurements.

Utilising and adapting existing infrastructure – in this specific case, the infrastructure of deployed optical fibres alongside railway tracks – for sensing and consequently condition monitoring of railway infrastructure represents such an approach. The network of installed optical fibres covers wide parts of the infrastructure primarily used for telecommunication and signalling to date. Hence, connecting one dark fibre to an interrogator unit discloses all relevant events taking place on or in the proximity of linear infrastructures. This already constitutes valuable information for infrastructure managers as they are able to monitor the infrastructure in question in real-time and can react immediately in case of disruptions.

When speaking of infrastructure condition monitoring a distinction must be made in advance, because answering the following question is decisive: *Is it necessary to know the exact failure or is a fault indication sufficient?*

The answer to this question determines the effort necessary to utilise already installed optical fibres for condition monitoring of railway infrastructure. The sensing principle is a reaction to external perturbations resulting in an altered backscatter which, in theory, makes it possible to conclude if an unusual event occurs at the specific position. Nevertheless, optical fibres alongside railway tracks do not always run parallel to the track because the distance between the cable guiding duct and the track varies. In addition, the fibre layout changes in complex areas such as stations or multi-tracked sections. The results of these circumstances may lead to dead

sensing zones. Another factor to be considered is fading of the signal resulting in reflections of the signal in adjacent channels. However, if a fault indication is adequately analysing the signal in the frequency-domain, potential faulty zones are revealed. In general, examinations focussing on the frequency content of the signal and applying several digital filters make it possible to distinguish between the condition of different assets and sections. This is especially relevant if it is necessary to rank the assets on the basis of their condition, in order to carry out the most urgent maintenance to prevent safety-critical conditions and thus track closures. However, if it is necessary to know the exact type of failure a thorough positioning and stationing process has to be considered. This includes gaining knowledge about the fibre layout and linking channels to track kilometres or rather positions along the track. In combination with asset data, this permits one to draw conclusions regarding the reason for signal anomalies. For instance, if channel *A* is linked to a track kilometre *XX* which is, in fact, an insulated rail joint it facilitates execution of a customised maintenance task for the rail joint.

The results presented in this work point out that the system is capable of distinguishing between different asset conditions and detecting of track defects (*RQ1* & *RQ2*). The shortcomings of the applied technology are the inability of assigning a signal pattern explicitly to a certain failure/defect and to conclude on the actual track geometry. Nevertheless, the latter is not necessarily mandatory as track recording vehicles are designed to fulfil this task in particular.

The distinction of different asset conditions is closely related to analyses of the deterioration process of an asset and the assessment of such forms the basis for planning and executing the necessary maintenance tasks. During the project, it was possible to monitor the deterioration of a white spot on an open track section. The white spot was a consequence of a malfunctioning weld leading to increased vehicle dynamics and finally to ballast break-up in this section. The deterioration process, as well as the improved track quality due to tamping, were monitored with DAS and thus confirmed by measurements of the track recording vehicle. To monitor the deterioration process it is necessary to filter the raw DAS data and to remove all the noise present. Afterwards, the standard deviation turned out to be a proper value for condition monitoring and trend analyses (*RQ3*). It must be noted that it is solely permissible to compare like with like, as several circumstances influence the signal pattern.

The results outline the enormous potential of the sensing system, but serious efforts have to made to derive valid results. The data amount is always critical as further aspects need to be covered when using DAS in operation. This includes considerations regarding data mining, data processing and finally data storage. The question to be answered here is which values should be stored. The sensing principle shows the response of the infrastructure to the load induced by train movements which vary among the different train types and compositions. During the course of the project, measurements of one specific reference train were considered at which the standard deviation of the filtered signal seems to be a valid value for condition monitoring. Also linked to this issue is the integration of DAS data into existing system architectures and, probably the more important aspect – what data needs to be stored. Considering the huge data amount, it may be expedient to delete all processed/raw data and keep some statistical values only. For instance, if the system is used as a wheel condition sensor, any value exceeding a threshold can be stored and transmitted to the railway undertaking and shall not be deleted in the system of the infrastructure manager until the necessary maintenance was executed. Also connected to this issue is the automated starting of the measurements. If DAS is used for condition monitoring, it is feasible to record train movements of interest only and consequently reduce data.

Furthermore, the positioning and stationing of fibre and channel are still challenging and requires a resolution. While answers to the first three research questions can be given quite easily, this is not the case when addressing RQ4 *"…can DAS replace other technologies and be a stand-alone application"*. This depends mainly on further research and serious efforts to tackle the issues depicted in this thesis. Paving the way for a successful implementation of DAS manufacturers should focus on delivering additional and/or more frequent information about the infrastructure condition which also provides more time for necessary development of the system. Suppliers must deliver a reasonable solution for infrastructure managers so that they benefit from this sensing technology. Otherwise, the system will end as a data-gathering giant not used by anyone. Conclusively, the answer to RQ4 is a definite "*maybe, the future will tell*".

In contrast to the conclusions above, the answer to RQ5 *"Can DAS assess executed maintenance"* seems fairly straightforward. Apart from a clear detection of maintenance work, it is possible to identify the specific work, which was proven in this thesis for tamping and grinding. In general, any maintenance work affecting the frequency spectrum of the track should be detectable with

DAS. However, this requires further research for example for identifying rail surface defects (head checks) and removing of such by grinding. Going into more detail provides information on decisive parameters such as tamping frequency, squeezing time and dominating frequency in the course of grinding. Additionally, the start and endpoints of maintenance activities can be identified with exact timestamps, which can clearly describe the processed length.

Finally, an answer should be given to the main question *"(How) Can infrastructure managers utilise DAS to increase knowledge about track condition?"*.

The statements above make it necessary to make a distinction between the demand of infrastructure managers who can be classified into three classes, based on their strategy regarding measurement, data processing and maintenance (see Figure 8.1).

	Class 1	Class 2	Class 3
Measurement	In-house IM owner of TRV (mostly)	In-house/out-tasking	Outsourced
Processing	In-house Track analysis department	In-house/out-tasking	Outsourced
Maintenance planning	In-house Dedicated department	In-house	In-house/outsourced
Maintenance execution	In-house Framework contract Tendering (for new-line)	Outsourced/out-tasking	Outsourced

Figure 8.1: Classification of maintenance strategies and infrastructure managers.

The classification made constitutes no judgement on whether a strategy or concept is good or bad. Rather, it is an attempt to highlight the benefits and potentials of DAS as an infrastructure condition monitoring application considering different states of data availability of infrastructure managers.

Infrastructure managers classified in class 1 usually own a track recording car and carry out track measurements in-house. Furthermore, data processing and maintenance planning are performed in-house in dedicated departments. Planned maintenance is executed in the course

of frameworks or tendering in case of new-line constructions. Infrastructure managers associated with class 1 perform measurements with the track recording vehicles several times a year and deploy the previously described monitor & prevent maintenance concept. Such infrastructure managers need to know the explicit type of failure to carry out the maintenance needed. This is mainly due to dense time tables, a high number of trains (mixed traffic usually) and less time for maintenance measures. These infrastructure managers have a lot of knowledge based in-house and are aware of the asset condition. For those managers, DAS may be a valuable data and information source when used for turnouts, insulated rail joints and the assessment of executed maintenance tasks. In the case of the first two, more research is necessary to strengthen the results. For the latter, the benefit has been identified yet the data issue has to be resolved.

Infrastructure managers assigned to the second group (class 2) have already outsourced some tasks. Most of them outsource the measurement tasks and analyse the data in-house or partially out-task it. The same holds true for the execution of maintenance, whereby the planning of the tasks takes place in-house. However, the boundary conditions in terms of traffic mix are almost the same as for class 1. This also applies for the benefits and requirements when using DAS – with some limitations – of course.

Class 3 needs further specification. Those who have outsourced also maintenance planning and have thus in principle control neither of track quality nor of maintenance tasks. Both are somehow contractually regulated in terms of track availability and kilometres to be maintained but it is in the responsibility of the contractor to determine when and how to carry out the maintenance. In this case information provided by DAS can serve as a quality check of track status and maintenance work.

Infrastructure managers assigned to class 3 and keeping maintenance planning in-house have access to data about track condition defined by specific contracts. For those it can be beneficial to get additional track information delivered by DAS as indications about occurring failures in order to prevent critical conditions. Even more, for those companies, it is mandatory to obtain a ranking of the most urgent assets which require maintenance. As they are mainly driven by budgetary constraints and have only limited money to execute maintenance, this permits shifting and distributing money where this is most needed. In the case of the former, DAS could

play a key role in supervising maintenance tasks. In this context, issues regarding maintained length could be tackled.

Independently of the infrastructure manager some general valid statements can be formulated. Modern asset management systems targeting sustainability require time series analyses of track data enabling prognoses and thus proactive maintenance. Distributed Acoustic Sensing can deliver valuable information on degradation. Furthermore, as soon as a rapid degradation is detected the measurement frequency can be adjusted utilising DAS.

9 OUTLOOK

This work presents results gained with one specific system or rather sensing technology, based on the very first developments of coherent optical time reflectometry systems initially applied in the oil and gas industry mainly for safety reasons. Such systems operate in intensity mode only, which does not allow one to draw conclusions about the asset's condition based solely on the raw backscattered data. Effects like fading may occur leading to dead detection zones or even channels showing a similar signal pattern. However, currently, the overwhelming part of the research focuses on phase optical time-domain reflectometry enabling direct detection of both amplitude and phase with limited fading occurrence. Phase-sensitive systems usually operate with higher sampling rates resulting in even more data as presented in this work. Furthermore, the distance that can be monitored is shorter than with conventional systems. Infrastructure managers who decide to go for DAS and to use it operationally as a monitoring application should specify which system to apply initially. Having said this, the question arises regarding the added value of phase-sensitive systems. Of course, in theory, the backscattered signal of those systems is sufficient meaning no more data processing afterwards, but in the case of railways, this has not been verified yet. Therefore, more research is necessary to tackle this issue.

Another aspect worth considering involves the layout of the optical fibre and thus the positioning and calibration. It may be beneficial to install new cables depending on the purpose. In this project already installed fibres were utilised which has, of course, some major advantages but also considerable disadvantages. Cables laid in the cable duct are protected against almost any external effects (except derailments which cause severe damage to the whole infrastructure) and malicious damage but have some serious shortcomings as the signal transmission may be affected by varying distances between cable duct and track. In addition, the deployment within the trough itself may also lead to changed scattering. The infrastructure condition and boundary conditions influence the measurement quality – as shown – considerably. While the impact of the superstructure (ballast, sleepers, rail) can be overcome – this work underpins that statement – this does not apply for the substructure. Condition monitoring and the assessment of such has been the subject of many research projects to date. However, the long-waved fractal value (Landgraf and Hansmann, 2018) seems to be promising.

The influencing factors mentioned must be considered when using DAS for condition monitoring. A reasonable solution could be clipping the fibre to the rail foot, but this may be destroyed in case of maintenance tasks, which is not the case when laid in a cable duct. Finally, the channels need to be referenced and linked to assets. This ensures that the changed signal pattern or rather recognised deterioration is assigned to the causative fault in order to carry out the right measure at the right position and time. The approach chosen in this project is, of course, not applicable to thousands of track kilometres. A potential solution could be the stationing and positioning based on maintenance work (tamping, as it shows the most characteristic pattern) by assigning the signal to the specific channel with the highest intensity. Another solution may be found by applying machine learning methods (deep learning). Such networks could improve/learn – this must be supervised at the beginning – and automate the stationing and calibration process.

Train tracking also represents a feasible field of application for DAS. The data of the specific train run have to be stored temporarily and in case of a detected fault (e. g. wheel flat), this has to be reported to the railway undertaking and the data can be deleted afterwards. Based on this, the company owning the vehicle is able to derive the necessary maintenance for the component in question. This holds true for the data of all train rides except those of the reference train. These must be specified in any case when utilising DAS for condition monitoring. Here, in a first step, it is not mandatory to know the explicit failure but rather to monitor the trend of a certain position. In the case of automatically detected anomalies (pattern recognition), the location needs to be investigated further and the reason for the changed signal pattern identified, whereby the data can be used for time series and trend analyses. In general, track failures occur neither within a couple of days nor within one or two weeks. They arise and develop over time, meaning that it is not necessary to store the data of each train ride of the reference train. It might be sufficient to keep the data of the reference train every two or three weeks. Actually, the measurement is a derivate of the vehicle-track interaction. On the one hand, it shows the reaction of the infrastructure due to the load of the train. If the signal pattern at one position remains constant over a period of time and anomalies occur only within one train movement, this is certainly because of the condition of the train. On the other hand, if the signal at the position deteriorates constantly the defect/failure can be assigned to the track/asset.

Finally, once integrated into the asset management strategy and system of an infrastructure manager, the system can be used for maintenance planning and documentation of these. The measurement intervals of DAS can be adjusted to the deterioration of the asset which consequently would also allow adjusting the measurement frequency of track recording vehicles. Moreover, this enables to assess track geometry with track recording vehicles when needed only, e.g. after maintenance or if critical values due to DAS data are assumed. Based on statistical values the optimal point in time could be chosen in order to keep the track quality at the determined level resulting in an improved planning process of necessary maintenance. DAS could be utilised here in a two-way approach in particular. Firstly, as additional information to measurements of other sensing devices and secondly as a supervision application for maintenance tasks. The former is closely related to condition monitoring. The latter includes maintenance documentation with respect to the beginning of the work, maintained length, working speed and quality assessment of the respective task. This information may be used for billing of executed/non-executed work.

The evaluations currently take place primarily on a manual basis, which must be overcome, especially considering the vast amount of data. At this point, machine learning can be a ground-breaking approach and pave the way for the implementation of DAS in the daily business of any infrastructure manager.

References

Abalde-Cela, S. *et al.* (2010) 'Surface-enhanced Raman scattering biomedical applications of plasmonic colloidal particles', *Journal of The Royal Society Interface*, 7(suppl_4). doi: 10.1098/rsif.2010.0125.focus.

Agrawal, G. (2006) *Nonlinear Fiber Optics*, *Nonlinear Fiber Optics*. Elsevier. doi: 10.1016/B978-0-12-369516-1.X5000-6.

Alfi, S. and Bruni, S. (2009) 'Mathematical modelling of train-turnout interaction', *Vehicle System Dynamics*, 47(5), pp. 551–574. doi: 10.1080/00423110802245015.

An, R. *et al.* (2018) 'Improved railway track geometry degradation modeling for tamping cycle prediction', *Journal of Transportation Engineering Part A: Systems*, 144(7), pp. 1–11. doi: 10.1061/JTEPBS.0000149.

Arndt, M. (2015) 'Modular concept of diagnostic and monitoring technologies', *Signal + Draht*, 6(107), pp. 38–45.

Asadzadeh, S. M. and Galeazzi, R. (2019) 'The predictive power of track dynamic response for monitoring ballast degradation in turnouts', *Proceedings of the Institution of Mechanical Engineers, Part F: Journal of Rail and Rapid Transit*, (April 2020). doi: 10.1177/0954409719883547.

Audley, M. and Andrews, J. (2013) 'The effects of tamping on railway track geometry degradation', *Proceedings of the Institution of Mechanical Engineers, Part F: Journal of Rail and Rapid Transit*, 227(4), pp. 376–391. doi: 10.1177/0954409713480439.

Auer, F. (2013) 'Multi-function track recording cars', *RTR*, (3+4), pp. 32–36.

Auer, F. *et al.* (2018) 'Smart Tamping – Fields of Application of the Turnout Tamping Assistance System', *ETR International Edition*, pp. 32–34.

Auer, F., Hauke, R. and Wenty, R. (2015) 'High-Tech-Stopfaggregate für nachhaltige Gleislageverbesserung', *EI - Der Eisenbahningenieur*, (11), pp. 18–22.

Barbir, O. *et al.* (2019) 'Compaction energy as an indicator for ballast quality', in *Proceedings of 12th World Congress on Railway Research*. Tokyo, pp. 1–6.

Barke, D. and Chiu, K. W. (2005) 'Structural health monitoring in the railway industry: A review', *Structural Health Monitoring*, 4(1), pp. 81–94. doi: 10.1177/1475921705049764.

Barnoski, M. K. *et al.* (1977) 'Optical time domain reflectometer', *Applied Optics*, 16(9), p. 2375. doi: 10.1364/AO.16.002375.

Barnoski, M. K. and Jensen, S. M. (1976) 'Fiber waveguides: a novel technique for investigating attenuation characteristics', *Applied Optics*. doi: 10.1364/ao.15.002112.

Bevan, A. *et al.* (2013) 'Development and validation of a wheel wear and rolling contact fatigue damage model', *Wear*. Elsevier, 307(1–2), pp. 100–111. doi: 10.1016/j.wear.2013.08.004.

Bisang, J., Frey, M. and Koller, S. (2017) 'Rolling stock condition monitoring with wayside train monitoring systems and RFID', *Signalling + Datacommunication*, 109(10), pp. 23–30.

Bogdański, S., Olzak, M. and Stupnicki, J. (1996) 'Numerical stress analysis of rail rolling contact fatigue cracks', *Wear*, 191(1–2), pp. 14–24. doi: 10.1016/0043-1648(95)06685-3.

Boyd, R. W. (2008) *Nonlinear Optics*, *Academic Press*.

Burstow, M. C. (2004) *Whole Life Rail Model Application and Development for RSSB (T115)-Continued Development of an RCF Damage Parameter*.

Caetano, L. F. and Teixeira, P. F. (2016) 'Predictive maintenance model for ballast tamping', *Journal of Transportation Engineering*, 142(4), pp. 1–9. doi: 10.1061/(ASCE)TE.1943-5436.0000825.

Cannon, D. F. *et al.* (2003) 'Rail defects: an overview', *Fatigue & Fracture of Engineering Materials & Structures*, 26(10), pp. 865–886. doi: 10.1046/j.1460-2695.2003.00693.x.

Cannon, D. F. and Pradier, H. (1996) 'Rail rolling contact fatigue research by the European Rail Research Institute', *Wear*, 191(1–2), pp. 1–13. doi: 10.1016/0043-1648(95)06650-0.

Clayton, P. and Hill, D. N. (1987) 'Rolling contact fatigue of a rail steel', *Wear*. Elsevier, 117(3), pp. 319–334. doi: 10.1016/0043-1648(87)90152-9.

Crickmore, R. I. and Hill, D. J. (2007) 'Detecting movement of traffic to be counted or controlled using treadles built into the road'. Great Britian.

134

DeCusatis, C. (ed.) (2014) *Handbook of Fiber Optic Data Communication*, *Handbook of Fiber Optic Data Communication: A Practical Guide to Optical Networking: Fourth Edition*. Elsevier. doi: 10.1016/C2012-0-00043-9.

Delepine-Lesoille, S. *et al.* (2010) 'Truly distributed optical fiber sensors for structural health monitoring: From the telecommunication optical fiber drawling tower to water leakage detection in dikes and concrete structure strain monitoring', *Advances in Civil Engineering*. doi: 10.1155/2010/930796.

Dirks, B., Enblom, R. and Berg, M. (2016) 'Prediction of wheel profile wear and crack growth – comparisons with measurements', *Wear*. Elsevier, 366–367, pp. 84–94. doi: 10.1016/j.wear.2016.06.026.

Dittmer, E. (2018) *Grundlagenanalyse der Ausbauentscheidung von Weichen*. Graz University of Technology.

Du, C. *et al.* (2020) 'A review of railway infrastructure monitoring using fiber optic sensors', *Sensors and Actuators, A: Physical*. Elsevier B.V., 303, p. 111728. doi: 10.1016/j.sna.2019.111728.

Erhard, F., Wolter, K. U. and Zacher, M. (2009) 'Improvement of track maintenance by continuous monitoring with regularly scheduled high speed trains', in *Railway Engineering–10th International Conference & Exhibition*.

European Commission (2019) *Report from the Commission to the European Parliament and the Council Sixth report on monitoring development of the rail market pursuant to Article 15(4) of Directive 2012/34/EU of the European Parliament and of the Council*. Brussels.

European Committee for Standardization (2010) *EN 13848-3. Railway applications - Track - Track geometry quality. Part 3: Measuring systems - Track construction and maintenance machines*.

European Committee for Standardization (2012) *EN 13848-4. Railway applications - Track - Track geometry quality. Part 4: Measuring systems - Manual and lightweight devices*.

European Committee for Standardization (2014) *EN 13848-6. Railway applications - Track - Track geometry quality. Part 6: Characterisation of track geometry quality*.

European Committee for Standardization (2017) *EN 13848-5. Railway applications - Track - Track geometry quality. Part 5: Geometric quality levels - Plain line, switches and crossings*.

European Committee for Standardization (2018) *EN 13848-2. Railway applications - Track - Track geometry quality. Part 2: Measuring systems - Track recording vehicles*.

European Committee for Standardization (2019) *EN 13848-1. Railway applications - Track - Track geometry quality. Part 1: Characterization of track geometry*.

Fellinger, M. (2020) *Sustainable Asset Management for Turnouts - From measurement data analysis to behaviour and maintenance prediction*. Graz University of Technology.

Fendrich, L. and Fengler, W. (2019) *Handbuch Eisenbahninfrastruktur*. 3rd edn, *Handbuch Eisenbahninfrastruktur*. 3rd edn. Berlin, Heidelberg: Springer Vieweg. doi: 10.1007/978-3-662-56062-4.

Fiber Optics Market by Cable Type, Optical Fiber Type, Application & Geography (2020). Available at: https://www.marketsandmarkets.com/Market-Reports/fiber-optics-market (Accessed: 9 May 2020).

Fischer, J. (1983) *Einfluss von Frequenz und Amplitude auf die Stabilisierung von Oberbauschotter*. Graz University of Technology.

Fontul, S. *et al.* (2018) 'Railway track condition assessment at network level by frequency domain analysis of GPR data', *Remote Sensing*, 10(4), pp. 1–26. doi: 10.3390/rs10040559.

Goryacheva, I. G., Soshenkov, S. N. and Torskaya, E. V. (2013) 'Modelling of wear and fatigue defect formation in wheel-rail contact', *Vehicle System Dynamics*, 51(6), pp. 767–783. doi: 10.1080/00423114.2011.602419.

Grossniklaus, R. (2016) 'Advances in Tamping Technology', in *AusRAIL*. Adelaide, p. 8.

Hansmann, F. (2018) *The Missing Link between Asset Data and Asset Management*. Edited by P. Veit. Verlag der Technischen Universität Graz. doi: 10.3217/978-3-85125-567-6.

Hansmann, F. and Landgraf, M. (2013) 'Fractal Analyses and their use in railway engineering | Wie fraktal ist die Eisenbahn?', *ZEVrail*.

Hartog, A. H. (2017) *An Introduction to Distributed Optical Fibre Sensors*. CRC Press. doi: 10.1201/9781315119014.

Healey, P. (1984) 'Fading in heterodyne OTDR', *Electronics Letters*. doi: 10.1049/el:19840022.

Healey, P. *et al.* (1984) 'OTDR in single-mode fibre at 1.5 μm using homodyne detection', *Electronics Letters*. doi: 10.1049/el:19840247.

Healey, P. and Malyon, D. J. (1982) 'OTDR in single-mode fibre at 1.5 μm using heterodyne detection', *Electronics Letters*, 18(20), p. 862. doi: 10.1049/el:19820585.

Hecht, J. (2015) *Understanding Fiber Optics*. 4th edn. Upper Saddle River: SPIE. doi: 10.1117/3.1445658.

Holzfeind, J. (2009) *For the Predictability of Track Quality Behaviour Analysis of Track Behaviour in Individual Cross-Sections*. Graz University of Technology.

Holzfeind, J. *et al.* (2015) 'Verschleißabhängige Komponente im Trassenpreissystem der Schweiz - ein Anreiz zur Rückbesinnung auf ein Gesamtoptimum', *ZEVrail*, 139(6), pp. 232–243.

Holzfeind, J., Nerlich, I. and Kull, Z. (2016) 'ANABEL – ein detailliertes Belastungs- und Beanspruchungsmonitoringsystem mit großem Potential', *ZEVrail*, 140(11/12), p. 18.

Hui, R. and O'Sullivan, M. (2009) *Fiber Optic Measurement Techniques*, *Fiber Optic Measurement Techniques*. Academic Press. doi: 10.1016/B978-0-12-373865-3.X0001-8.

Hummitzsch, R. (2009) *For the Predictability of Track Quality Behaviour - Statistical Analysis of Track Behaviour for the Creation of a Prediction Model*. Graz University of Technology.

Izumita, H. *et al.* (1992) 'Fading Noise Reduction in Coherent OTDR', *IEEE Photonics Technology Letters*. doi: 10.1109/68.122361.

Izumita, H. *et al.* (1997) 'Stochastic amplitude fluctuation in coherent OTDR and a new technique for its reduction by stimulating synchronous optical frequency hopping', *Journal of Lightwave Technology*, 15(2), pp. 267–278. doi: 10.1109/50.554377.

Johansson, A. *et al.* (2011) 'Simulation of wheel-rail contact and damage in switches & crossings', *Wear*. Elsevier B.V., 271(1–2), pp. 472–481. doi: 10.1016/j.wear.2010.10.014.

Juarez, J. C. and Taylor, H. F. (2005) 'Polarization discrimination in a phase-sensitive optical time-domain reflectometer intrusion-sensor system', *Optics Letters*. OSA, 30(24), p. 3284. doi: 10.1364/OL.30.003284.

Juškaitis, R. *et al.* (1994) 'Interferometry with Rayleigh backscattering in a single-mode optical fiber', *Optics Letters*. The Optical Society, 19(3), p. 225. doi: 10.1364/ol.19.000225.

Kassa, E., Andersson, C. and Nielsen, J. C. O. (2006) 'Simulation of dynamic interaction between train and railway turnout', *Vehicle System Dynamics*, 44(3), pp. 247–258. doi: 10.1080/00423110500233487.

Kassa, E. and Nielsen, J. C. O. (2008) 'Dynamic interaction between train and railway turnout: Full-scale field test and validation of simulation models', *Vehicle System Dynamics*, 46(SUPPL.1), pp. 521–534. doi: 10.1080/00423110801993144.

Kassa, E., Sramota, J. and Kaynia, A. (2017) *DESTination RAIL – Decision Support Tool for Rail Infrastructure Managers: D1.3 Report on monitoring Switches and Crossings*. Available at: https://cordis.europa.eu/project/id/284995.

Kowarik, S. *et al.* (2020) 'Fiber optic train monitoring with distributed acoustic sensing: Conventional and neural network data analysis', *Sensors (Switzerland)*, 20(2), pp. 1–12. doi: 10.3390/s20020450.

Laferrière, J. *et al.* (2007) 'Reference Guide to Fiber Optic Testing', *Jdsu*.

Lamb, C. and Dakin, J. P. (1990) 'Distributed fibre optic sensor system'. United Kingdom.

Landgraf, M. (2018) *Smart data for sustainable Railway Asset Management*. Graz: Verlag der technischen Universität Graz. doi: 10.3217/978-3-85125-569-0.

Landgraf, M. and Hansmann, F. (2018) 'Fractal analysis as an innovative approach for evaluating the condition of railway tracks', *Proceedings of the Institution of Mechanical Engineers, Part F: Journal of Rail and Rapid Transit*, p. 095440971879576. doi: 10.1177/0954409718795763.

Li, H.-N., Li, D.-S. and Song, G.-B. (2004) 'Recent applications of fiber optic sensors to health monitoring in civil engineering', *Engineering Structures*, 26(11), pp. 1647–1657. doi: 10.1016/j.engstruct.2004.05.018.

Lienhart, W. *et al.* (2016) 'Condition monitoring of railway tracks and vehicles using fibre optic sensing techniques', in *Transforming the Future of Infrastructure through Smarter Information: Proceedings of the International Conference on Smart Infrastructure and Construction, 27?29 June 2016*. ICE Publishing (Cambridge Centre for Smart Infrastructure & Construction), pp. 45–50. doi: 10.1680/tfitsi.61279.045.

Liokumovich, L. B. *et al.* (2015) 'Fundamentals of Optical Fiber Sensing Schemes Based on Coherent Optical Time Domain Reflectometry: Signal Model Under Static Fiber Conditions', *Journal of Lightwave Technology*, 33(17), pp. 3660–3671. doi: 10.1109/JLT.2015.2449085.

Loendersloot, R. and Mostafa, N. (2018) *DESTination RAIL – Decision Support Tool for Rail Infrastructure Managers: D1.5 Implementation of a Complete Vibration Monitoring System on Irish Rail Bridge*.

Lumley, D. E. (2001) 'Time-lapse seismic reservoir monitoring', *Geophysics*. doi: 10.1190/1.1444921.

Marschnig, S. (2016) *iTAC - innovative Track Access Charges*. Graz: Verlag der technischen Universität Graz.

Marschnig, S. and Holzfeind, J. (2013) 'Verursachungsgerechte Kostenzuordnung der Fahrbahnerhaltungsarbeiten am Beispiel des Verschleißmodells der SBB', *ZEVrail*.

Marschnig, S. and Vidovic (2019) 'Estimating future tamping demands using the Swiss Wear Factor', in *Proceedings of 12th World Congress on Railway Research*. Tokyo, p. 6.

Marschnig, S., Vidovic, I. and Brantegger, M. (2019) 'Trassenpreise auf Basis der Richtlinie 2012/34/EU – ein erster Benchmark', *Eisenbahningenieur EI*, (6), pp. 6–8.

Martinez Pereira, A. and Jones, M. (Geophysicist) (2010) *Fundamentals of borehole seismic technology*. Schlumberger.

Matta, F. *et al.* (2008) 'Distributed Strain Measurement in Steel Bridge with Fiber Optic Sensors: Validation through Diagnostic Load Test', *Journal of Performance of Constructed Facilities*, 22(4), pp. 264–273. doi: 10.1061/(ASCE)0887-3828(2008)22:4(264).

McAnaw, H. E. (2003) 'The system that measures the system', *NDT and E International*, 36(3 SPEC.), pp. 169–179. doi: 10.1016/S0963-8695(02)00055-5.

Mittermayr, P. *et al.* (2019) 'OBAL measurement system Wheel profile measurement at train speeds up to 250 km / h', in *Proceedings of 12th World Congress on Railway Research*. Tokyo, pp. 4–7.

Mittermayr, P., Stephanides, J. and Maicz, D. (2011) 'Argos®- A decade of operational experience in wayside train monitoring', *IET Conference Publications*, 2011(581 CP). doi: 10.1049/cp.2011.0605.

Motil, A., Bergman, A. and Tur, M. (2016) '[INVITED] State of the art of Brillouin fiber-optic distributed sensing', *Optics & Laser Technology*, 78, pp. 81–103. doi: 10.1016/j.optlastec.2015.09.013.

Mullens, S. J., Lees, G. P. and Duvivier, G. (2010) 'Fiber-optic distributed vibration sensing provides technique for detecting sand production', in *Proceedings of the Annual Offshore Technology Conference*. doi: 10.4043/20429-ms.

Muster, H. *et al.* (1996) 'Rail rolling contact fatigue. The performance of naturally hard and head-hardened rails in track', *Wear*, 191(1–2), pp. 54–64. doi: 10.1016/0043-1648(95)06702-7.

Neuhold, J. (2020) *Tamping within sustainable track asset management*. Graz University of Technology.

Neuhold, J., Vidovic, I. and Marschnig, S. (2020) 'Preparing Track Geometry Data for Automated Maintenance Planning', *Journal of Transportation Engineering, Part A: Systems*, 146(5), p. 04020032. doi: 10.1061/JTEPBS.0000349.

Neuper, G., Neuhold, J. and Landgraf, M. (2018) 'Effekte von Schwellenbesohlungen auf das langfristige Qualitätsverhalten des Gleises', *ZEVrail*, 142(8), p. 13.

Nicklisch, D. *et al.* (2010) 'Geometry and stiffness optimization for switches and crossings, and simulation of material degradation', *Proceedings of the Institution of Mechanical Engineers, Part F: Journal of Rail and Rapid Transit*, 224(4), pp. 279–292. doi: 10.1243/09544097JRRT348.

Oakley, L. H. *et al.* (2011) 'Identification of Organic Materials in Historic Oil Paintings Using Correlated Extractionless Surface-Enhanced Raman Scattering and Fluorescence Microscopy', *Analytical Chemistry*, 83(11), pp. 3986–3989. doi: 10.1021/ac200698q.

ÖBB-INFRASTRUKTUR AG (2019) *Geschäftsbericht 2019*.

Offenbacher, S. (2019) *Ballast Evaluation as Part of Tamping Measures*. Graz University of Technology.

Offizielles Kursbuch: Grafische Fahrpläne (2020). Available at: https://www.fahrplanfelder.ch/de/archiv/grafische-fahrplaene.html (Accessed: 7 April 2020).

ORE (1987) *D 161.1 / RP 4 The dynamic effects due to increasing axle load from 20 to 22.5 t and the estimated increase in track maintenance costs The dynamic effects due to increasing axle load from 20 to 22.5 t and the estimated increase in track maintenance*. Utrecht.

Owen, A., Duckworth, G. and Worsley, J. (2012) 'OptaSense: Fibre Optic Distributed Acoustic Sensing for Border Monitoring', in *2012 European Intelligence and Security Informatics Conference*. IEEE, pp. 362–364. doi: 10.1109/EISIC.2012.59.

Park, J. and Taylor, H. F. (2003) 'Fiber Optic Intrusion Sensor using Coherent Optical Time Domain Reflectometer', *Japanese Journal of Applied Physics*, 42(Part 1, No. 6A), pp. 3481–3482. doi: 10.1143/JJAP.42.3481.

Peng, F. *et al.* (2014) 'Real-time position and speed monitoring of trains using phase-sensitive OTDR', *IEEE Photonics Technology Letters*. doi: 10.1109/LPT.2014.2346760.

Qin, Z., Chen, L. and Bao, X. (2012) 'Continuous wavelet transform for non-stationary vibration detection with phase-OTDR', *Optics Express*. doi: 10.1364/oe.20.020459.

Rail Cargo Group - Wagon equipment (2020). Available at: https://www.railcargo.com/en/services/wagonload/wagon-equipment (Accessed: 6 May 2020).

Railway Group Standard (2019) *Permissible Track Forces and Resistance to Derailment and Roll-Over of Railway Vehicles Permissible Track Forces and Resistance to Derailment and Roll-Over of Railway Vehicles*. Available at: www.rssb.co.uk/railway-group-standards. (Accessed: 15 April 2020).

Rogers, A. (1999) 'Distributed optical-fibre sensing', *Measurement Science and Technology*. doi: 10.1088/0957-0233/10/8/201.

Di Sante, R. (2015) 'Fibre optic sensors for structural health monitoring of aircraft composite structures: Recent advances and applications', *Sensors (Switzerland)*, 15(8), pp. 18666–18713. doi: 10.3390/s150818666.

Santos, J. L. and Farahi, F. (eds) (2014) *Handbook of Optical Sensors*, *Handbook of Optical Sensors*. CRC Press. doi: 10.1201/b17641.

SBB (2020) *Dark fibre*. Available at: https://bahninfrastruktur.sbb.ch/de/produkte-dienstleistungen/sbb-telecom/dark-fibre.html (Accessed: 27 March 2020).

SBB Fleet strategy (2020). Available at: https://company.sbb.ch/en/media/background-information/fleet-strategy.html (Accessed: 6 May 2020).

SBB Swiss Federal Railway (2019) *SBB Facts and Figures*.

Shannon, C. E. (1949) 'Communication in the Presence of Noise', *Proceedings of the IRE*, 37(1), pp. 10–21. doi: 10.1109/JRPROC.1949.232969.

Shimizu, K., Horiguchi, T. and Koyamada, Y. (1992) 'Characteristics and Reduction of Coherent Fading Noise in Rayleigh Backscattering Measurement for Optical Fibers and Components', *Journal of Lightwave Technology*. doi: 10.1109/50.144923.

Smart Railways Market by Solution (2020). Available at: https://www.researchandmarkets.com/reports/4968512/smart-railways-market-by-solution-rail-asset (Accessed: 9 May 2020).

Solomon, B. (2001) *Railway Maintenance: The Men and Machines That Keep the Railroads Running*. St. Paul: MBI.

Stack, J. R., Harley, R. G. and Habetler, T. G. (2004) 'An amplitude modulation detector for fault diagnosis in rolling element bearings', *IEEE Transactions on Industrial Electronics*, 51(5), pp. 1097–1102. doi: 10.1109/TIE.2004.834971.

Taylor, H. F. and Lee, C. E. (1993) 'Method For Fiber Optic Intrusion Sensing. US5194847A'. USA. Available at: https://patents.google.com/patent/US5194847A/en (Accessed: 28 May 2019).

Tennyson, R. C. *et al.* (2001) 'Structural health monitoring of innovative bridges in Canada with fiber optic sensors', *Smart Materials and Structures*. doi: 10.1088/0964-1726/10/3/320.

142

The European Parliament and the Council of the European Union (2012) *Directive 2012/34/EU of the European Parliament and of the Council of 21 November 2012 on the establishing a single European railway area (recast)*. Belgium.

Thyagarajan, K. and Ghatak, A. (2007) *Fiber Optic Essentials*. Wiley-IEEE Press. doi: 10.1002/9780470152560.

Tribble, K. *et al.* (2018) *Installation Considerations for Rail*. Washington, D.C. Available at: https://www.fiberopticsensing.org.

Tricker, R. (2002) *Optoelectronics and Fiber Optic Technology*, *Optoelectronics and Fiber Optic Technology*. Elsevier Ltd. doi: 10.1016/b978-0-7506-5370-1.x5000-4.

Udd, E. and Spillman Jr., B. (2011) *Fiber Optic Sensors: An Introduction for Engineers and Scientists*. 2nd edn. New Jersey: John Wiley & Sons.

UIC (2016) *UIC ASSET MANAGEMENT WORKING GROUP UIC Railway Application Guide Practical implementation of Asset Management*. Paris.

Union, I. T. (2013) 'ITU-T telecommunication standardization sector'. Geneva.

Veit, P. (1999) *Projekt Strategie Fahrweg*. Graz University of Technlogy.

Veit, P. (2007) 'Track Quality - Luxury or Necessity?', *RTR special: Maintenance & renewal, Railway Technical Review*, pp. 8–12.

Veit, P. and Marschnig, S. (2009) 'Technische und wirtschaftliche Aspekte zum Thema Schwellenbesohlung - Teil 2: Wirtschaftlichkeit im Netz der ÖBB', *ZEVrail*.

Vermeij, I., Venekamp, D. and Boom, P. (2011) 'Using Gotcha to obtain real-time data gathered from wayside monitoring systems to optimize the LCC', *RTR Special – Wayside Train Monitoring Systems*.

Vidovic, I. (2016) *The track behaviour after formation rehabilitation*. Graz University of Technology.

Vidovic, I. and Landgraf, M. (2019) 'Fibre Optic Sensing as Innovative Tool for Evaluating Railway Track Condition?', in *International Conference on Smart Infrastructure and Construction 2019 (ICSIC)*. ICE Publishing, pp. 107–114. doi: 10.1680/icsic.64669.107.

Vidovic, I., Landgraf, M. and Marschnig, S. (2017) 'Impact of substructure improvement on track quality', in *3rd International symposium Railway geotechnical engineering*. Paris: IFSTTAR, p. 10.

Vidovic, I. and Marschnig, S. (2019) 'FOSphAT – Fiber optic sensing for peramanent and holistic assessment of track', in *Proceedings of 12th World Congress on Railway Research*. Tokyo, p. 5.

Walter, S. (2016) *Long-Term Railway Infrastructure Development Expansion of the Integrated Timetable on Mixed-Traffic Passenger Railway Networks*. Graz University of Technology.

Wenty, R. (2016) 'Kontinuierliche Gleisdurcharbeitungstechnologie im internationalen Vergleich', *EIK - Eisenbahningenieurkalender*, pp. 63–75.

Weston, P. F., Ling, C. S., Goodman, C. J., *et al.* (2007) 'Monitoring lateral track irregularity from in-service railway vehicles', *Proceedings of the Institution of Mechanical Engineers, Part F: Journal of Rail and Rapid Transit*. doi: 10.1243/0954409JRRT64.

Weston, P. F., Ling, C. S., Roberts, C., *et al.* (2007) 'Monitoring vertical track irregularity from in-service railway vehicles', *Proceedings of the Institution of Mechanical Engineers, Part F: Journal of Rail and Rapid Transit*. doi: 10.1243/0954409JRRT65.

Wiesmeyr, C. *et al.* (2018) 'Train tracking and train condition monitoring by Distributed Acoustic Sensing', in *Proceedings of 7th Transport Research Arena TRA 2018,*. doi: 10.5281/ZENODO.1456474.

Wilczek, K. *et al.* (2017) 'swissTAMP - Big Data für ein proaktives Anlagenmanagement Fahrweg', *ZEVrail*, 141(5), pp. 1–15.

Wilfling, P. A. (2017) *Der Weg zur Smarten Weiche*. Graz University of Technology.

Wu, H. *et al.* (2015) 'Separation and Determination of the Disturbing Signals in Phase-Sensitive Optical Time Domain Reflectometry (Φ-OTDR)', *Journal of Lightwave Technology*. doi: 10.1109/JLT.2015.2421953.

Wuttke, J., Krummrich, P. M. and Rösch, J. (2003) 'Polarization oscillations in aerial fiber caused by wind and power-line current', *IEEE Photonics Technology Letters*. doi: 10.1109/LPT.2003.811143.

Yazawa, E. and Takeshita, K. (2002) 'Development of Measurement Device of Track Irregularity using Inertial Mid-chord Offset Method', *Quarterly Report of RTRI*, 43(3), pp. 125–130. doi: 10.2219/rtriqr.43.125.

Zaayman, L. (2017) *The Basic Principles of Mechanised Track Maintenance*. 3rd edn. Bingen: PMC Media House.